National Research Council Canada
Conseil national de recherches Canada

PERFORMANCE EVALUATION OF VARIABLE-SURFACE AREA BIOREACTORS FOR CELLULOSE UTILIZATION

BY
BIOREACT ENGINEERING

Canada
NRCC 22784

85-3207/

This report summarizes work carried out under contract to the Division of Energy, National Research Council of Canada. It has been published in accordance with the policy of the National Research Council of Canada of making information on energy research and development available to all interested groups. Publication by the National Research Council of Canada does not signify that the contents necessarily reflect the views or policies of the National Research Council of Canada, nor does mention of trade names or commercial products constitute endorsement or recommendation for use. Furthermore, no warranty or representation is made with respect to the accuracy or completeness of the information contained in this report. This report is reproduced here from camera-ready copy prepared by the contractor. The abstract was translated by the National Research Council of Canada.

Le présent rapport constitue un résumé des travaux effectués à contrat par la Division de l'énergie, Conseil national de recherches du Canada (CNRC). Sa publication est conforme à la politique du CNRC qui est de diffuser l'information disponible sur la recherche et le développement énergétiques auprès de tous les groupes intéressés. Son contenu n'exprime pas nécessairement les opinions ou politiques du Conseil national de recherches du Canada et la mention de marques ou produits commerciaux ne doit pas être considérée comme une approbation ou une recommandation d'utilisation. De plus, aucune garantie ni représentation ne peut être faite quant à l'exactitude ou à l'intégralité du contenu du rapport, qui a été reproduit à partir d'une copie prête à l'impression préparée par le sous-traitant. Le résumé a été traduit par le Conseil national de recherches du Canada.

Copyright 1984 by
National Research Council of Canada

Permission is granted to quote short excerpts and to reproduce figures and tables from this report, provided that the source of such material is fully acknowledged.

Additional copies of this report are available free of charge from:

Division of Energy
Bioenergy Program
Building R-105
National Research Council of Canada
Ottawa, Ontario, Canada
K1A 0R6

Copyright 1984 par
Conseil national de recherches du Canada

De courtes citations et la reproduction de figures et tableaux du présent rapport sont autorisées sous réserve que la source en soit clairement mentionée.

Des exemplaires supplémentaires gratuits peuvent être obtenus à l'adresse suivante:

Division de l'énergie
Programme d'énergie de biomasse
Edifice R-105
Conseil national de recherches du Canada
Ottawa (Ontario) Canada
K1A 0R6

FINAL REPORT

PERFORMANCE EVALUATION OF VARIABLE-SURFACE AREA BIOREACTORS FOR CELLULOSE UTILIZATION

Prepared for

Division of Energy Research and Development
Bldg. M-55, Suite 381
National Research Council
Montreal Road
Ottawa, Ontario
K1A OR6

by

BioReact Engineering
c/o Dr. Paul P. Matteau, PEng.
Royal Military College of Canada
Department of Chemical Engineering
Kingston, Ontario.
K7L 2W3

April, 1984

TABLE OF CONTENTS

	Page
SUMMARY	xi
SOMMAIRE	xiii
INTRODUCTION	1
WORK UNDERTAKEN	3
TECHNICAL DISCUSSION	7
REACTOR DESIGN/OPERATION	8
Immobilization Procedure	10
REACTOR EVALUATION	11
Inert Flow Experiments	11
Enzymatic Hydrolysis	14
Fermentation	19
CONCLUSIONS	29
RECOMMENDATIONS	33
TABLES	35
FIGURES	53
APPENDIX 1 - Longer-Term Operation of Reactors	119
APPENDIX 2 - Paper Presented at 5th Bioenergy R&D Seminar	137

LIST OF TABLES

		Page
1	Description and designation of reactors	36
2	Effect of needle size on gravity-formed calcium alginate beads	37
3	Pressure drops observed in packed-bed reactors using different sizes of packing	38
4	Steady-state glucose concentration for enzymatic hydrolysis of cellobiose and salicin (Run 1)	39
5	Steady-state glucose concentration for enzymatic hydrolysis of cellobiose (Run 2)	40
6	Serial batch growth of yeast using decreasing levels of salts in the medium	41
7	Serial batch growth of yeast using decreasing levels of yeast extract in the medium	42
8	Operational parameters and results obtained for fermentation reaction using reactor TUB 1 with 1%, 2% and 5% glucose medium	43
9	Operational parameters and results obtained for fermentation reaction using reactor TAP 2 with 1%, 2% and 5% glucose medium	44
10	Operational parameters and results obtained for fermentation reaction using reactor RAD 1 with 1%, 2% and 5% glucose medium	45
11	Operational parameters and results obtained for fermentation reaction using reactor TAP 1 with 8% and 12% glucose medium .	46
12	Operational parameters and results obtained for fermentation reaction using reactor TAP 2 with 8% and 12% glucose medium .	47
13	Operational parameters and results obtained for fermentation reaction using reactor RAD 2 with 8% and 12% glucose medium .	48
14	Comparison of productivities obtained from TAP 1, TAP 2 and RAD 2 based on calculations from ethanol analysis and carbon dioxide production rate data	49

LIST OF TABLES (Concluded)

		Page
15	Operational parameters and results obtained for fermentation reaction using reactor TAP 1 packed with ion-exchange resin and with 8% and 12% glucose medium	50
16	Operational parameters and results obtained for fermentation reaction using reactor TAP 1 packed with alginate beads and with 8% and 12% glucose medium	50
17	Operational parameters and data obtained for reactors prior to start of tracer analyses	51
A1	Operational parameters and results obtained for long-term fermentation of 8% glucose with alginate beads in TAP 1 . . .	124
A2	Operational parameters and results obtained for long-term fermentation of 8% glucose with ion-exchange resin in TAP 1 .	125
A3	Operational parameters and results obtained for long-term fermentation of 8% glucose with ion-exchange resin in RAD 1	126

LIST OF FIGURES

		Page
1	Schematic of tubular reactor	54
2	Schematic of radial-flow reactor (original)	55
3	Schematic of tapered-bed reactor (original)	56
4	Diagram of modified radial-flow and tapered bed reactors . . .	57
5	Schematic of reactor evaluation system	59
6	Relationship between radius and length of a 1 litre capacity tubular reactor	60
7	Relative linear velocities in various lengths of 1 litre capacity tubular reactors	61
8	Effect of variation in volumetric flow rate on pressure drop in different 1 litre capacity tubular reactors	62
9	Relationship between radius and height for a radial-flow reactor of 1 litre capacity	63
10	Relative linear velocity of fluid passing through a radial-flow reactor	64
11	Effect of variation in volumetric flow rate on the pressure drop in different 1 litre capacity radial-flow reactors . . .	65
12	Variation in exit radius as a function of reactor length for a 1 litre capacity tapered-bed reactor	66
13	Relative linear velocities of fluid passing through various lengths of 1 litre capacity tapered-bed reactors	67
14	Effect of height of 1 litre capacity tapered-bed on the exit fluid velocity	68
15	Effect of variation in volumetric flow rate on the pressure drop in different 1 litre capacity tapered-bed reactors . . .	69
16	General procedure for the preparation of calcium alginate encapsulated cells	70
17	Pressurized large-scale calcium alginate bead-forming device .	71

LIST OF FIGURES (Continued)

		Page
18	Tracer analysis through short tubular reactor packed with calcium alginate beads formed with 1.024 mm needles	72
19	Filter paper activity of T. reesei 9414 grown on 2% Solka-Floc	74
20	Filter paper activity of T. harzianum E58 grown on 2% Solka-Floc	75
21	Carboxymethylcellulase activity of T. reesei 9414 grown on 2% Solka-Floc	76
22	Carboxymethylcellulase activity of T. harzianum E58 grown on 2% Solka-Floc	77
23	*b*-glucosidase activity of T. reesei 9414 grown on 2% Solka-Floc	78
24	*b*-glucosidase activity of T. harzianum E58 grown on 2% Solka-Floc	79
25	Variation in dry weight and pH of T. reesei culture grown on 2% Solka-Floc	80
26	Variation in dry weight and pH of T. harzianum E58 culture grown on 2% Solka-Floc	81
27	Encapsulated cell-associated activity of culture solids during growth of T. reesei 9414 and T. harzianum E58 on 2% Solka-Floc	82
28	Dynamic response of TUB 1 for 10 mM cellobiose hydrolysis at a dilution rate of 0.18 h^{-1} (Run 1)	83
29	Steady-state conversions of 10 mM cellobiose as a function of dilution rate for reactors TUB 1, TAP 1 and RAD 1 (Run 1) .	84
30	Steady-state conversion of 5 mM cellobiose as a function of dilution rate for reactors TUB 2, TAP 2 and RAD 1 (Run 2) .	85
31	Steady-state conversion of 7.5 mM cellobiose as a function of dilution rate for reactors TUB 2, TAP 2 and RAD 1 (Run 2) .	86

LIST OF FIGURES (Continued)

		Page
32	Steady-state conversion of 10 mM cellobiose as a function of dilution rate for reactors TUB 2 and TAP 2 (Run 2)	87
33	Steady-state conversion of 20 mM cellobiose as a function of dilution rate for reactors TUB 2, TAP 2 and RAD 1 (Run 2) .	88
34	Steady-state conversions of cellobiose (5, 7.5, 10 and 20 mM) as a function of dilution rate for reactor TUB 2 (Run 2) . .	89
35	Steady-state conversions of cellobiose (5, 7.5, 10 and 20 mM) as a function of dilution rate for reactor TAP 2 (Run 2) . .	90
36	Comparison of the steady-state conversion of 10 mM cellobiose and a mixture of 10 mM cellobiose and 10 mM glucose in the reactors TUB 2 and TAP 2	91
37	Glucose elution profiles obtained after steady-state conversion had been achieved in reactors TUB 2 and TAP 2 . .	93
38	Comparison of 10 mM cellobiose hydrolysis using TUB 2 with 100% active beads and with 50% active beads	94
39	Response surface obtained by modelling of data obtained from cellobiose hydrolysis with TUB 2	95
40	Dynamic start-up response of reactors TUB 1, TAP 2 and RAD 1 operating at 5% glucose at a dilution rate of 0.9 h^{-1} . . .	96
41	Correlation between alcohol concentration based on carbon dioxide production rates and measured alcohol levels in reactor effluent	98
42	Dynamic response of reactors TAP 1, TAP 2 and RAD 2 as determined using carbon dioxide production rates	101
43	Glucose utilization at 8% feed as a function of dilution rates in reactors TAP 1, TAP 2 and RAD 2	104
44	Glucose utilization at 12% feed as a function of dilution rates in reactors TAP 1, TAP 2 and RAD 2	105
45	Alcohol productivities based on effluent alcohol and carbon dioxide production rates: (a) TAP 1; (b) TAP 2; (c) RAD 2 .	106

LIST OF FIGURES (Concluded)

		Page
46	Size distribution of yeast-containing calcium alginate beads at various times after initial preparation and use	109
47	Dynamic response of reactor TAP 1 packed with calcium alginate beads and with ion-exchange resin	111
48	Glucose utilization at 8% feed as a function of dilution rates in reactor TAP 1 packed with calcium alginate beads and ion-exchange resin	112
49	Response of step input of 5% isopropanol into TAP 1 containing ion-exchange immobilized yeast cells	113
50	Response of step input of 5% isopropanol into TAP 1 containing calcium alginate immobilized yeast cells	114
51	Response of step input of 5% isopropanol into TAP 2 containing calcium alginate immobilized yeast cells	115
52	Response of step input of 5% isopropanol into TUB 1 containing calcium alginate immobilized yeast cells	116
53	Response of step input of 5% isopropanol into RAD 1 containing calcium alginate immobilized yeast cells	117
A1	Carbon dioxide production rate data for TAP 1 containing calcium alginate immobilized yeast cells	127
A2	Carbon dioxide production rate data for TAP 1 containing ion-exchange resin immobilized yeast cells	130
A3	Carbon dioxide production rate data for RAD 1 containing ion-exchange resin immobilized yeast cells	133

SUMMARY

The objective of this work was to compare the performance of two types of packed-bed variable-surface area reactors with that of tubular reactors. The evaluation was carried out using two different types of biological reactions: an enzymatic hydrolysis using enzymes associated with non-growing cells and a model fermentation in which the cells were reproducing.

One reactor configuration was in the form of a cone, or a tapered-bed, and the other consisted of a cartridge-type reactor which permitted a radial flow of the fluids. Two reactors, each of 1 litre capacity, were tested from each of these types.

Theoretical analyses showed that operation of the radial-flow reactor results in the smallest pressure drop across the packed catalyst bed for reactors having the same bed volume. Experimental results with both inert flow experiments and under reactive conditions bore this out. The radial-flow reactor was found to be less suitable than the others for both types of reaction, as substantial channelling was observed to occur at the top of the reactor bed, especially with the easily compressible calcium alginate beads which were being used.

As predicted, operation of the tapered-bed reactors resulted in lower pressure drops than that observed in the tubular reactors. The upflow mode of fluid flow, however, resulted in bed separation and compaction in all but the shortest tapered-bed reactor chosen. This was due in part to the compressible nature of the packing material (calcium alginate beads). This work has also demonstrated that use of other than variable-surface area reactors in fermentations can result in unacceptably high pressure drops across the reactor bed.

The data obtained from the enzymatic hydrolysis have permitted the evaluation of the kinetic constants required for the modelling and simulation of the process. The data from the fermentation have shown the same trends as the hydrolysis and additional work will be required prior to a reliable model being constructed.

This work has shown the usefulness of using a computer based on-line data acquisition system for the determination of the state of the fermentation process.

The use of compressible particles, such as calcium alginate beads has been shown to result in operational difficulties in most of the reactors tested. This was not the case with the shortest of the tapered-bed reactors. This system was subsequently tested for long term stability using both alginate beads and an incompressible immobilizing agent (an ion-exchange resin) in the fermentation reaction. The results obtained indicate that the ion-exchange resin is much less effective for longer term operation than is the calcium alginate immobilized system when used in variable-surface area reactors. As the former immobilizing system does have some practical advantages over the latter method, it is recommended that additional studies be carried out in order to properly evaluate these two immobilization procedures.

SOMMAIRE

L'objectif du présent travail était de comparer le rendement de deux types de réacteurs à surface variable et à lit compact au rendement de réacteurs tubulaires. On a fait l'évaluation en utilisant deux types différents de réactions biologiques: une hydrolyse enzymatique réalisée à l'aide d'enzymes associées à des cellules dépourvues de croissance et une fermentation type dans laquelle les cellules se reproduisent.

L'un des réacteurs avait la forme d'un cône, ou était à lit conique, et l'autre était du type cartouche, permettant un écoulement radial des fluides. Pour chacun de ces types, on a mis à l'essai deux réacteurs ayant chacun une capacité de 1 litre.

Des analyses théoriques de réacteurs ayant des lits de même volume ont montré que le réacteur à écoulement radial donnait la plus faible perte de charge dans le lit de catalyseur compact. Les expériences réalisées aussi bien avec un écoulement de matière inerte qu'en conditions réactives ont confirmé ce résultat. On a trouvé que le réacteur à écoulement radial ne convenait pas aussi bien que les autres pour les deux types de réactions: on a observé un phénomène appréciable de création de cheminements préférentiels à la partie supérieure du lit, particulièrement lorsqu'on utilisait les grains d'alginate de calcium facilement compressibles.

Comme prévu, les réacteurs à lit conique ont produit des pertes de charge moins importantes que les réacteurs tubulaires. Cependant, l'écoulement ascendant du fluide a produit le tassement et la séparation du lit dans tous les réacteurs choisis, à l'exception du réacteur à lit conique le plus court. Cette caractéristique était attribuable en partie à la nature compressible du matériau de remplissage (grains d'alginate de calcium). Le présent travail a aussi permis de démontrer que l'utilisation de réacteurs autres que ceux à surface variable, pour la fermentation, pouvait produire de trop grandes pertes de charge dans le lit du réacteur.

Les données obtenues à partir de l'hydrolyse enzymatique ont permis d'évaluer les constantes cinétiques requises pour la modélisation et

la simulation de la réaction. Les données obtenues à partir de la fermentation ont permis d'observer les mêmes tendances qu'à partir de l'hydrolyse et il faudra effectuer d'autres travaux avant de pouvoir construire un modèle faible.

Le travail a montré l'utilité d'un système d'acquisition de données en direct géré par ordinateur pour déterminer l'état de la réaction de fermentation.

On a montré que l'utilisation de particules compressibles, par exemple de grains d'alginate de calcium, créait des problèmes de fonctionnement dans la plupart des réacteurs mis à l'essai. Le plus court des réacteurs à lit conique faisait exception. On a ensuite effectué des essais en vue d'évaluer la stabilité à long terme de ce système en utilisant des grains d'alginate et un agent immobilisant incompressible (une résine à échange ionique) dans la réaction de fermentation. D'après les résultats obtenus, la résine à échange ionique est beaucoup moins efficace que le système immobilisé à alginate de calcium pour une utilisation à plus long terme dans les réacteurs à surface variable. Étant donné que le premier système d'immobilisation présente certains avantages pratiques que n'offre pas la dernière méthode, on recommande de faire d'autres études afin d'évaluer convenablement ces deux méthodes d'immobilisation.

INTRODUCTION

The objective of this contract is to design and construct four variable-surface area reactors and to study/compare their performance relative to tubular reactors. The variable-areas reactors included two tapered-bed reactors and two radial-flow reactors. The various reactors were initially evaluated under inert conditions in order to determine the effect of the geometries on the flow and operational properties using different sizes of packing material for the packed-bed. The reactors were subsequently evaluated using an enzymatic hydrolysis reaction and a gas-producing fermentation. The former process involved the use of calcium alginate encapsulated fungal mycelium in order to hydrolyse cellobiose to glucose. The latter process involved the use of immobilized yeast for the model, gas-producing fermentation of glucose to ethanol. The immobilization procedures used here included both calcium alginate encapsulation of the yeast as well as some use of a macroporous ion-exchange resin.

The major advantage postulated in the use of these variable-surface area bioreactors was a reduced pressure drop across the multi-phase reactions as a result of an increase in the surface area of the packed-bed in the direction of flow. This change in surface area results in a decrease in the superficial velocity of the fluids passing through the bed. Additionally, during the fermentation process, these novel geometries would permit the gas produced during the reaction to pass more readily through the reactive bed.

Initial efforts were devoted to the design and construction of the six reactors to be used for this project. Each reactor system was constructed so as to permit its isothermal operation under restricted flow conditions. The operation of each reactor was then evaluated, first under no reaction or inert conditions and then for both the enzymatic hydrolysis of cellobiose and then the fermentation of glucose to ethanol and carbon dioxide. These experiments were designed to determine if any variations in the performance of the reactors could be attributed to a change in the geometry of the reactor.

WORK UNDERTAKEN

Reactor Design/Construction

The parameter to be evaluated in the design of the packed-bed reactors was the ratio of the height to diameter. As a result of modelling of the pressure drop across packed-beds for each of the geometries, it had been decided that two height-to-diameter ratios for each reactor geometry would be evaluated. Any variation in performance as a result of a change in this parameter would permit subsequent optimization studies to be carried out in relation to the packed-bed particle diameter and to the type of immobilization method to be used.

Tubular Reactors: A schematic showing the critical dimensions and construction details of the two tubular reactors is presented as Figure 1. The original jacketed reactors were fabricated from polycarbonate tubing. The acrylic cement which was used to join various sections proved to be unsuitable in that several leaks developed in the reactors. A new set of reactors was therefore constructed using acrylic tubing. No major sealing problems were encountered using these units. The end-plates for the reactors were machined from blocks of Delrin and as indicated, were bolted to the flanges which had been placed at each end.

Radial-Flow Reactors: The radial-flow reactors were constructed of acrylic tubing with stainless-steel mesh applied to the surfaces which had been holed using 2 mm drill bits. The initial design required that the effluent be drawn off using a second pump as is shown in Figure 2. Each reactor system was subsequently modified to permit pressurized operation. A diagram of these systems is presented as Figure 4a. In order to operate these systems isothermally, the complete unit was immersed in a controlled-temperature water bath.

Tapered-Bed Reactor: The tapered-bed reactors as depicted in Figure 3 were also initially designed to operate with a draw-off of the effluent. Again, in order to facilitate data acquisition, each reactor was subsequently modified in order to operate as a pressurized unit (Figure 4b). The taller of the two reactors was constructed of styrene-acrylonitrile whereas the shorter unit was formed using ABS plastic. Isothermal operation was ensured by seating these reactors in constant-temperature water baths.

Reactor Evaluation

The evaluation of the reactor was carried out in three distinct phases: (a) inert or non-reactive flow experiments; (b) enzymatic hydrolysis of cellobiose; and (c) fermentation of glucose to ethanol and carbon dioxide.

The initial "inert" experiments were carried out to determine the base effects of liquid flow through the various reactor configurations. In this phase of the work we were interested in determining the pressure drops which would occur across each of the packed beds using the different geometries. The variables evaluated were the volumetric liquid flow through the beds and the packed-bed particle diameter. Experiments to determine the ease with which the packed bed could be fluidized were carried out by determining the degree of bed expansion as a function of the volumetric liquid flow rates. Addititionally, some tracer experiments were carried out in order to determine the residence time distributions in the reactors and to develop the analytical techniques which would be required for such studies using the reactive systems. This latter information also permitted the comparison of the reactor void volume (packing density) with that which had been calculated based on the liquid displacement volume of the catalyst bed.

The next two phases of the work were carried out, more or less, in parallel. Initially, some microbiological experiments were carried out in order to determine the effects of growth conditions on both the fungi which were to be used for the hydrolytic experiments and on the yeast which were to be used for the fermentation. Once these growth parameters had been established, alternate runs consisting of the enzymatic hydrolysis and the fermentation were carried out. Normally, one reactor from each geometry was used simultaneously in order to obtain comparable data within a given run. An overall system diagram is presented as Figure 5.

Based on the data obtained after six months of work, it was decided, in consultation with the project manager, that the remainder of the experimental work period would be devoted to the fermentation reaction and that this process would be carried out at higher substrate concentrations and at lower dilution rates so as to obtain data for 100% conversions of the substrate. The data obtained from all the fermentation runs suggested that the best reactor for carrying out this process was the short tapered-bed reactor. A recommendation

has been made to the project manager for the extension of this contract for a period of one month in order that this unit be evaluated for continuous, longer-term operation using encapsulated and adsorbed yeast cells.

TECHNICAL DISCUSSION

REACTOR DESIGN/OPERATION

Novel enzyme and cell immobilization techniques require research to determine the type of bioreactors to be used in conjunction with these biological catalytic particles. One type of reactor of major interest for carrying out continuous catalytic processes is the packed- or fixed-bed reactor. There are many advantages to using packed-bed reactors and normally, the preferred geometry for such a system is an upright cylindrical reactor with either bottom feed (upflow) or feed from the top (downflow). A unique feature of the packed-bed reactor is that there exists a pressure drop or resistance to flow across the reactor. This pressure drop depends on such parameters as bed height, feed rate, feed temperature, and composition as well as the catalyst packing density. This negative aspect of this reactor is further compounded during certain biological reactions wherein a substantial amount of gas is released due to the fermentation. The increased pressure drop thus results in reduced flows, as well as gas hold-up and channelling of the fluids in the reactor. Augmenting the flow merely acts to increase further the pressure differential across the packed-bed and further results in compaction of the bed and additional reduction in the hydraulic permeability of the resulting bed.

In order to circumvent this negative aspect and still maintain the positive qualities of the packed-bed reactor, two novel reactor geometries were considered: a radial-flow packed-bed reactor (RFPBR) and a tapered packed-bed reactor (TPBR). In both geometries there is an increased bed surface area in the direction of flow which results in a reduction in the fluid velocity through the reactor. This should result in a lower pressure drop across an equivalent height of bed in a tubular reactor. When used for a process such as a gas-producing fermentation, the increased surface area should result in a reduction in the bed resistance to both gas and liquid flow.

In order to test the above hypothesis with respect to the effect of the reactor geometry on the pressure drop, the pressure drop predicted by the Kozeny-Carman equation was determined for various volumetric flow rates through one litre packed-bed reactors. This model was then applied to each of the three geometries for a series of bed depths. Figures 6 through 8 present data

for the tubular packed-bed reactors. Figure 6 presents the relationship between the length and radius of such reactors. Figure 7 presents the linear liquid velocities which occur in these reactors relative to the longest reactor studied (1 metre). Finally, the calculated relative pressure drops encountered at flow rates from 0.1 to 4.1 litres/hour are presented in Figure 8. Similar data are presented in Figures 9 through 11 for the radial-flow packed-bed reactors and in Figures 12 to 15 for the tapered packed-bed reactors.

Based on these simulations, it can be expected that under identical reaction conditions (catalyst particle size, flow rates, temperature, substrate concentration), the pressure drops encountered in tubular packed-bed reactors will be approximately twice that encountered in tapered-bed reactors and up to 20 times greater than those encountered in radial-flow packed-bed reactors.

These results served as the basis for the choice of the dimensions of each pair of reactors to be used in this study. The dimensions of each reactor are presented in Table 1, along with the abbreviations used to identify each reactor. As can be seen, for each of the two new geometries, dimensions at each of the the extremities of the previously presented curves were chosen. The tubular reactor dimensions were chosen on the basis of the height to diameter ratio. The taller unit has a ratio of 23 while the shorter unit has a height to diameter ratio of 9.7.

Reactor Construction/Operation

In their final form, both tubular and radial-flow reactors were constructed of acrylic plastic. The taller tapered-bed reactor was constructed of styrene-acrylonitrile and the shorter tapered-bed reactor was constructed of ABS plastic. Details of construction are presented in Figures 1 through 4.

All reactors were operated isothermally through the use of either a heat-exchange jacket (tubular reactors) or by immersing the reactors in a constant-temperature water bath. A schematic of the general system is presented in Figure 5. As can be seen, the collection reservoir connected to the exit of the reactors was controlled using electronically timed relays. This permitted the collection of timed samples as well as the continuous measurement of the gas produced during the fermentation.

Immobilization Procedure

Encapsulation: The general procedure that was used to immobilize the fungal mycelium is presented in Figure 16. Immobilization of the yeast cells was carried out in the same manner, but the cells were separated by centrifugation rather than by filtration. Initial experiments with each of the reactors, showed that a new supply of sodium alginate produced a much more viscous solution than had been previously obtained. In order to have a mixture with approximately the same extrusion charactersitics (for bead formation), it was found necessary to decrease the sodium alginate concentration to 1.5%.

In order to scale-up the production of calcium alginate beads, a pressurized bead-forming system was designed and constructed. The unit, as depicted in Figure 17, has the advantage of forming up to 5 litres of beads without refilling the reservoir. Additionally, the orifice diameter is easily changed by changing the size of needle on the connectors to give a variation in the size of gravity-formed beads. Data obtained for various needle sizes used are presented in Table 2.

Adsorption: Use of a macroporous anion exchange resin (Ambergard XE-352) was carried out in some of the developmental runs in order to determine if any gross variations occurred as a result of using a much smaller particle size (0.5 - 1.3 mm OD). Some recent work (A.J. Daugulis, personal communication) has suggested that this medium is particularly suitable for the immobilization of both bacteria and yeast. In order to use this support medium, the resin was treated with a 0.5% sodium hypochlorite solution according to the manufacturer's (Rohm and Haas) suggested method of preparation and then transferred into the reactor where it was washed with distilled water. The inoculated growth medium was then recycled through the reactor for a period of 24 hours. This provided a good cell mass within the reactor for start-up.

REACTOR EVALUATION

Inert Flow Experiments: In order to separate those effects which occurred during the course of the catalytic reaction from those which resulted from fluid flow through a packed-bed, a series of flow studies were carried out. One of the parameters of interest was the pressure drop across the packed-bed. Another aspect which was studied was the degree of bed expansion or fluidization which resulted from the fluid flow. A third parameter of interest was the residence time distribution. Determination of the base values associated with each of these parameters would permit some insight into the effects which would be subsequently observed during the biological reactions.

The pressure drop studies and the tracer analyses were carried out with the reactors completely filled with the catalyst. The bed expansion studies, on the other hand, were carried out using the tall tubular and tapered reactors filled with approximately 650 ml of the inert particles.

A summary of the results of the pressure drop studies is presented in Table 3. The highest pressure drops were obtained with the ion exchange resin (smallest particle size) and were of the order of 40 mm Hg in the tall tubular reactor. There was a very small resistance to the flow of liquid in all but the two tubular reactors. Any large pressure drops encountered in the fermentation reactions were, therefore, a result both of the gas being formed in the reactor and of the compaction of the catalytic bed.

The bed expansion studies were carried out to determine the degree of fluidization which might be encountered with each of the particle sizes. Preliminary studies indicated that some bed segregation was occurring, especially at higher flow rates, resulting in bed compaction and increased or erratic pressure drops. The studies were carried out in the tall tubular reactor (TUB 2), using the ion exchange resin, as well as three sizes of calcium alginate beads. The results showed that, with flow rates of up to 3.6 litres/hour, only the ion exchange resin bed expanded appreciably. At this flow, the height of the bed increased by 45%. With the calcium alginate beads, no bed expansion was observed, except in the case of the smallest of the alginate beads used (needle size of 0.813 mm). A 5% increase in bed height

was obtained in this case. When the tall tapered-bed reactor was tested under similar conditions, the ion-exchange bed expanded by approximately 10% at a flow rate of 3.6 liters/hour, whereas no measurable variation was observed with the alginate beads. These data on pressure drop and bed expansion suggested that problems might be encountered when attempting to use the ion exchange resin in the tubular or tapered-bed reactors at high flow rates.

The determination of the residence time distributions with some of the reactors was carried out in order to develop a method for tracer studies to be used in conjunction with the fermentation reaction. This is particularly important as an accurate determination of the liquid and gas volumes in the packed bed during fermentation is critical to the modelling of the system. Initial tracer studies were carried out using fluorescein which can be easily detected at a wavelength of 460 nm. Unfortunately, it was found that this compound was easily adsorbed onto the ion-exchange resin. No such problem was encountered when using the calcium alginate beads. A typical result obtained using this compound with the short tubular reactor (TUB 1) is presented in Figures 18a and 18b. Subsequent studies showed that use of this compound with the fermentation medium was impractical, as its absorbance was masked by colouring matter in the medium. It was finally decided that tracer studies would be carried out using isopropanol at a level of 5% in the culture medium. Isopropanol was also being used as the internal standard for the chromatographic determination of ethanol. Therefore, little effort was required in developing the analytical method to be used. This compound was, therefore, used with the fermentation reactors to verify flow behaviour under reactive conditions.

Generally, it was found that little axial dispersion occurred in the tubular reactors. The tapered-bed reactors, on the other hand, showed some deviation from plug-flow behaviour. This could be expected as a result of the change in the bed cross-sectional area in the direction of flow. Tracer experiments with the radial-flow reactors were inconclusive, as channelling of the dye occurred at the top of the reactor. Tighter packing of the reactor reduced but did not eliminate this effect. This also proved to be a problem with the cellobiose hydrolysis system where the cells were not growing. During the fermentation process this channelling did not appear to pose the same

kind of problem. It is suspected that this was due to the increase in the size of the alginate beads during the fermentation process.

These results were the basis for carrying out the continuous hydrolysis and fermentation experiments. The results obtained here suggested that problems might be encountered in using the radial-flow reactors for the enzymatic hydrolysis and in using the tubular reactors with the fermentation process. This phase of the work also permitted the development of standard operating procedures with each of the reactors as well as the determination of any difficulties which might be encountered with the equipment.

Enzymatic Hydrolysis

Microorganisms/Medium: The fungi used for this study were both species of Trichoderma, one obtained from Forintek Canada Corporation (Trichoderma harzianum E58) and the other from the National Research Council (Trichoderma reesei 9414). Growth was initiated by adding 50 ml of inoculum to 400 ml of Vogel's medium contained in 1 litre flasks. The fungi were then grown with shaking (rotary) at 30°C using 2% Solka Floc as the carbon source.

Reactor Packing: After 5 days of growth at 30°C, fungal pellets and mycelium were removed from the shake flasks and separated from the culture medium by filtration through Whatman glass fiber filters. The fungus was resuspended in a volume of distilled water equal to four times that of the original culture and sodium alginate (1.5% w/v) was added. This mixture was then homogenized in a food processor. The resultant viscous suspension was extruded through a 2 mm orifice into a stirred 4% calcium chloride solution. After hardening overnight in the calcium chloride solution, the beads were wet-packed into the reactors.

It was noticed that after approximately 24 hours at 50°C (reaction condition for cellobiose hydrolysis) some shrinkage of the alginate beads occurred. Additional beads were then added in order to obtain a firmly packed, but not compressed, bed.

Growth/Activity of Fungi: In order to choose between the two species of Trichoderma, an eight-day growth experiment was carried out. During this time, the enzymatic activities of the whole culture, the culture filtrate, and the culture solids were assayed using standard techniques. These included, carboxymethylcellulase activity (CMCase), filter paper activity (FPase), and β-glucosidase activity or salicin activity (SALase). The results obtained are presented in Figures 19 to 24. The variations in the dry weight and the pH of the cultures are presented in Figures 25 and 26. Additionally, the daily enzyme activities associated with the solids which were encapsulated in calcium alginate beads are presented in Figure 27. These results suggested that the organism which contained the most mycelium-associated enzyme activity was T. harzianum E58, and that the best age of culture for immobilization is approximately 5 days.

Reactor Operation: The effect of reactor configuration on the efficiency of cellobiose hydrolysis by mycelium-associated β-glucosidase was studied in two sets of experiments, referred to below as Run 1 and Run 2. All reactors were operated at 50°C, a temperature at which the fungus is in a no-growth condition. The substrates (cellobiose or salicin) were prepared in a 0.02 mol/liter sodium acetate buffer, pH 4.8, containing 2 g/l of calcium chloride. The substrate medium was not sterilized and no contamination problems were encountered.

Experiments were carried out in a discontinuous fashion, with sodium acetate buffer being recirculated through the reactors overnight. In the morning, prior to start-up, 1 liter of substrate was rapidly pumped through each reactor in order to displace the buffer solution. Glucose produced from the hydrolysis of cellobiose was measured by means of the glucose oxidase-peroxidase assay method.

Evaluation of Reactor Performance (Run 1): The first major run compared the three reactor TUB 1, TAP 1 and RAD 1 (see Table 1 for descriptions). The beads in these reactors, prepared as described above, were not spherical, but rather shaped like a comma and approximately 2 mm x 4 mm in size. Each reactor was packed with 570 ml (displaced volume) of beads.

The reactors were normally operated on 10 mM cellobiose for 6 - 8 hours at one dilution rate. The dynamic responses of each of the reactors were very similar in that the length of time required to reach the steady-state levels of conversions were approximately the same. An example of this dynamic response is represented in Figure 28. Generally, the lower the dilution rate used, the longer it took to establish a steady-state level of conversion. The steady-state conversions of cellobiose as a function of the dilution rate are presented in Figure 29. As can be seen, TUB 1 was more efficient than the other reactors in carrying out the enzymatic hydrolysis at low dilution rates. At higher dilution rates, little difference in the effectivenes of the reactors was observed.

At even the lowest flow rates used, the maximum conversion of cellobiose, in this run, never exceeded 60%. This resulted in a maximum glucose concentration of 2 mg/ml (Table 4). It is thought that some deactivation of the beads might have occurred as a result of storage at 30°C for 48 hours.

In order to look more closely at the possibility that some form of enzyme inhibition was occurring, the substrate was changed to salicin, a cellobiose analogue. As can be seen in Table 4, 10 mM salicin gave results comparable to that obtained with cellobiose. Doubling the concentration of salicin but maintaining the same flow rate resulted in an even lower steady-state value for the product. These results suggested that the enzyme activity is subject to substrate inhibition at very low levels and to product inhibition at glucose concentrations of approximately 2 mg/ml.

Reactor Performance (Run 2): Run 2 compared the three reactors TUB 2, TAP 2 and RAD 1 (see Table 1 for descriptions). As a result of a minor modification to the bead-forming unit, the beads used in these reactors were spherical and approximately 2 mm in diameter. Due to their smaller size and more uniform shape, it was possible to pack 770 ml (displaced volume) into each of the reactors.

While the reactors still exhibited dynamic responses similar to that obtained in Run 1, the length of time necessary to achieve steady-state was considerably shorter. It was therefore possible to operate the reactors at several dilution rates in a single day. The steady-state conversions obtained from these three reactors are summarized in Table 5. The efficiency of each reactor type in hydrolyzing a given concentration of cellobiose is compared in Figures 30 to 33 . It is clear that little difference exists between the results obtained using either the tubular or the tapered-bed reactor. On the other hand, the radial flow reactor consistently gave much lower results than the other two. It is thought that this was due to a shrinkage of the calcium alginate bead bed which permitted channelling of the substrate at the top of the reactor. In the case of the other two reactors, this effect was not critical, as both units were operated in an upflow manner.

The effect of substrate concentration on the rate of hydrolysis using the tubular reactor is presented in Figure 34, and with the tapered-bed reactor in Figure 35. The results obtained are consistent with what could be expected for a single-step enzymatic reaction in a plug-flow reactor. Both of these reactors were subsequently operated at various dilution rates on a feed solution containing 10 mM cellobiose and 10 mM glucose (Figure 36). The results obtained here indicate that at high dilution rates (low conversion),

the decrease in activity is approximately 50% whereas at low dilution rates, (high conversion) the decrease in activity is of the order of 10%. This suggests that substrate inhibition is likely more important than is product inhibition for this process.

In an attempt to determine the steady-state level of glucose which had accumulated in the beads, the tubular and the tapered reactors were initially operated at a low dilution rate using 7.5 mM cellobiose. Once both had stabilized at 100% conversion, the glucose was eluted by passing the buffer solution through them. As can be seen in Figure 37, the elution profiles for the two reactors were similar. Integration of these data showed that the glucose concentration in each reactor was 4.2 mg/(ml of reactor bed).

In order to determine whether or not the whole bed was reactive, the calcium alginate beads from the tubular reactor were mixed with an equal volume of inert beads. The reactor was then packed with a volume of beads equal to that which had been removed from it. The reactor was then operated using a 10 mM cellobiose medium at various dilution rates. As can be seen from the results presented in Figure 38, it is clear that, at the lower dilution rates, only a fraction of the bed was being utilized for the hydrolyis reaction. At higher dilution rates, this was even more evident as one-half of the active catalyst bed consistently produced a conversion greater than 50% of that obtained with the whole bed.

Modelling/Simulation: In order to determine the kinetic parameters of the cellobiose hydrolysis using the packed-beds of encapsulated β-glucosidase the data from the tubular reactor in Run 2 were evaluated in an integrated form of the Michaelis-Menton expression for a single substrate, irreversible reaction. As the reactor was effectively a plug-flow reactor, substrate inhibition is expected to be more critical than product inhibition. This was confirmed in experiments presented in the previous section. The data were then evaluated in the integrated form of the equation for both an uninhibited and a substrate-inhibited single-step enzyme reaction in a plug-flow reactor using a non-linear least squares technique. The non-inhibited model resulted in a sum of squares of the residuals of 112 whereas the subtrate-inhibition model resulted in a sum of squares of the residuals of 52. The kinetic constants as evaluated for this latter model were: Km = 3.129 mmol/litre; Ks = 15.78 mmol/litre and ; kE = 0.1878 mmol/min. Substitution of these values back into the integrated equation permitted the simulation of the response surface of the reactor with respect to flow rate and substrate concentration. The resultant response surface is presented in Figure 39.

The integrated form of this model incorporating substrate inhibition is given by:

$$XS_0 - Km(\ln(1-X)) + S_0(2X - X^2)/(2Ks) = kE/Q$$

where:

X = fraction conversion of substrate

S_0 = initial substrate concentration

Km = Michaelis constant

Ks = substrate inhibition constant

kE = maximal activity of total enzyme in the reactor

Q = volumetric flow rate

Fermentation

Microorganisms/Medium: The yeast used for this study were both species of Saccharomyces, one obtained from the National Research Council (Saccharomyces cerevisiae NRC 202076 and the other was a brewing yeast originally obtained from the Labatt Brewing Company. This latter yeast was used in the initial studies, whereas the former was used for all the continuous fermentations. Cells were typically grown without aeration at 30°C in a 5% glucose medium containing 0.5g KH_2PO_4, 0.5 g NaCl, 0.35 g $MgSO_4$, 2.0g $(NH_4)_2SO_4$ and 1.0 g of yeast extract per litre of solution. As a complete medium was required for the fermentation process, a set of serial batch reactions were carried out using the brewing yeast in order to determine the minimum nutrient requirements for both growth and fermentation. In a series of experiments, therefore, the salts were reduced to 0, 20, 40, 60, and 80 per cent of that used in the basic medium. In another series of experiments the level of yeast extract was varied in a similar fashion. The results of these experiments are presented in Table 6 & 7. The results showed that some slight reductions in both the salts and the yeast extract could be tolerated before a decrease in both the growth and the level of alcohol production occurred. Additional experiments were carried out to determine if the yeast were tolerant to various levels of calcium chloride. Results showed that levels of calcium chloride of up to 4% (maximum tested) did not reduce the amount of alcohol produced by the organism. Higher levels of calcium chloride did, however, result in the formation of a heavy precipitate upon autoclaving of the medium. This precipitate could result in substantial operational difficulties when the medium was passed through the packed-bed reactors.

Cell Immobilization and Reactor Packing: The yeast was grown in 2 litres of 5% glucose medium at 30°C for 24 hours. The cells were centrifuged, resuspended in 8 litres of distilled water, and then homogenized with sodium alginate (1.5% w/v) in a food processor to produce a viscous suspension. Using the bead-forming unit, this suspension was extruded through needles having a diameter of 1.024 mm into a stirred 4% calcium chloride solution. After hardening overnight in the calcium chloride solution, the beads were transferred into

8 litres of aerated 5% glucose medium every 24 hours for a period of 3 to 5 days. This incubation period at 30°C permitted the growth of the yeast cells within the calcium alginate beads. The medium used during bead incubation, as well as that used during the fermentations, contained 1.5 g of calcium chloride per litre of medium. This helped to maintain the rigidity of the beads by minimizing the loss of calcium from the beads. After this incubation period, the beads were wet-packed in the reactors.

Reactor Evaluation: The response of five reactors to fermentation conditions was examined in four complete sets of experiments, referred to below as Runs 1 to 4. Since operating conditions for each run were different, each is described separately below.

RUN 1: Here the aim was to compare the efficiency of fermentation in the three reactors TUB 1, TAP 2, and RAD 1 (see Table 1 for description). Each reactor was wet-packed with 500 ml (displaced volume) of freshly-prepared yeast beads. The reactors, maintained at 30°C, were operated at a dilution rate of 0.15 h^{-1} for 24 hours on sterile 5% glucose medium in order to allow cell mass within the reactors to increase and stabilize. After this initial period, the reactors were operated in a discontinuous fashion. Overnight, and on weekends, yeast cell viability was maintained by pumping 5% glucose medium through the reactors for 20 minutes every 1.5 hours. As during bead incubation, the 5% glucose medium contained 1.5 g of calcium chloride per litre of medium. Daily experiments were carried out using either 5% or 2% glucose medium; the lower glucose level medium was of the same composition as the 5% medium, but contained proportionately less of each component. Daily start-up involved the initial rapid passage of 2 liters of either 2% or 5% glucose medium through each reactor, followed by pump adjustment to the desired dilution rate. All medium used in this run was sterile.

As these reactors had not been previously been tested under fermentation conditions, few scientifically sound experimental data were obtained from this run. From the limited experiments conducted during this run, it was obvious that the operation of the tubular reactor for fermentation was resulting in severe pressure drops across the reactor. Operating on a 2% glucose medium at a dilution rate of 1.0 h^{-1}, typical pressure drops of 6 kPa were obtained.

Pressure drops of two to three times this value were consistently obtained when using the 5% glucose medium. Both the radial and the tapered reactors operated at much lower pressures, typically in the range of 1 - 2 kPa. Based on these results, it was decided to not operate the tubular reactor on glucose concentrations above 5%.

RUN 2: The second run used the same reactors as in the first run. A more systematic approach to the comparison of the three reactors was adopted. Whereas in the first run no attempt was made to measure the rate of carbon dioxide production, in this run each reactor was operated in a pressurized mode to permit the continuous monitoring of the gas flow. As previously, the reactors were operated in a discontinuous fashion. Overnight and on weekends, sterile 5% glucose medium was intermittently passed through the reactors. Daily start-up was the same as described above, except that non-sterile medium was used. Daily runs lasted from 10 to 14 hours.

Three concentrations of glucose medium were used in this run -- 1%, 2% and 5%. Tables 8 to 10 summarize the results obtained from the three reactors after 10 hours operation under a given set of conditions. The reactors were initially operated on 5% glucose medium and pressure drops were measured by means of mercury manometers. It soon became apparent that the pressure drops in both the tapered and the tubular reactor were greater than that which could be measured with the manometers. Consequently, the manometers were replaced with pressure gauges which could read to 250 kPa. These high pressure drops seemed to be caused by compaction of the calcium alginate beads against the top screening in each of the reactors. This compaction appeared to result from a flotation of the beads, likely due to an accumulation of carbon dioxide within the beads. Bed separation was clearly visible in both the tubular and the tapered reactors. Three distinct zones were formed. The lowest zone was highly agitated as a result of both the inlet liquid flow and the gas which was being produced. This represented a rather small fraction of the total bed. A middle zone contained no beads but only free cells suspended in the medium. The top region consisted of a highly compacted mass of calcium alginate beads through which both liquid and gas could be seen to percolate. It is very difficult to determine to what extent these beads contributed to the reactor productivity. When the tubular reactor was dismantled and repacked after

3 days of operation, the alginate beads at the top of the reactor had already begun to lose their rigidity and were found to be very flat. A similar but much less severe situation existed in the tapered reactor. After approximately 10 days of operation it was found that the pressure drop across the tubular reactor had risen to over 150 kPa. As the pump was incapable of operating against such a pressure, it was decided to incline the reactor at 30° to the horizontal. Subsequent operation of the reactor in this position resulted in relatively low pressure drops.

The results tabulated in Table 8 were obtained after 10 hours operation for a given set of conditions (approximately steady-state values). An example of the daily dynamic behaviour of the reactors is presented in Figure 40. Figure 40a presents the glucose utilization for the three reactors and Figure 40b the level of ethanol production. In general, the tubular and the tapered reactors gave the same results while the radial reactor tended to respond more slowly.

During this run it was found that, as a result of ineffective storage of the collected samples (refrigeration temperature too high), glucose levels in the samples tended to fluctuate. This also affected the measurement of ethanol concentrations in the samples. In addition, the low ethanol levels obtained by operating the reactors on 1% and 2% glucose were found to be at the resolution limit of the detector of the gas chromatograph which was being used.

Once some of the difficulties involving the gas metering were remedied, and despite the somewhat erratic ethanol measurements, it was found that the correlation between the rate of carbon dioxide and ethanol production was very good. An example of this correlation is illustrated in Figure 41. It was decided that for subsequent runs, the dynamic response of each of the reactors would be monitored by means of the rate of gas production, and that glucose and ethanol assays would be carried out only after steady-state values had been reached. Continuous gas monitoring could be carried out by coupling the gas meters which were being used to a minicomputer data acquisition system.

RUN 3: This run was used to evaluate the performance of the reactors TAP 1, TAP 2 and RAD 2. As a result of the high pressures which had developed in the tubular reactor, it had been decided that no additional work would be carried out with this type of reactor.

It had been noticed during the previous runs that the alginate beads containing the yeast increased in size during both the batch incubation and during the first few days of reactor operation. For this reason, each of the reactors were wet-packed with 400 ml (displaced volume) of freshly prepared, incubated beads. The reactors were then operated continuously at a low dilution rate (0.3 h^{-1}) on sterile 5% glucose medium for 48 hours to encourage bead expansion which was apparently due to an increase in the cell mass within the beads. Within 48 hours, the beads had expanded to completely fill the reactors.

As a result of consultation with the project manager, it had been decided to carry out a series of runs at higher glucose concentrations (8% and 12%). The media used for these experiments had the same compositions as that used for the 5% glucose medium except that the level of each component was increased proportionately. Unlike the previous two runs, the reactors in this run were operated continuously. Typically, an experiment would commence in the late afternoon by adjustment of the flow rate to give the desired dilution rate. The reactors were then operated on sterile medium at that flow overnight. The dynamic response of each reactor was continuously monitored by means of a minicomputer which had been linked to the gas meters (one for each reactor). From the gas production data, it was obvious that steady-state operation was normally achieved after approximately 16 hours of operation. At this time, several samples were collected from each reactor over a period of 4 to 5 hours and analyzed for residual glucose and ethanol. Additionally, in order to permit a complete mass balance to be carried out, the dry weight of yeast cells which were being swept from the reactors were determined. The results presented are the average of these analyzed samples. On weekends, the reactors were operated continuously on sterile medium at a dilution rate of 0.3 h^{-1}.

The dynamic reponses of the reactors to a change in operating conditions based on the gas production data are presented in Figure 42. The reaction parameters which were measured after steady-state had been reached are summarized in Tables 11 to 13. It is evident from these data that, although

the tapered reactor TAP 2 experienced the greatest pressure drops and RAD 2 the least, none of the reactors developed very large pressure differentials. As can be seen from these data, there does not exist a correlation between the dilution rate, or glucose feed concentration and the dry weight of yeast cells which are being washed from the reactors. In all cases, the dry cell weight was approximately 0.06 g dry cell matter per 100 ml of effluent.

The efficiency of fermentation by the three reactors is compared in Figures 43 and 44. At both 8% and 12% glucose fed, TAP 2 utilized more of the available glucose than the other reactors, followed by the other tapered reactor and then the radial reactor. These results indicate that a tapered-bed might be the most suitable for carrying out a fermentation with immobilized cells. The results also suggest that the most efficient operation of the tapered-bed reactor would be at a glucose concentration of 8% and at dilution rates of between 0.5 and 1.0 h^{-1}. The use of substrate concentrations substantially higher that 8% appears to be counter-productive. As Figures 45a, b and c indicate, approximately the same, or even higher productivities were obtained for the tapered bed reactors at a given dilution rate using 8% glucose medium as compared to 12% glucose. It is not obvious from the data whether this is also the case for the radial flow reactor.

Table 14 compares the productivities (based on reactor volume) for the three reactors being operated on 8% and 12% glucose medium as determined from either the actual effluent ethanol concentrations (gas chromatograph) or as calculated from the carbon dioxide production rate after 16 hours of operation. It is evident that the two sets of data are virtually identical. Some variations are, however, evident in these comparisons. These results show that the rate of carbon dioxide production is in fact a very good measure of the behaviour of this fermentation system. Additionally, the use of a minicomputer data acquisition system to monitor and constantly analyze the state of the reaction results in a drastic reduction in the number of time-consuming assays that would otherwise be performed.

The reactors in this run were initially operated on 8% glucose and then on the 12% glucose medium. Before the reactors were shut-down, the systems were again operated with the 8% glucose feed at a dilution rate of 0.7 h^{-1}. As can be seen from the data in Tables 11 to 13, the productivities obtained were

significantly lower than when the reactors were initially operated under these conditions. This decrease in activity is difficult to explain, especially, as is indicated below, when the total cell mass had in fact increased over this period.

Upon dismantling the reactors, it became obvious that there was a substantial mass of free cells within the reactor. Each reactor was found to contain approximately 14 g (dry weight) of free cells and 70 g (dry weight) of yeast cells associated with the calcium alginate beads. However, what fraction of the overall reaction was being carried out by either the free or immobilized yeast cells is unknown.

As mentioned previously, the calcium alginate beads containing the yeast increased in size during the batch incubation and in the first few days of reactor operation. The size distribution of the beads at various stages of the fermentation process is depicted in Figure 46. The size distribution was essentially the same after one week of operation at either 8% or 12% glucose medium. The bimodal distribution of the bead sizes is likely due to a geometric effect. That is, those beads which were in the bottom of the reactors were obviously larger that those which were at the top of the reactor. This can be accounted for by the fact that more growth would occur at the bottom -- availability of some oxygen, and the presence of higher ethanol concentrations at the top -- dehydration and cell starvation.

In order to determine the total cell weight which was in the reactor at any given time, samples of the yeast-containing calcium alginate beads were taken immediately after formation of the beads, immediately prior to loading into the reactors (after incubation), after the runs had been carried out with the 8% glucose (approximately 10 days) and again after the experiments with the 12% glucose had been completed. The dry weights of cell matter found in the beads, based on 100 ml displaced volume were respectively: 0.17 g; 3.76 g; 10.3 g; and 11.4 g. The final value was subsequently used, as indicated above, to determine the total cell mass which was associated with the calcium alginate beads in the reactors.

Run 4: The final run attempted to determine the effect of using a smaller particle size in the best of the reactors for the fermentation reaction. Two short tapered-bed reactors (TAP 1) were used. One was loaded with the encapsulated yeast beads and the other was loaded with the macroporous ion-exchange resin. The resin-containing reactor was initially loaded with approximately 2 g (dry weight) of freshly grown yeast cells. The other reactor was packed with 400 ml (displaced volume) of incubated yeast-containing beads (average diameter of 2.7 mm). In order to encourage cell growth, both reactors were operated for 24 hours on 5% sterile glucose medium at a dilution rate of 0.3 h^{-1} and subsequently for a further 16 hours at the same flow rate on 8% glucose medium. The reactors were then operated on 8% sterile glucose medium at various dilution rates until a steady-state had been reached. As had been done previously, the dynamic responses for the reactors were constantly monitored using the carbon dioxide production rate data. An example of the dynamic response is presented as Figure 47. As can be seen, steady-state conditions are approximated after 16 hours of operation.

The steady-state conditions in the two reactors after overnight operation at a given dilution rate are presented in Table 15 and 16. The pressure drop in the reactor packed with ion-exchange resin was greater than in the reactor containing the calcium alginate beads. Neither reactor,however, developed a pressure drop during the course of the run, comparable to those previously obtained with the other reactors.

An unexpected result obtained was that a significantly greater mass of yeast cells were being constantly swept from the resin filled reactor during the course of the run. We had expected that the ion exchange resin would act not only as an immobilizing agent, but would also act as a much more efficient filtering device for the free cells in the reactor. When the reactors were disassembled at the end of the run, it was found that the resin-packed reactor contained 10 g (dry weight) of free yeast cells and the alginate-packed reactor contained 5.5 g. On the other hand, the resin reactor was found to contain 20 g of immobilized yeast cells and the alginate reactor 56 g.

In view of these results, the substantially higher productivities obtained with the alginate system as given in Table 16 are not surprising. At dilution rates of greater than 0.5 h^{-1}, the alginate-packed reactor had productivities twice those of the resin-packed reactors. At lower dilution rates, the differences, as expected, were not as great. Figure 48 shows the differences in reactor capacities more dramatically. Here the amount of substrate utilized as a function of dilution rate is plotted.

Additional longer term continuous runs with these two immobilization procedures should be carried out in order to determine whether these methods of immobilization have inherent problems with respect to long term stability.

Reactor Residence Time Distributions: In order to obtain data about the residence time distributions within each of the reactors, a series of tracer studies were carried out using a standard 8% glucose culture medium containing 5% isopropanol. This solution was passed through the reactors each of which had been packed with active yeast-containing calcium alginate beads. Fractions (approximately 15 ml) of the effluent were collected and analyzed using the gas chromatograph.

Initial studies were carried out with the two tapered-bed reactors used in Run 4 containing the ion-exchange resin and the calcium alginate beads. Subsequently, the beads were removed from the reactor and packed into a new reactor. This repacked system was then operated continuously for approximately 18 hours on the 8% glucose medium. At this time, the analyses of the effluent showed that a pseudo steady-state had been reached (based on a 3 hour average of carbon dioxide production rate, effluent glucose and ethanol and dry cell weight). These results are presented in Table 17.

The results obtained for the effect of a step input to the reactors tested are presented in Figures 49 to 53. The concentration of isopropanol detected relative to the inlet isopropanol concentration is plotted as a function of the volume of medium passed through the reactor. The slopes of these curves, especially when compared to the results obtained with the inert reactor (Figure 18a), indicate that axial dispersion of the fluid occurs within the reactors during the fermentation.

CONCLUSIONS

The data reported here suggest definite operational advantages in using packed-bed variable-area reactors for catalytic processes such as the enzymatic hydrolysis of cellobiose to glucose and the subsequent fermentation of glucose to alcohol.

The data obtained from a theoretical analysis of fluid flow through a packed-bed indicated that the radial-flow reactor was less susceptible to large pressure drops than were either the tubular or the tapered-bed reactors. Flow experiments using these reactors confirmed these findings.

The radial-flow reactor, on the other hand, was found to be less suitable for use with loosely-packed catalyst particles. Tracer analyses showed that settling of the particles resulted in a substantial fraction of the bed being by-passed. This was less severe when the bed was firmly packed or when, as in the case during the fermentation process, the beads increased in size as a result of growth of the yeast within them.

During the course of the enzymatic hydrolysis experiments, it was found that even low cellobiose concentrations resulted in substantial deactivation of the immobilized enzymes. Modelling of the results obtained showed that there was an excellent fit of the data with a model based on substrate inhibition. The kinetic parameters obtained from a non-linear least squares fit of the data to this model agree with those previously reported for this enzyme. No kinetic advantage resulted from using the variable-surface reactors, nor was any operational advantage found to be achieved for this enzymatic process. If such an enzyme system were to be coupled with a fermentation reactor, with recycle, it would be advantageous to go to a non-uniform reactor cross-section, as carry-over of carbon dioxide would occur.

The use of calcium alginate beads for the enzymatic reaction proved to be very effective. The reactors could be operated under non-sterile conditions for long periods of time and little deterioration of the beads occurred.

During the course of the fermentation reaction, there were definite operational advantages in the use of the variable-surface area reactors. Use of the radial-flow reactor resulted in the lowest pressure drops at all levels of operation. The tubular reactor proved to be ineffective, because carbon dioxide produced within the beads caused flotation and subsequent compaction of

the bed. Extremely high pressure drops were obtained in this reactor. The use of the tapered-bed reactor combined the advantages of the tubular and radial-flow reactor (upflow and variable-surface area). Of the two reactors tested, the shorter tapered reactor presented the least difficulties during operation. No compaction of the reactor bed was observed and the pressure drops across the reactor were very low.

Definite problems were encountered with the calcium alginate beads used in the fermentation reactors. Bed compaction resulted in bead deformation and subsequently bead disintegration in all but the shorter of the tapered-bed reactors. It has been recommended that this reactor be used in a longer-term continuous process with both the alginate beads and with an ion-exchange resin which is less deformable. The results of these studies will be appended to the final report.

A reactor design which combines the advantages of all three reactors would be desireable. A suggested design is a wedge-shaped reactor, in which the end surfaces are flat and in a pie-shape. Such a reactor would have the same advantage as the radial-flow reactor insofar as the change in surface area is concerned and could be operated in an upflow mode. Additionally, such a reactor could be easily scaled-up.

The use of a minicomputer based data acquisition system for the determination of the continuous performance of the fermentation reactor and for limited control of the process proved to be quite valuable. Such a system could also be used for on-line sample acquisition and subsequent analysis. In this work it was found that this system not only saved countless hours of needless analytical time, but also produced a permanent record of the data which was being constantly obtained. It is highly recommended that further development of such systems be carried out.

RECOMMENDATIONS

1. Although no major problems were encountered with the use of the tubular reactor with the enzymatic hydrolysis, theoretical calculations show that this type of reactor is much more susceptible to large pressure drops than are the variable-surface area reactors. It is therefore recommended that their use be discouraged because of their limited applicability.

2. The use of calcium alginate for the immobilization of cell-associated enzymatic activity seems to be very effective. Additional studies should be carried out to determine the overall and intrinsic kinetics of the β-glucosidase enzyme immobilized in this fashion. Such studies should include as parameters, the enzyme concentration, the calcium alginate bead size, the substrate concentration and should be carried out in batch, differential stirred-tank and integral reactors.

3. As the soluble β-glucosidase enzyme is much less stable than the cell-associated activity, additional studies involving the screening of fungi known to have high activities should be carried out.

4. Studies should be initiated on a coupled cellulose hydrolysis and cellobiose hydrolysis reactor system as well as a cellobiose/fermentation reactor system. This latter system will be essential in order to remove as quickly as possible the inhibiting glucose from the cellobiose reactor.

5. Kinetic studies should be carried out with various solvent producing organisms in order that basic design parameters might be determined. Again, as in the case of the enzymatic hydrolysis, such studies should involve a wide range of substrate concentrations and reactor types.

6. Additional work should be carried out with the design and operation of scaled-up variable surface reactors. A modification to those designs which have been tested in this study would be the use of a pie or wedge-shaped reactor which combines the operational advantages of all the reactors tested.

7. Additional work whould be carried out on the development of a cost-effective on-line data acquisition and control system for the testing of packed-bed immobilized enzyme/cell reactors.

TABLES

TABLE 1: Description and designation of reactors

Reactor Type/ Designation	Height (cm)	Diameter (cm)	
		Inlet(D1)	Exit(D2)
Tubular			
TUB 1	49.3	5.1	5.1
TUB 2	87.7	3.8	3.8
Tapered-Bed			
TAP 1	16.0	1.9	15.0
TAP 2	45.0	1.3	7.6
Radial-Flow			
RAD 1	8.2	1.3	12.7
RAD 2	24.7	1.3	7.6

TABLE 2: Effect of the needle size on gravity-formed calcium alginate beads

Calcium Alginate Bead Parameter	Needle Diameter (mm)			
	1.024	0.813	0.643	0.404
Diameter Measured (mm)[1] Calculated (mm)[2]	3.15 2.97	2.92 2.61	2.55 2.44	1.91 1.96
Ratio	1.52	1.33	1.24	1.00
Surface Area (cm^2)	0.312	0.268	0.205	0.114
Ratio	2.74	2.35	1.80	1.00
Volume ($cm^3 x 10^{+3}$)	16.39	13.07	8.70	3.63
Ratio	4.52	3.60	2.40	1.00
Bead Displacement (no./ml)	61	77	115	276
Void Volume[3] (ml liquid/ml bed)	0.38	0.33	N/A	0.34

NOTES:

[1] Diameters were measured using calipers (average of 100)
[2] Values were calculated based on 100 ml of displaced liquid volume
[3] Void volume was that which was determined from the free liquid which was removed from a volume of wet-packed beads.

TABLE 3: Pressure Drops observed in packed-bed reactors using different sizes of packing

Reactor and Type of Packing*	Maximum Flow Rate (liters/hour)	Pressure Drop (kPa)
TUB 1		
ION	5.0	1.3
Small	6.1	0.1
Medium	6.1	2.3
Large	6.1	0
TUB 2		
ION	5.0	4.9
Small	5.9	2.0
Medium	N/A	N/A
Large	5.9	3.0
TAP 1		
ION	N/A	N/A
Small	6.1	0
Medium	6.1	0
Large	6.1	3.0
TAP 2		
ION	5.0	1.2
Small	6.1	0.4
Medium	6.1	0
Large	6.1	6.0
RAD 1		
ALL	6.0	0
RAD 2		
ALL	6.0	0

* ION -- Ion-Exchange Resin
Small -- Calcium Alginate Beads Formed from 0.813 mm Needle
Medium -- Calcium Alginate Beads Formed from 1.024 mm Needle
Large -- Calcium Alginate Beads Formed from 2.0 mm Orifice

TABLE 4: Steady-state glucose concentrations and conversions as a function of dilution rates for enzymatic hydrolysis of cellobiose and salicin (Run 1)

S_0 (mM)	Reactor								
	TUB 1			TAP 1			RAD 1		
	D (h^{-1})	(mg/ml)	% Conv	D (h^{-1})	(mg/ml)	% Conv	D (h^{-1})	(mg/ml)	% Conv
10 Cell	0.18	2.1	58.3	0.18	1.7	47.2	0.18	1.5	41.7
	0.26	2.0	55.5	0.28	1.5	41.7	0.28	1.4	38.9
	0.42	1.1	30.5	0.42	1.0	27.8	0.35	0.94	26.1
	1.04	0.32	8.9	0.81	0.44	12.2	0.95	0.33	9.2
10 Sal	0.3	1.35	75.0	----	---	---	----	---	--
20 Sal	0.3	1.2	33.4	----	---	---	----	---	--

TABLE 5: Steady-state glucose concentrations and conversions as a function of dilution rates for enzymatic hydrolysis of cellobiose and salicin (Run 1)

S_o (mM)	Reactor								
	TUB 2			TAP 2			RAD 1		
	D (h^{-1})	(mg/ml)	% Conv	D (h^{-1})	(mg/ml)	% Conv	D (h^{-1})	(mg/ml)	% Conv
5	0.29	1.8	100	0.30	1.8	100	0.41	1.0	57
	0.62	1.8	100	0.60	1.8	100	0.60	1.0	57
	0.88	1.6	89	0.84	1.6	89	0.94	0.84	46
	1.9	1.0	57	1.9	0.92	51	2.0	0.44	24
	3.5	0.6	32	3.5	0.55	31	3.5	0.26	14
7.5	0.27	2.7	100	0.32	2.7	100	0.31	1.8	65
	0.56	2.6	97	0.6	2.5	94	0.6	1.4	51
	0.88	2.3	85	0.97	2.0	74	0.92	1.4	52
	1.47	1.5	54	1.56	1.4	53	1.56	0.75	28
	2.4	0.9	33	2.52	0.9	33	----	----	--
10	0.22	3.6	100	0.23	3.6	100	0.23	2.9	80
	0.32	3.6	100	0.34	3.6	100	0.35	2.0	57
	0.6	2.7	75	0.64	2.7	75	0.68	2.1	58
	1.2	1.8	49	1.26	1.7	47	1.26	1.1	32
	2.0	1.0	28	2.07	0.83	23	2.02	0.56	15
15	0.30	4.4	81	0.32	3.8	70	0.32	3.8	70
20	0.054	7.2	100	0.096	7.2	100	0.36	2.4	33
	0.32	5.0	70	0.37	4.7	65	----	---	--
	0.57	3.5	48	0.66	3.4	47	----	---	--
	1.2	1.6	22	1.23	1.3	18	----	---	--
30	0.27	6.0	56	0.3	5.6	52	0.3	3.5	32

TABLE 6: Serial batch growth of yeast using decreasing levels of salts in the culture medium

Batch Number, Incubation Time and Parameter*	% of Standard Salts					
	100	80	60	40	20	0
1 -- 48 h						
Ethanol	1.40	1.43	1.80	1.60	1.22	0.90
Glucose	11.8	20.8	14.7	21.1	35.8	55.0
Cell Dry Weight	0.96	0.96	1.38	1.18	1.02	1.32
2 -- 48 h						
Ethanol	2.23	2.00	1.87	1.61	1.24	1.01
Glucose	4.5	44.2	37.1	56.3	61.4	74.2
Cell Dry Weight	1.66	1.04	1.17	1.07	1.25	1.11
3 -- 72 h						
Ethanol	2.51	3.20	2.75	2.47	1.29	1.95
Glucose	0.2	1.0	4.0	8.3	30.7	66.6
Cell Dry Weight	1.14	1.31	1.46	1.18	1.33	1.0
4 -- 48 h						
Ethanol	2.04	1.49	1.37	1.28	0.92	1.06
Glucose	8.0	51.2	53.8	92.2	105	105
Cell Dry Weight	1.40	0.89	0.99	0.78	0.92	0.86
5 -- 72 h						
Ethanol	3.31	2.54	2.24	1.70	1.89	0
Glucose	0.8	2.0	8.0	27.8	33.3	36.5
Cell Dry Weight	1.16	1.03	1.29	1.11	1.42	0.93

* Measurements made after indicated incubation period:
Ethanol (%)
Residual Glucose (mg/ml) from original 100 mg/ml medium
Cell Dry Weight (mg/ml)

TABLE 7: Serial batch growth of yeast using decreasing levels of yeast extract in the culture medium

Batch Number, Incubation Time and Parameter*	Yeast Extract Concentration (g/L)					
	1.0	0.8	0.6	0.4	0.2	0
1 -- 48 h						
Ethanol	1.80	1.54	1.29	1.10	0.80	0.33
Glucose	28.2	51.2	91.5	64.0	74.2	100
Cell Dry Weight	1.26	1.11	1.03	0.91	1.22	0.81
2 -- 72 h						
Ethanol	3.34	3.42	3.08	2.40	1.72	0
Glucose	0.82	8.6	25.6	63.4	46.1	N/D
Cell Dry Weight	0.65	1.01	0.90	0.86	0.85	N/D
3 -- 48 h						
Ethanol	1.68	1.92	1.09	0.99	0.67	N/D
Glucose	22.4	52.5	69.1	71.7	100	N/D
Cell Dry Weight	1.06	1.15	1.19	1.22	1.12	N/D
4 -- 48 h						
Ethanol	1.56	1.40	1.65	1.19	0.85	N/D
Glucose	48.0	85.8	69.1	79.4	105	N/D
Cell Dry Weight	1.18	1.12	1.02	0.97	1.06	N/D

* Measurements made after indicated incubation period:
Ethanol (%)
Residual Glucose (mg/ml) from original 100 mg/ml medium
Cell Dry Weight (mg/ml)

TABLE 8: Operational parameters and results obtained for fermentation reaction using reactor TUB 1

Glucose (%)	Dilution (h^{-1})	Maximum Ethanol (%)	Residual Glucose (mg/ml)	Gas Rate (L/h)	Pressure Drop (kPa)	Productivity [3] (g EtOH/L/h)
5	0.9	2.05	0.06	11	12.6	18.5
	1.5	1.1	1.2	12	28	16.5
	2.1	1.1	N/D	15	41	23.1
	2.7 [1]	0.95	2.35	19	80	25.7
2	0.9	0.7	0	5	17	6.3
	2.1 [2]	0.2	0.8	6	10	4.2
	2.7	0.4	0.1	10	165	10.8
1	0.95 [2]	0.25	0.03	2.6	10.7	2.4
	2.5 [2]	0.25	0.2	5.5	7	6.2
5	0.8 [2]	1.6	0.4	8	7	12.6

[1] Manometer removed and replaced by pressure gauge
[2] Reactor turned 30° to the horizontal
[3] Productivities based on reactor volume (1 litre)

TABLE 9: Operational parameters and results obtained for fermentation reaction using reactor TAP 2

Glucose (%)	Dilution (h^{-1})	Maximum Ethanol (%)	Residual Glucose (mg/ml)	Gas Rate (L/h)	Pressure Drop (kPa)	Productivity [2] (g EtOH/L/h)
5	0.9	2.1	0.06	11	12.6	18.5
	1.5	1.5	0.7	12	21	22.5
	2.1	1.6	N/D	19	14	33.6
	2.7 [1]	1.3	0.75	19	27	35.1
2	0.9	0.7	0	2	10	6.3
	1.5	0.3	0.1	5	7	4.5
	2.1	0.4	0.5	6	0	8.4
	2.7	0.7	0	10	7	19.9
1	0.95	0.35	0.01	0.7	0	3.3
	2.5	0.25	0.2	4	4	6.2
5	0.8	1.8	0.4	7.5	7	14.4

[1] Manometer removed and replaced by pressure gauge
[2] Productivities based on reactor volume (1 litre)

TABLE 10: Operational parameters and results obtained for fermentation reaction using reactor RAD 1

Glucose (%)	Dilution (h^{-1})	Maximum Ethanol (%)	Residual Glucose (mg/ml)	Gas Rate (L/h)	Pressure Drop (kPa)	Productivity [1] (g EtOH/L/h)
5	0.9	1.95	0.24	8	1.3	17.6
	1.5	1.3	0.7	11	2.7	19.5
	2.1	1.3	N/D	15	6	27.3
	2.7	0.8	2.0	13	2.7	21.6
2	0.9	0.7	0.1	4	2.7	6.3
	1.5	0	0.3	5	5	0
	2.1	0.3	0.9	6	4	6.3
	2.7	0.4	0.1	7	5.3	10.8
1	0.95	0.1	0.3	1.9	2	0.95
	2.5	0	0.7	4	4	0
5	0.8	1.8	0.4	10	5.3	14.4

[1] Productivities based on reactor volume (1 litre)

TABLE 11: Operational parameters and results obtained for fermentation reaction using reactor TAP 1 with 8% and 12% glucose medium

Glucose (%)	Dilution (h^{-1})	Maximum Ethanol (%)	Residual Glucose (mg/ml)	Gas Rate (L/h)	Pressure Drop (kPa)	Effluent Cell Weight (g/100ml)	Productivity[1] (g EtOH/L/h)
8	0.25	3.88	0.05	5	21	0.06	9.7
	0.56	3.64	0.11	11	17	0.05	20.4
	0.73	3.79	0.55	14	17	0.06	27.7
	1.1	3.18	2.2	19	17	0.06	35.0
12	0.27	5.65	0.1	8	14	0.08	15.2
	0.35	5.62	1.5	9.8	10	0.07	19.7
	0.5	4.74	3.0	12	12	0.07	23.7
	0.76	3.78	5.1	14.3	10	0.07	28.7
8	0.75	3.1	2.8	11	12	0.05	23.2

[1] Productivities based on reactor volume (1 litre)

TABLE 12: Operational parameters and results obtained for fermentation reaction using reactor TAP 2 with 8% and 12% glucose medium

Glucose (%)	Dilution (h^{-1})	Maximum Ethanol (%)	Residual Glucose (mg/ml)	Gas Rate (L/h)	Pressure Drop (kPa)	Effluent Cell Weight (g/100ml)	Productivity[1] (g EtOH/L/h)
8	0.27	3.80	0.05	5.3	24	0.08	10.3
	0.62	3.79	0.09	13	39	0.05	23.5
	0.80	3.98	0.20	16.8	43	0.05	31.8
	1.26	3.23	1.26	21	31	0.06	40.7
12	0.29	5.73	0.1	8.9	19	0.06	16.6
	0.41	5.46	1.35	10.3	12	0.05	22.4
	0.57	4.73	2.76	13	26	0.05	27.0
	0.86	4.03	5.1	16.5	24	0.04	34.7
8	0.86	3.1	2.7	12	16	0.03	26.7

[1] Productivities based on reactor volume (1 litre)

TABLE 13: Operational parameters and results obtained for fermentation reaction using reactor RAD 2 with 8% and 12% glucose medium

Glucose (%)	Dilution (h^{-1})	Maximum Ethanol (%)	Residual Glucose (mg/ml)	Gas Rate (L/h)	Pressure Drop (kPa)	Effluent Cell Weight (g/100ml)	Productivity[1] (g EtOH/L/h)
8	0.22	3.72	0.35	4.5	4.7	0.07	8.2
	0.51	3.10	0.80	8.0	6.7	0.05	15.8
	0.67	3.16	1.60	10.8	6.7	0.05	21.2
	1.02	2.54	2.52	13.5	8.7	0.05	25.9
12	0.24	5.64	1.0	6.5	4.7	0.06	13.5
	0.31	5.20	1.75	7.7	6.7	0.07	16.1
	0.45	5.16	2.8	10	6.7	0.07	23.2
	0.68	4.22	4.7	14	6.7	0.05	28.7
8	0.66	2.84	3.2	7.8	8.0	0.06	18.7

[1] Productivities based on reactor volume (1 litre)

TABLE 14: Comparison of productivities[1] obtained from TAP 1, TAP 2 and RAD 2 based on calculations from ethanol analysis or carbon dioxide rate production data

S_0 (%)	Reactor								
	TAP 1			TAP 2			RAD 2		
	D (h^{-1})	Productivity (g EtOH/L/h)		D (h^{-1})	Productivity (g EtOH/L/h)		D (h^{-1})	Productivity (g EtOH/L/h)	
		EtOH	CO_2		EtOH	CO_2		EtOH	CO_2
8	0.25	9.7	9.5	0.27	10.3	10.7	0.22	8.2	8.6
	0.56	20.4	20.9	0.62	23.5	24.7	0.51	15.8	15.2
	0.73	27.7	26.6	0.80	31.8	31.9	0.67	21.2	20.5
	1.10	35.0	36.1	1.26	40.7	39.9	1.02	25.9	25.7
12	0.27	15.2	15.2	0.29	16.6	17.0	0.24	13.5	12.4
	0.35	19.7	18.6	0.41	22.4	19.6	0.31	16.1	14.6
	0.50	23.7	22.8	0.57	27.0	24.7	0.45	23.2	22.4
	0.76	28.7	27.2	0.86	34.7	31.4	0.68	28.7	26.6

[1] Productivities based on reactor volume (1 litre)

TABLE 15: Operational parameters and results obtained for fermentation reaction using reactor TAP 1 packed with ion-exchange resin and at 8% glucose medium

Dilution Rate (h^{-1})	Maximum Ethanol (%)	Residual Glucose (mg/ml)	Gas Rate (L/h)	Pressure Drop (kPa)	Effluent Cell Weight (g/100ml)	Productivity[1] (g EtOH/L/h)
0.27	3.1	0.7	5.0	10.7	0.11	8.4
0.37	2.6	2.6	5.6	16	0.10	9.6
0.52	1.8	4.7	5.8	12	0.09	9.4
0.84	1.2	5.8	6.4	15	0.09	10.1

[1] Productivities based on reactor volume (1 litre)

TABLE 16: Operational parameters and results obtained for fermentation reaction using reactor TAP 1 packed with calcium alginate beads and at 8% glucose medium

Dilution Rate (h^{-1})	Maximum Ethanol (%)	Residual Glucose (mg/ml)	Gas Rate (L/h)	Pressure Drop (kPa)	Effluent Cell Weight (g/100ml)	Productivity[1] (g EtOH/L/h)
0.19	3.6	0.06	4.3	5	0.05	6.8
0.25	3.6	0.08	5.7	6.7	0.03	9.0
0.36	3.3	0.25	8.0	10.7	0.07	11.9
0.57	3.1	1.0	11.2	10.7	0.03	17.7
0.95	2.1	3.7	13.3	8.0	0.05	20.0

[1] Productivities based on reactor volume (1 litre)

TABLE 17: Operational parameters and data obtained from reactors prior to start of tracer analyses[1]

Reactor	Dilution Rate (h^{-1})	Effluent Ethanol (%)	Effluent Glucose (mg/ml)	Gas Rate (L/h)	Pressure Drop (kPa)	Effluent Cell Weight (g/100ml)
TAP 1 [2]	0.25	3.1	0.7	5.0	10.7	0.08
TAP 1 [3]	0.36	3.3	0.25	8.0	10.7	0.07
TAP 2 [4]	0.45	3.5	0.22	8.0	10.7	0.04
TUB 1 [4]	0.45	3.4	0.15	9.1	18.7	0.067
RAD 1 [5]	0.44	3.0	1.35	8.3	7.3	0.053

NOTES:
1. Tracer studies were carried out in the order shown
2. Contained ion-exchange immobilized cells
3. Contained calcium alginate immobilized cells
4. Bed separation was found to occur
5. Additional inert beads were added to ensure tightly packed reactor (external void volume was 950 ml for RAD 1)

FIGURES

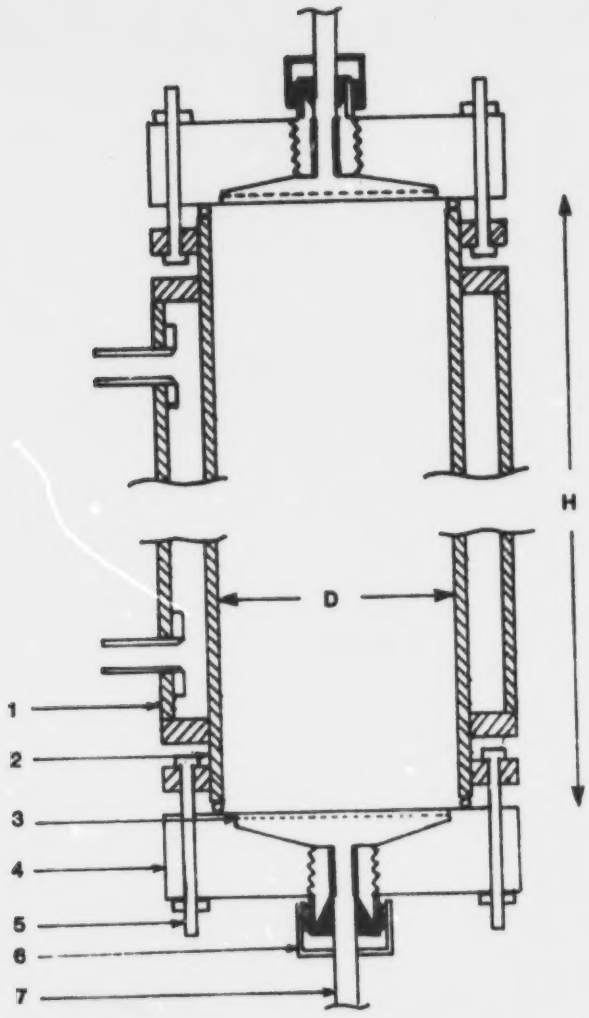

(1) Heat Exchanger

(2) Tubular Reactor

(3) Retaining Screen (Stainless Steel)

(4) Cap (Delrin)

(5) Retaining Bolts (Stainless Steel)

(6) Tubing Connector (Polyethylene)

(7) Tubing (Polyethylene)

FIGURE 1: Schematic diagram of tubular reactor

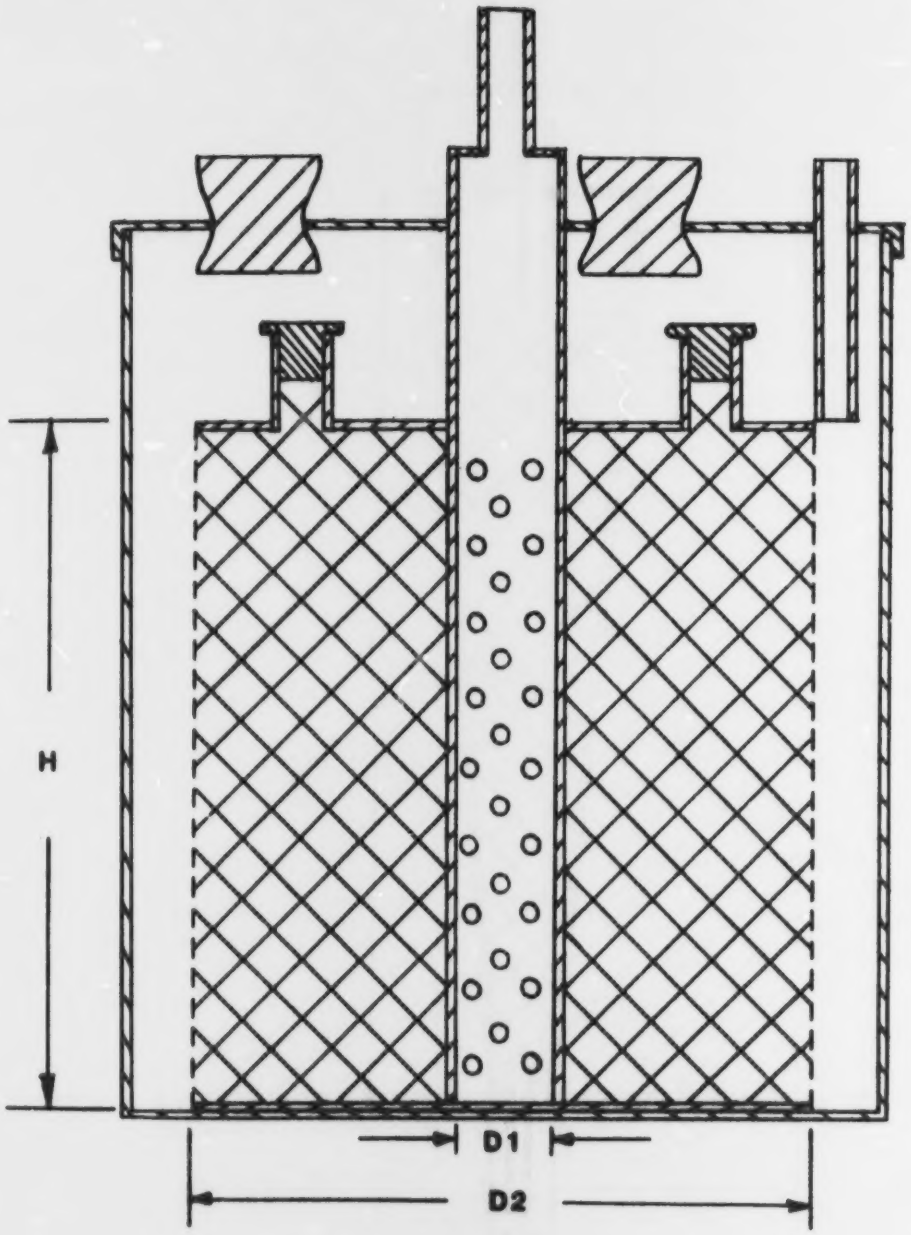

FIGURE 2: Schematic diagram of original radial-flow reactor

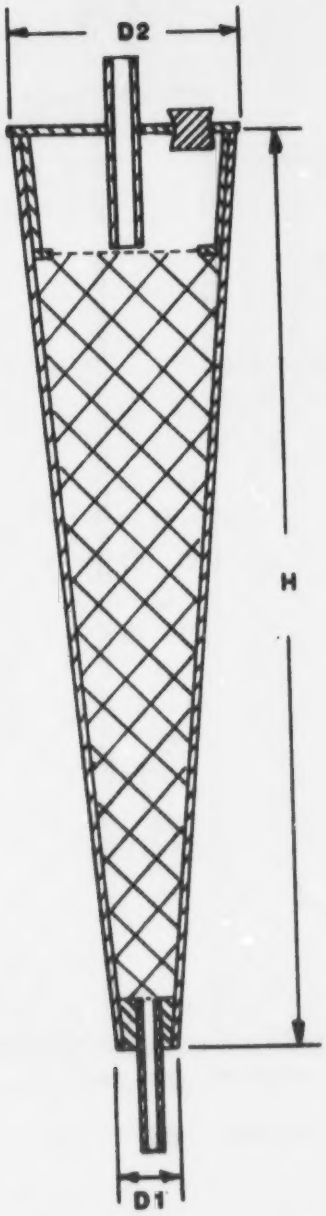

FIGURE 3: Schematic diagram of original tapered-bed reactor

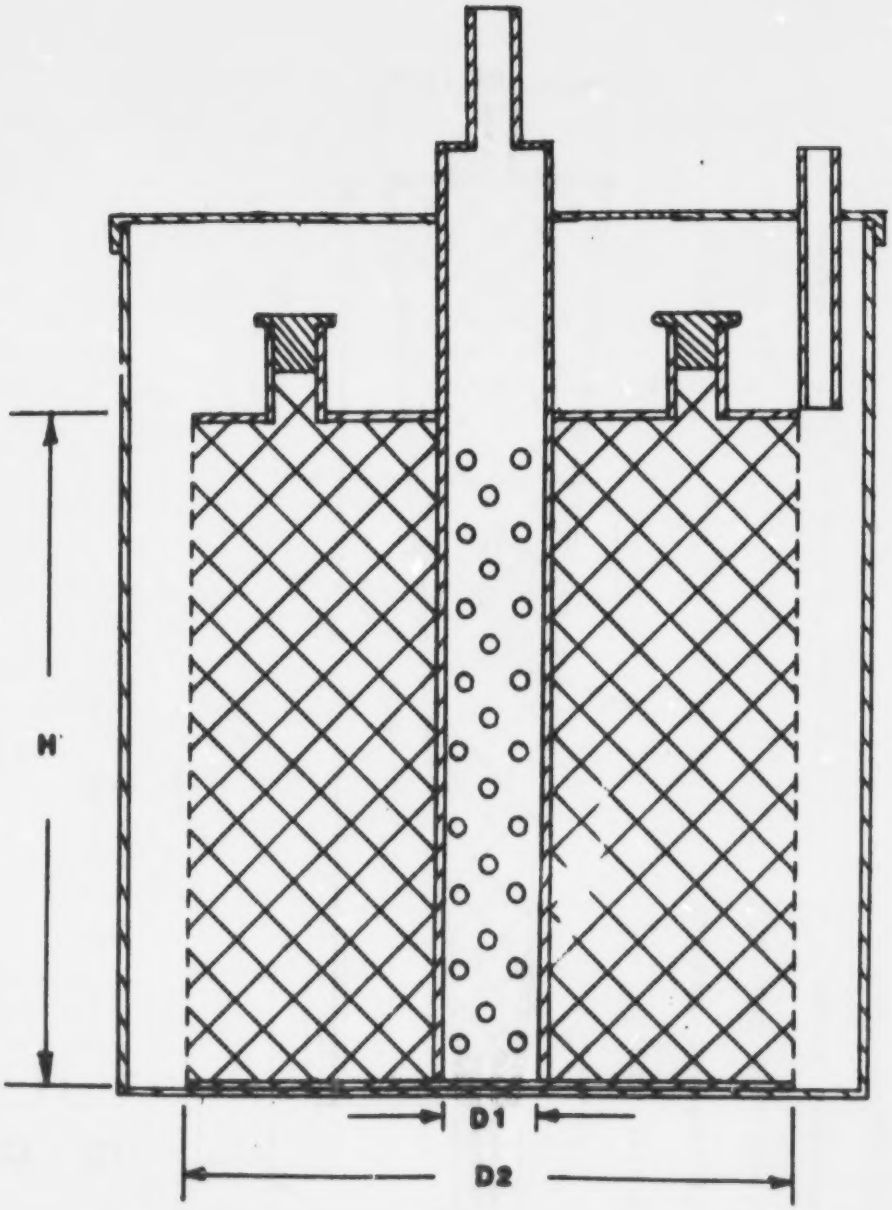

FIGURE 4(a): Schematic diagram of modified radial-flow reactor

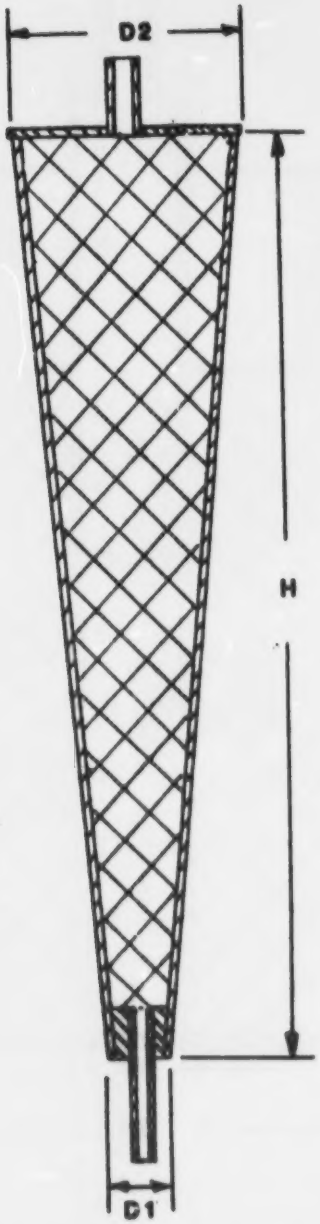

FIGURE 4(b): Schematic diagram of modified tapered-bed reactor

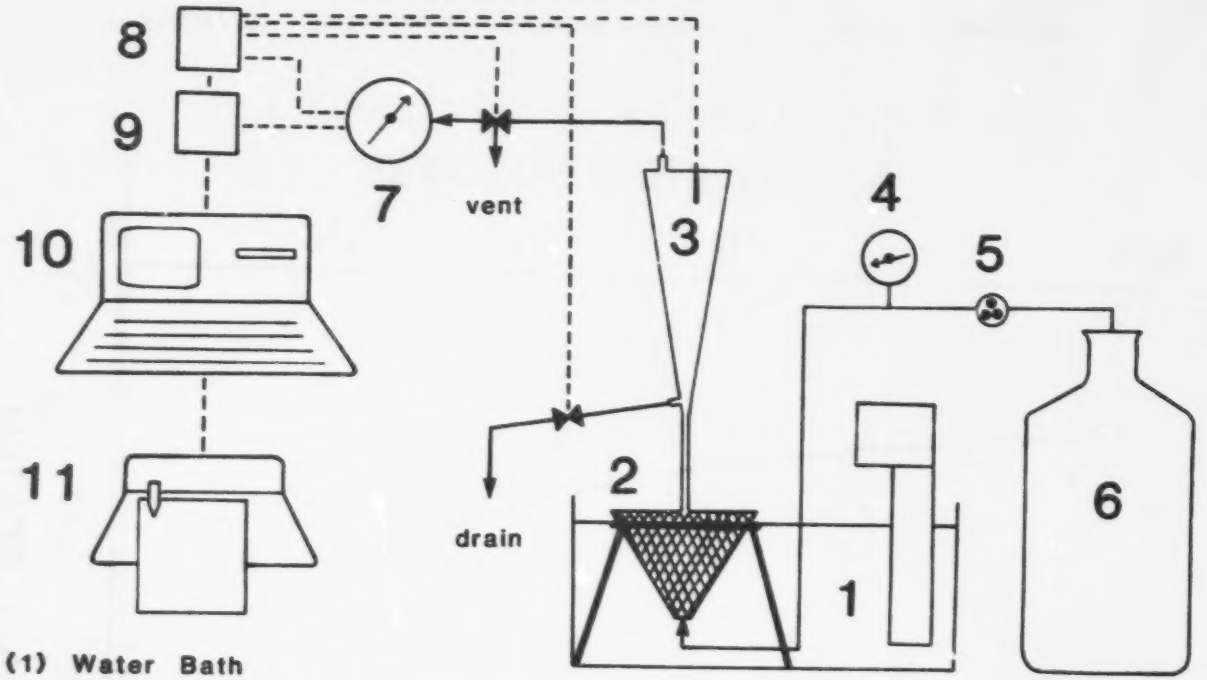

(1) Water Bath

(2) Packed-Bed Reactor

(3) Gas/Liquid Separator

(4) Pressure Gauge

(5) Peristaltic Pump

(6) Nutrient Medium

(7) Gas Meter

(8) Relay Actuator

(9) Digital Voltmeter

(10) HP85 Computer

(11) Printer / Plotter

FIGURE 5: Schematic diagram of reactor evaluation system

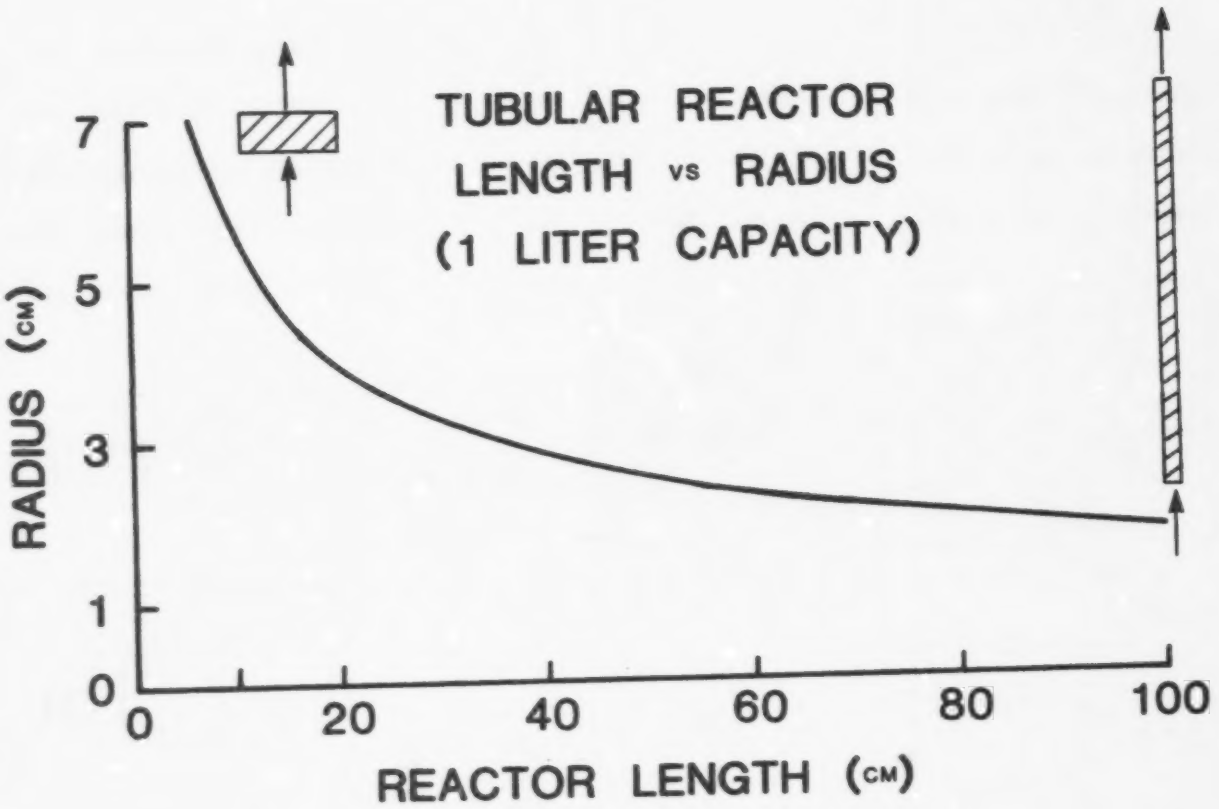

FIGURE 6: Relationship between radius and length of a one liter capacity tubular reactor

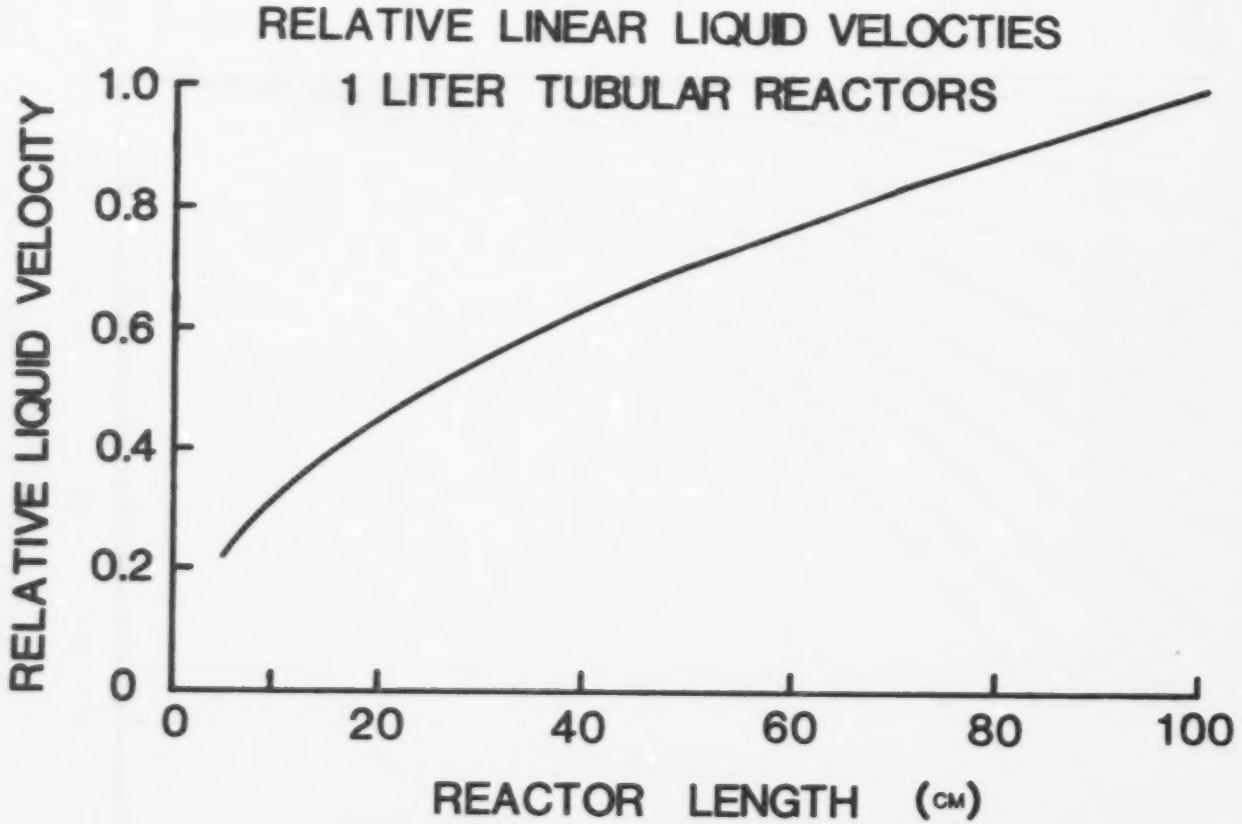

FIGURE 7: Relative linear velocities in various lengths of one liter capacity tubular reactors

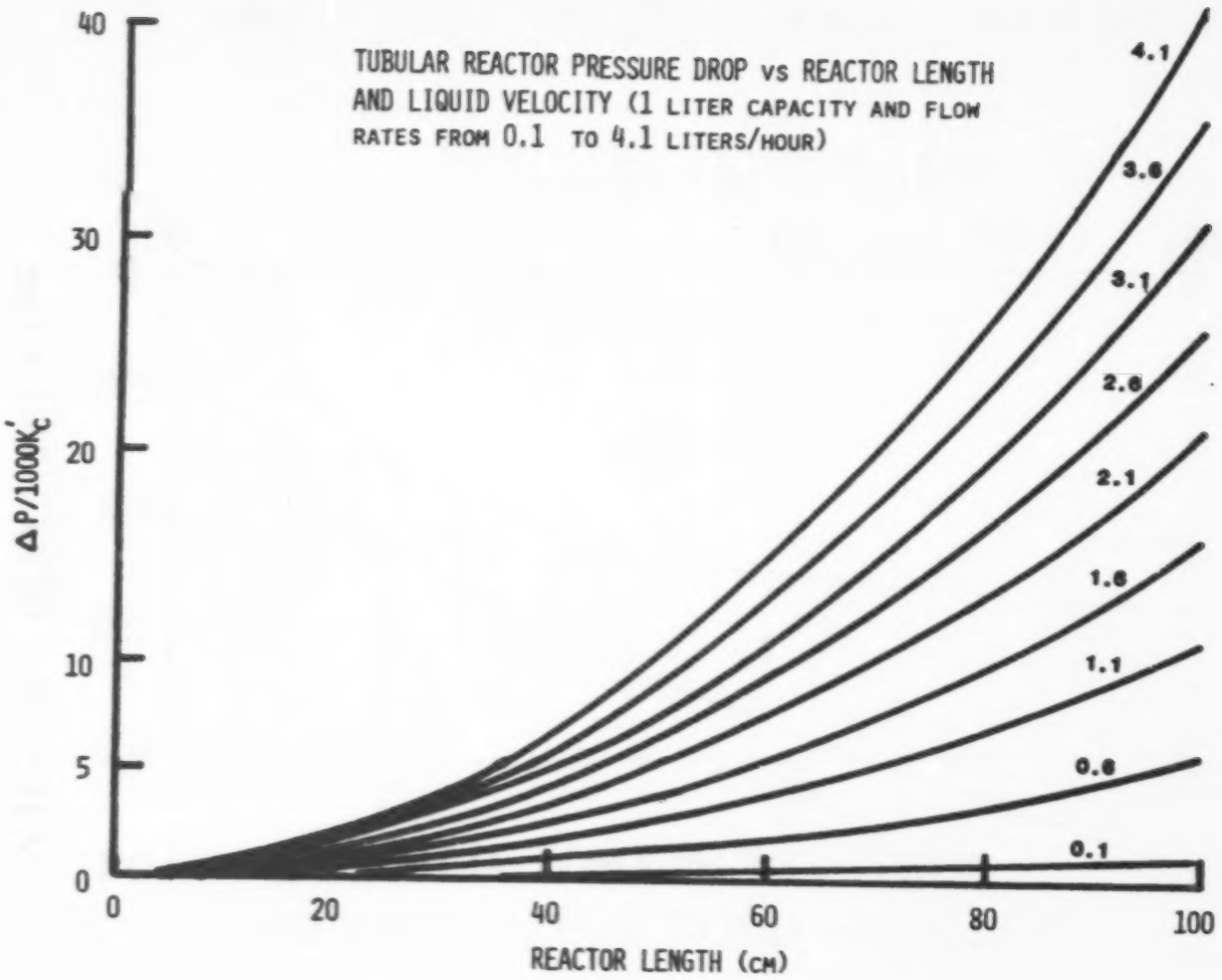

FIGURE 8: Effect of variation in volumetric flow rate on pressure drop in different one liter capacity tubular reactors

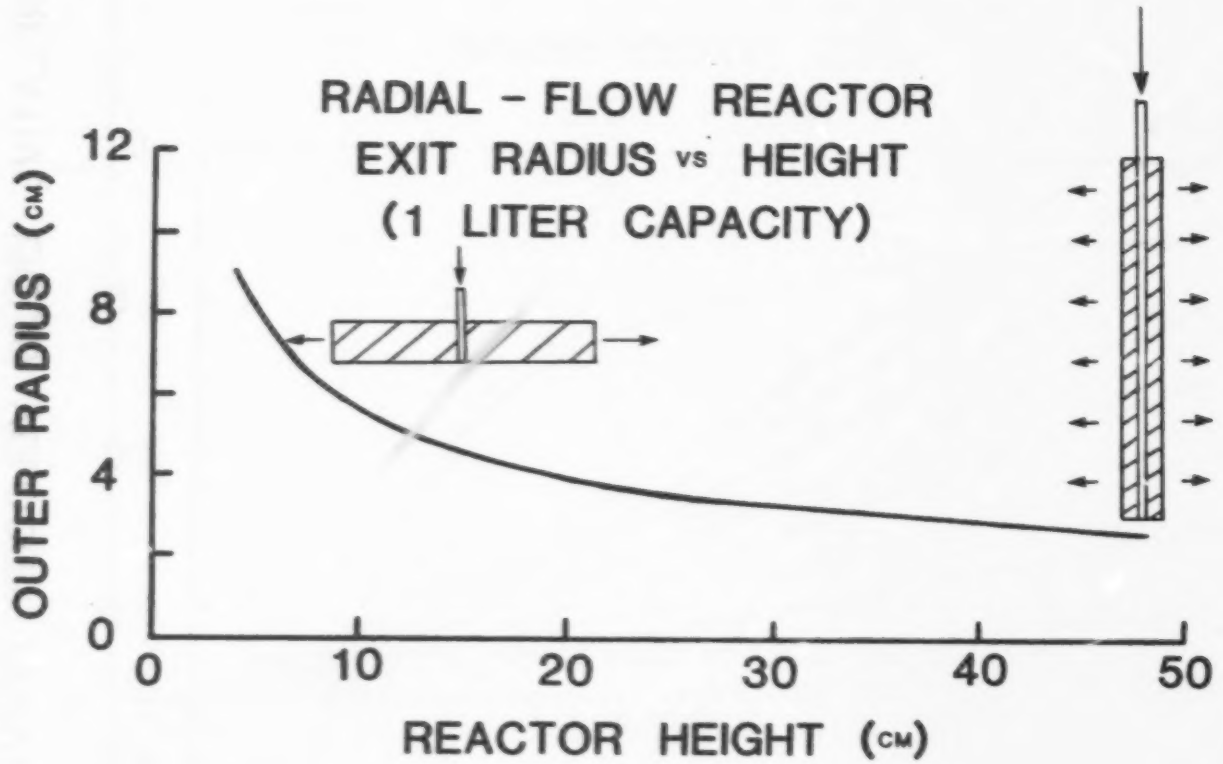

FIGURE 9: Relationship between radius and height for a radial-flow reactor of one liter capacity

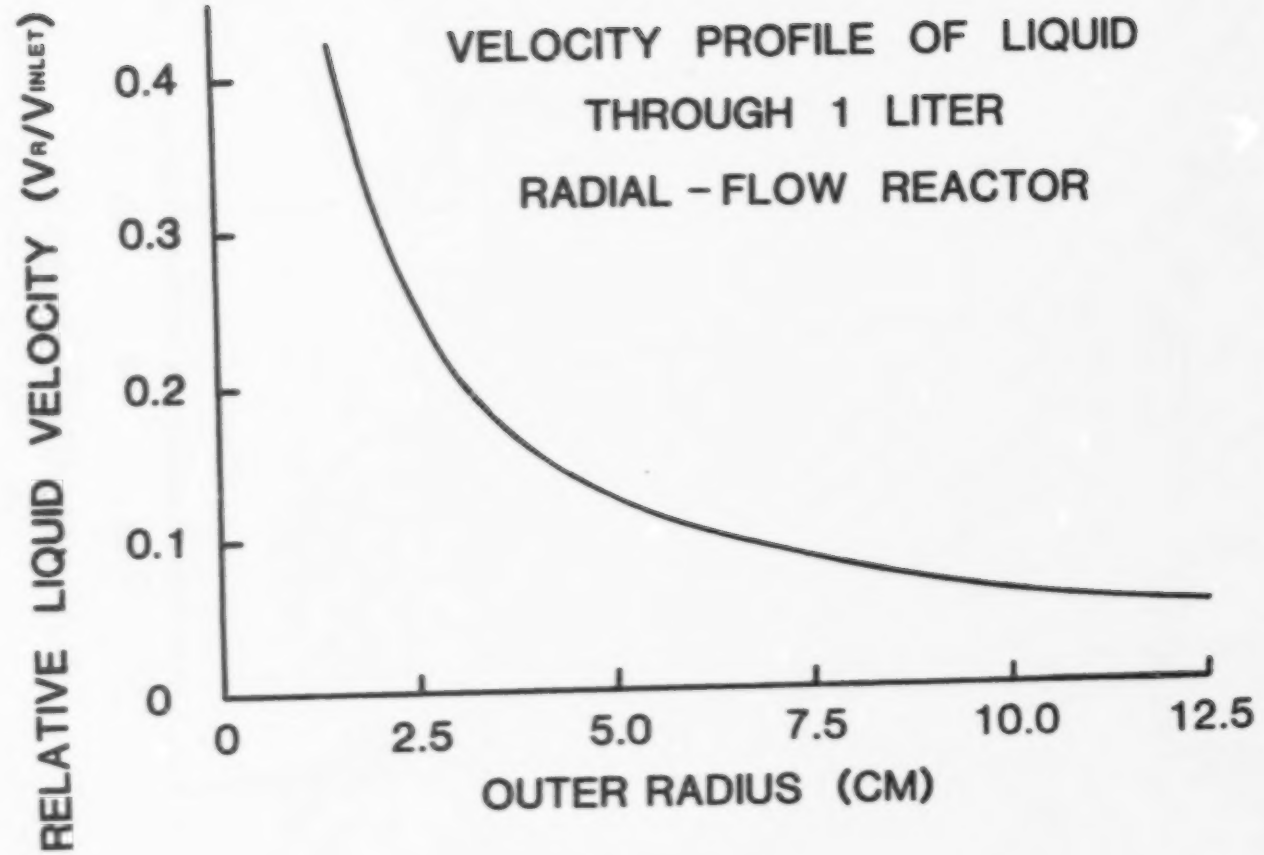

FIGURE 10: Relative linear velocity of fluid passing through a radial-flow reactor

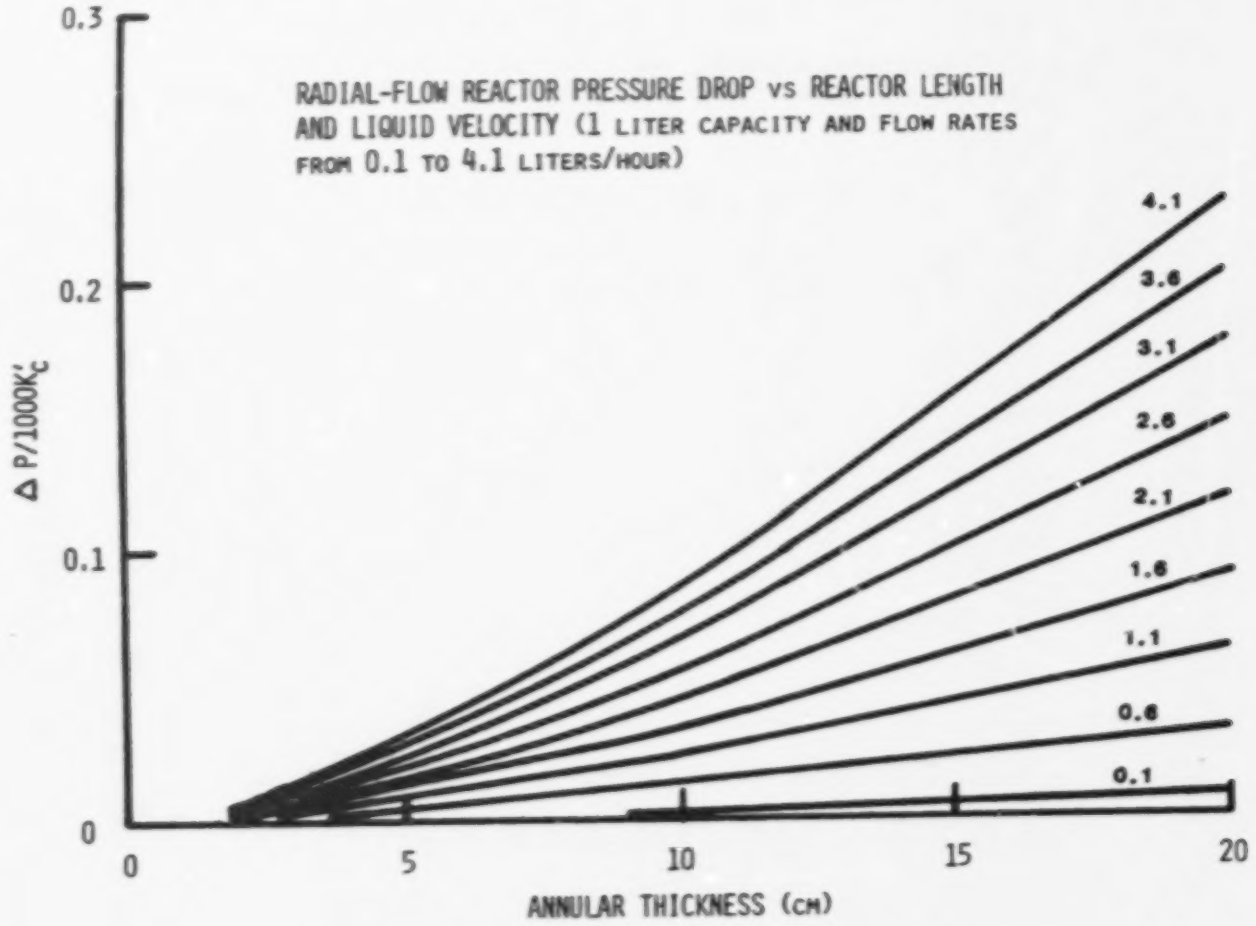

FIGURE 11: Effect of variation in volumetric flow rate on the pressure drop in different one liter capacity radial-flow reactors

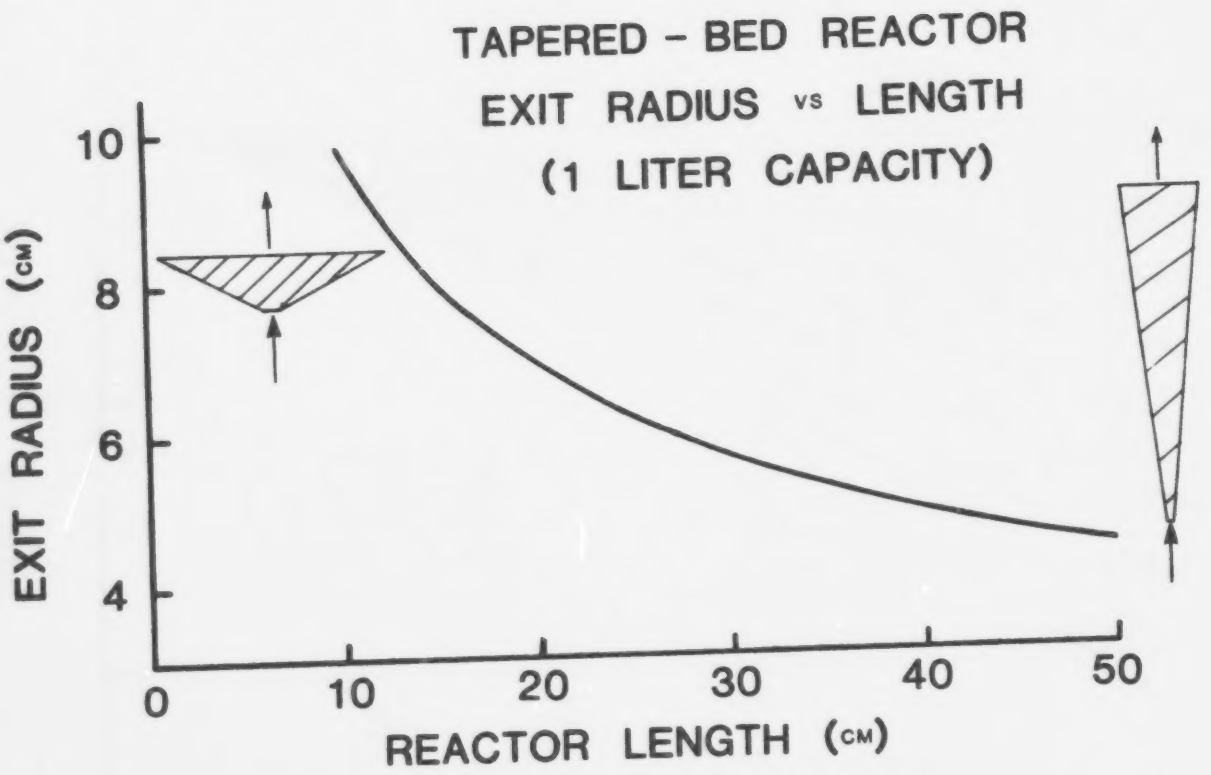

FIGURE 12: Variation in exit radius as a function of reactor length for a one liter capacity tapered-bed reactor

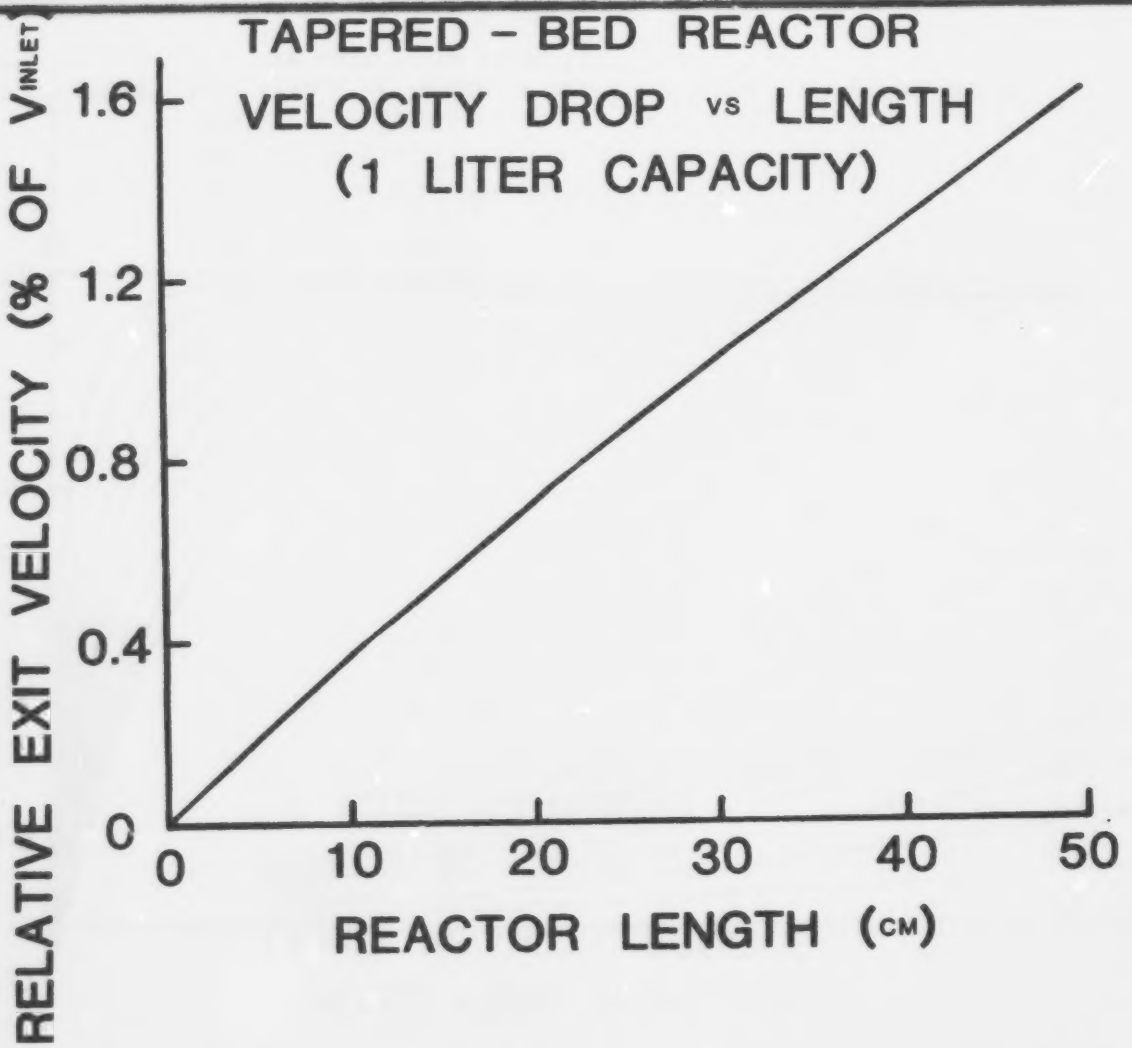

FIGURE 13: Relative linear velocities of fluid passing through various lengths of one liter capacity tapered-bed reactors

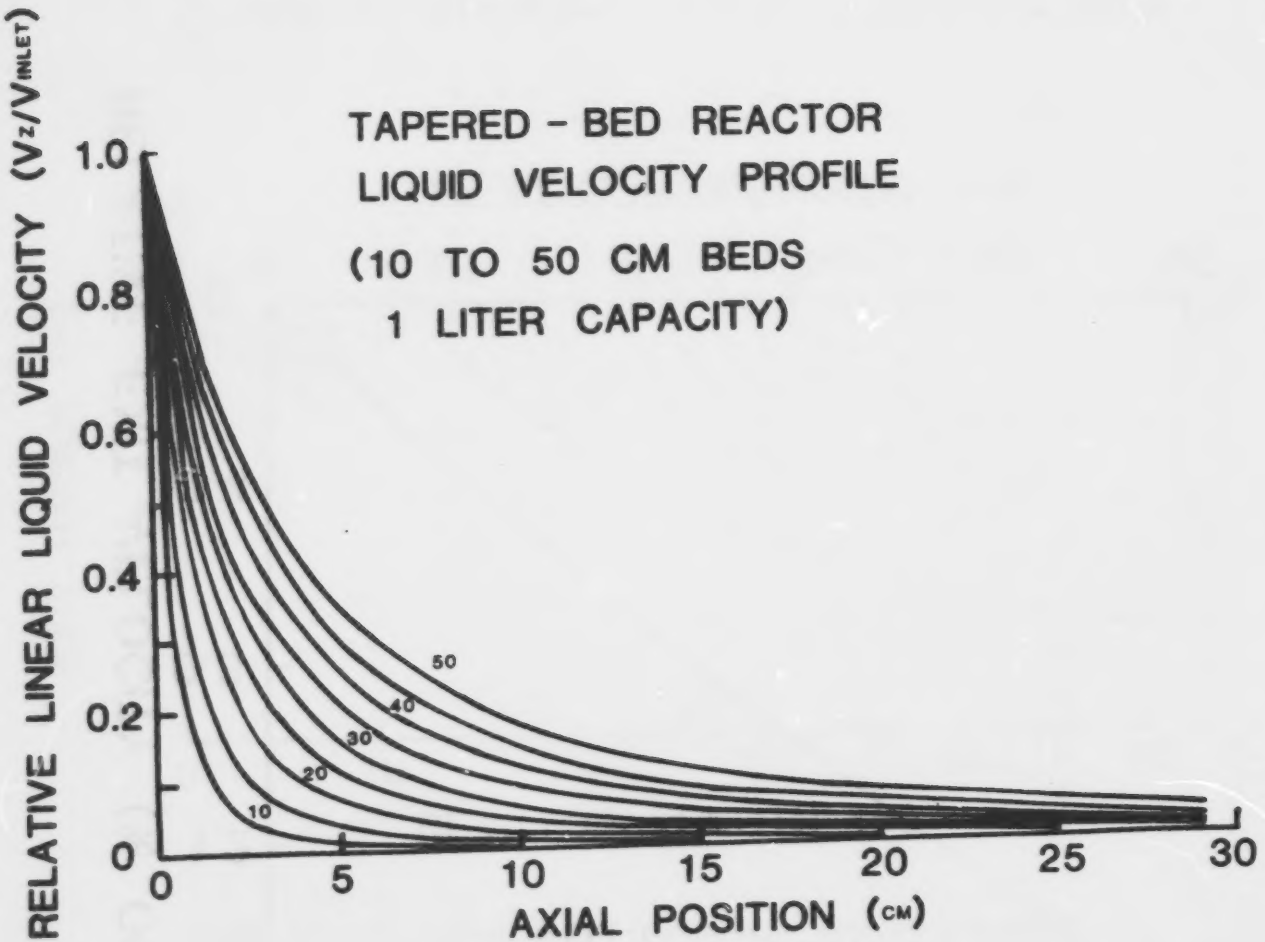

FIGURE 14: Effect of length of one liter capacity tapered-bed on the exit fluid velocity

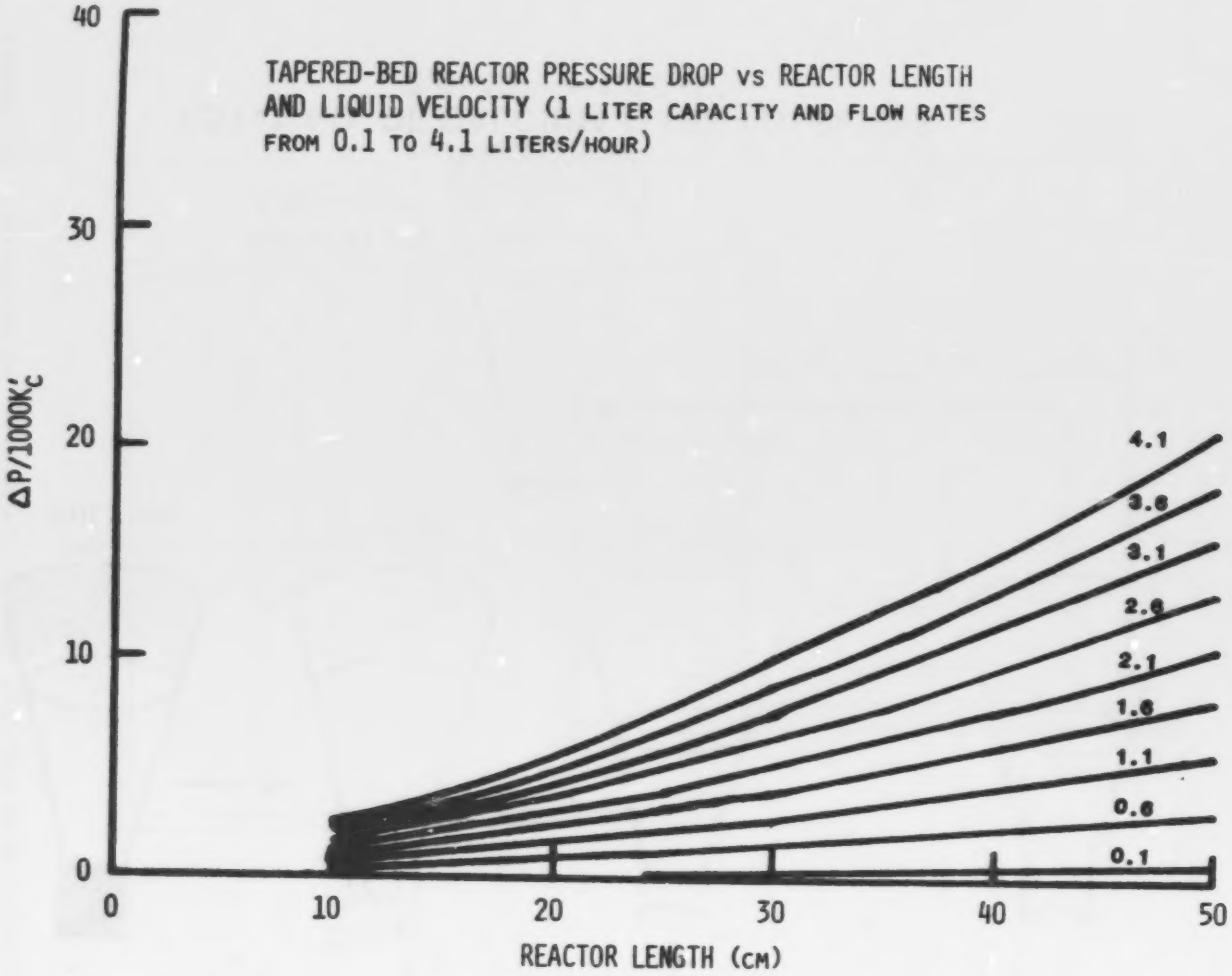

FIGURE 15: Effect of variation in volumetric flow rate on the pressure drop in different one liter capacity tapered-bed reactors

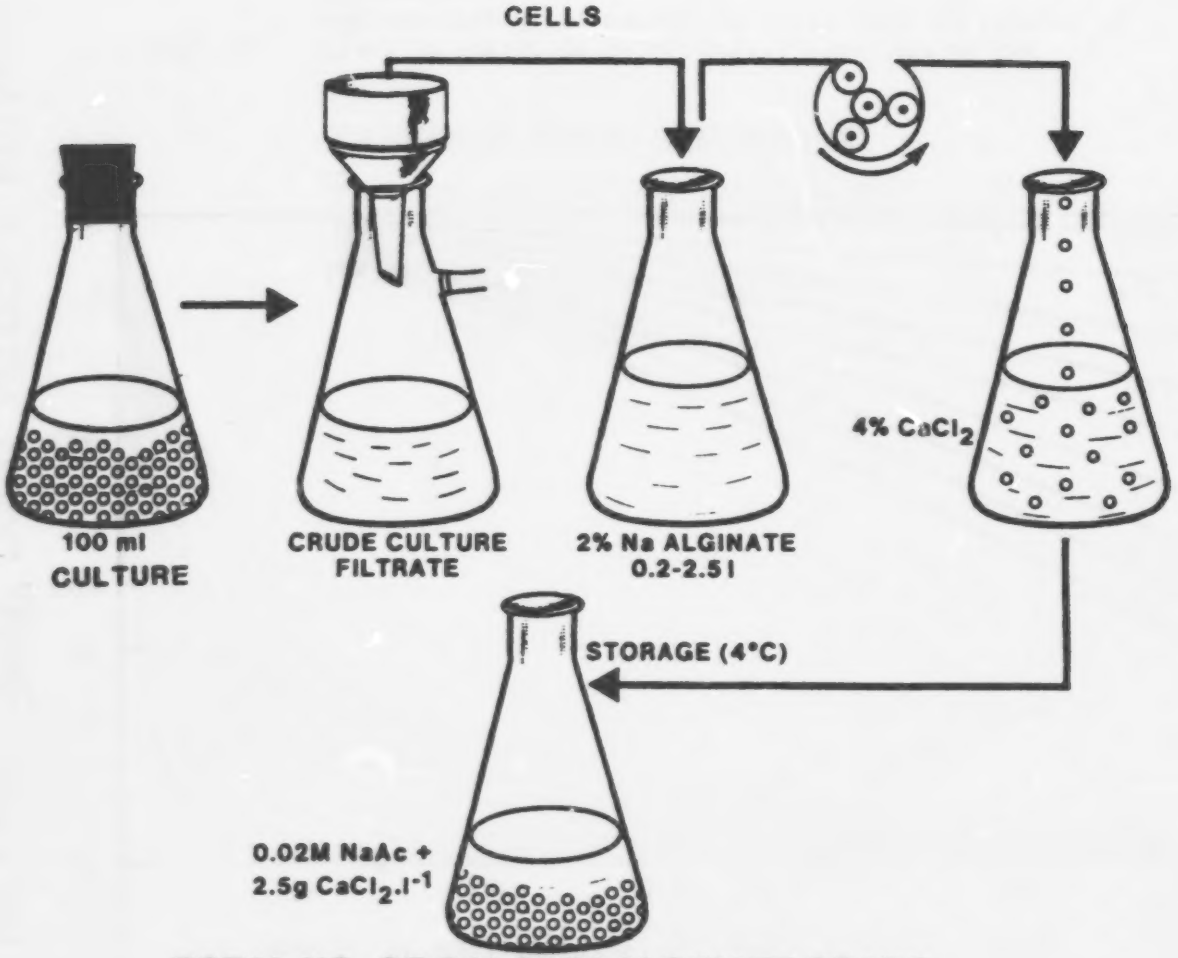

FIGURE 16: General procedure for the preparation of calcium alginate encapsulated cells

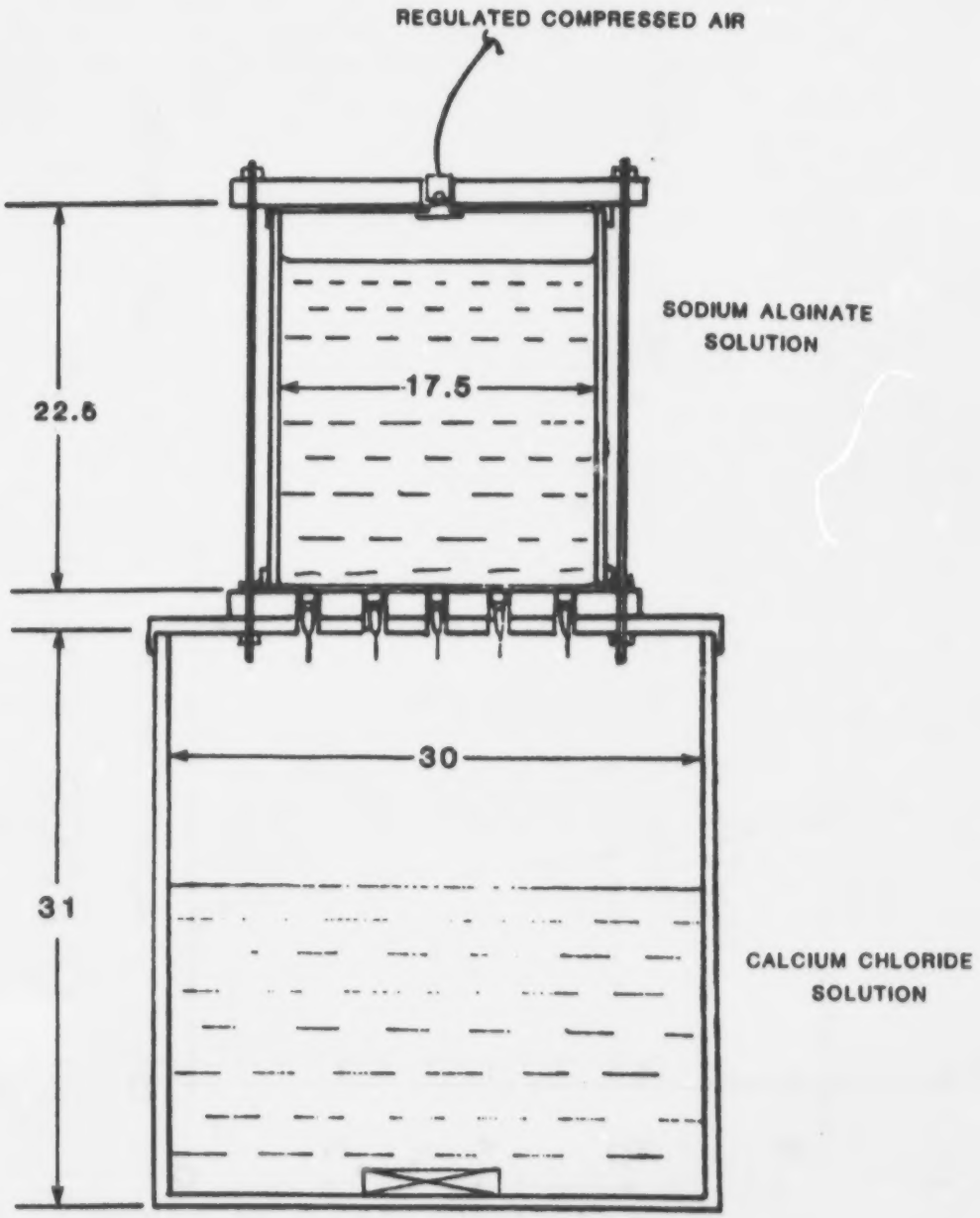

FIGURE 17: Pressurized large-scale calcium alginate bead-forming device

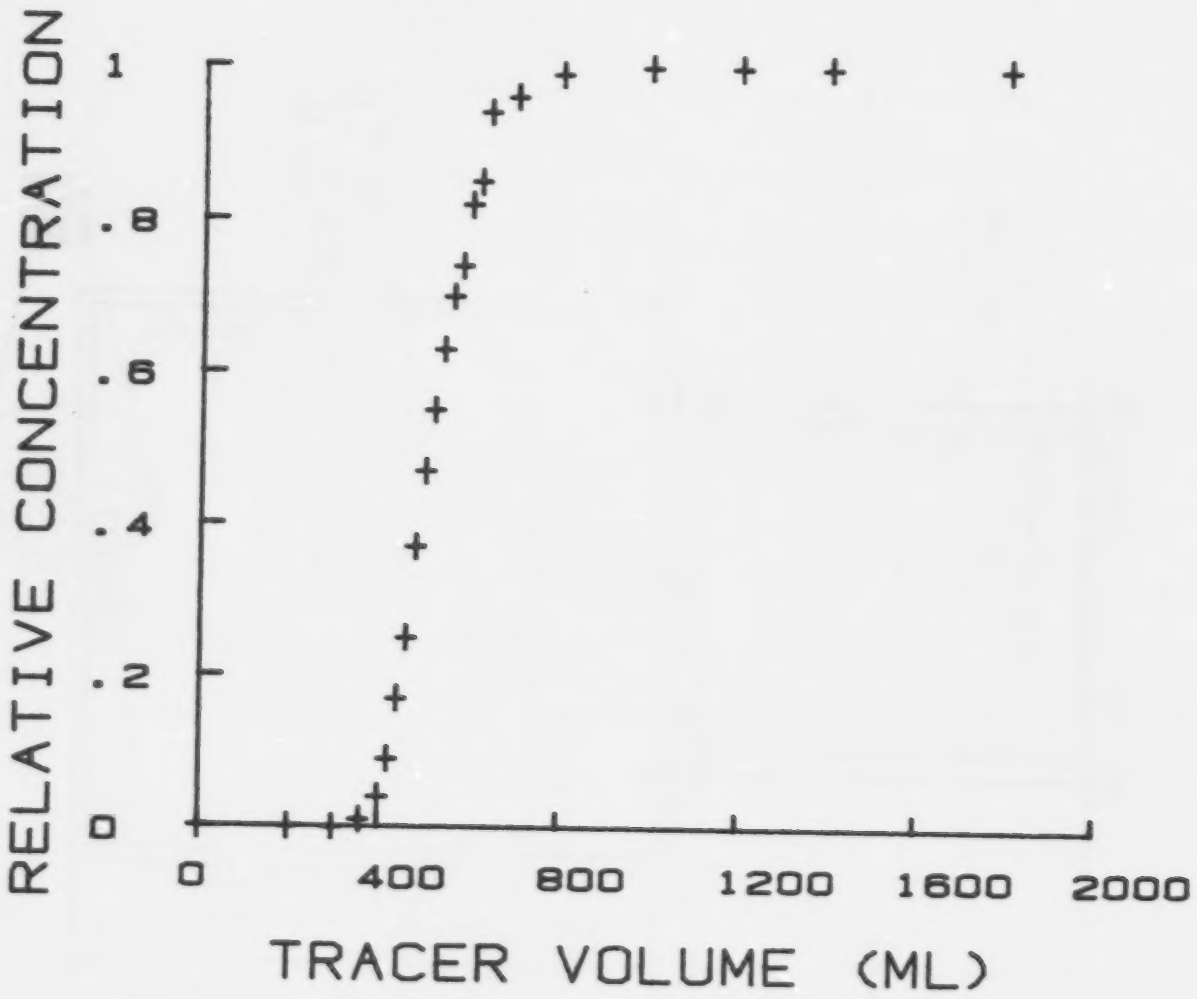

FIGURE 18(a): Tracer analysis through short tubular reactor packed with calcium alginate beads formed with 1.024 mm needles

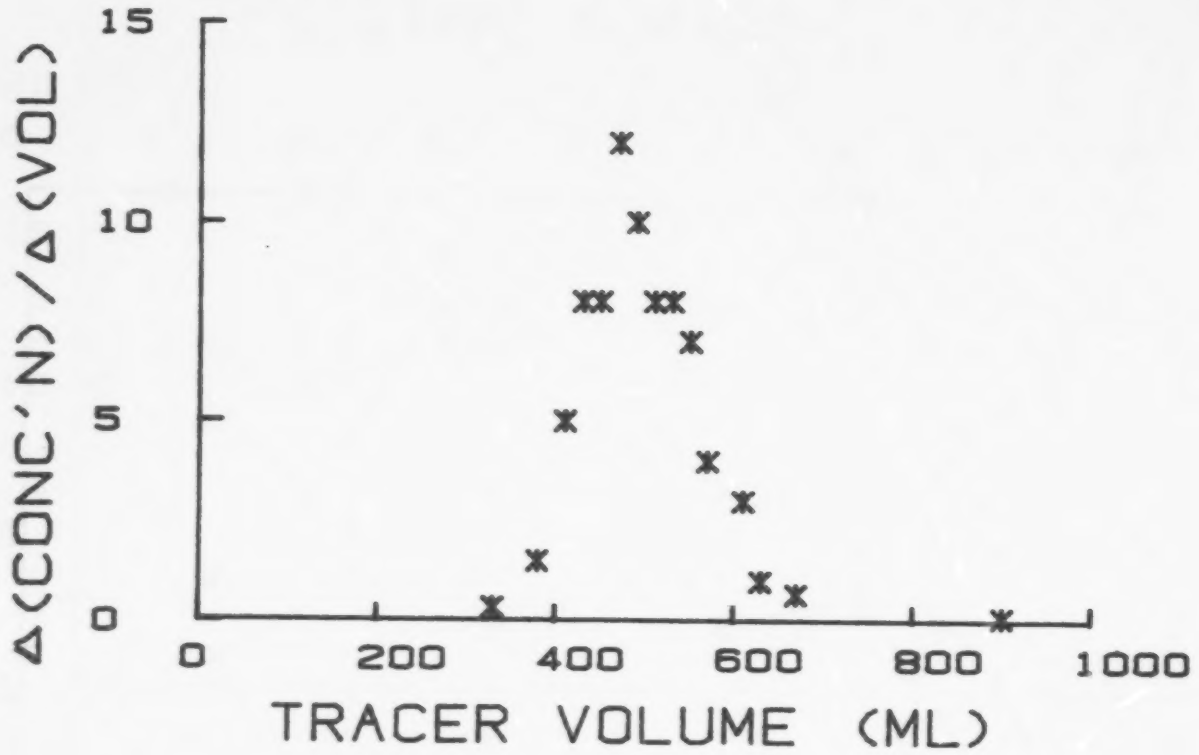

FIGURE 18(b): Tracer analysis through short tubular reactor packed with calcium alginate beads formed with 1.024 mm needles

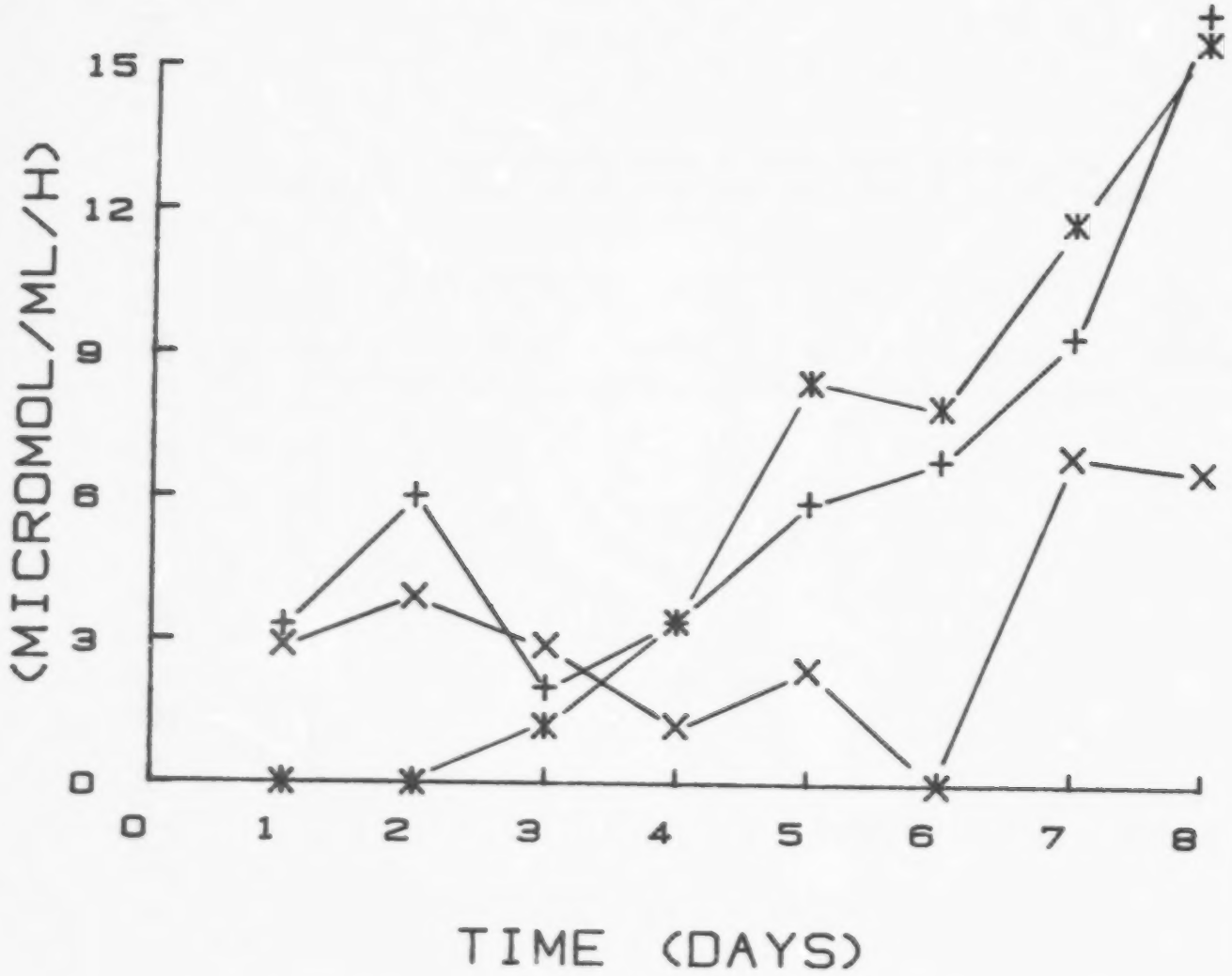

FIGURE 19: Filter paper activity of T. reesei 9414 grown on 2% Solka-Floc. Symbols: (×) culture solids; (+) culture filtrate; (✳) whole culture

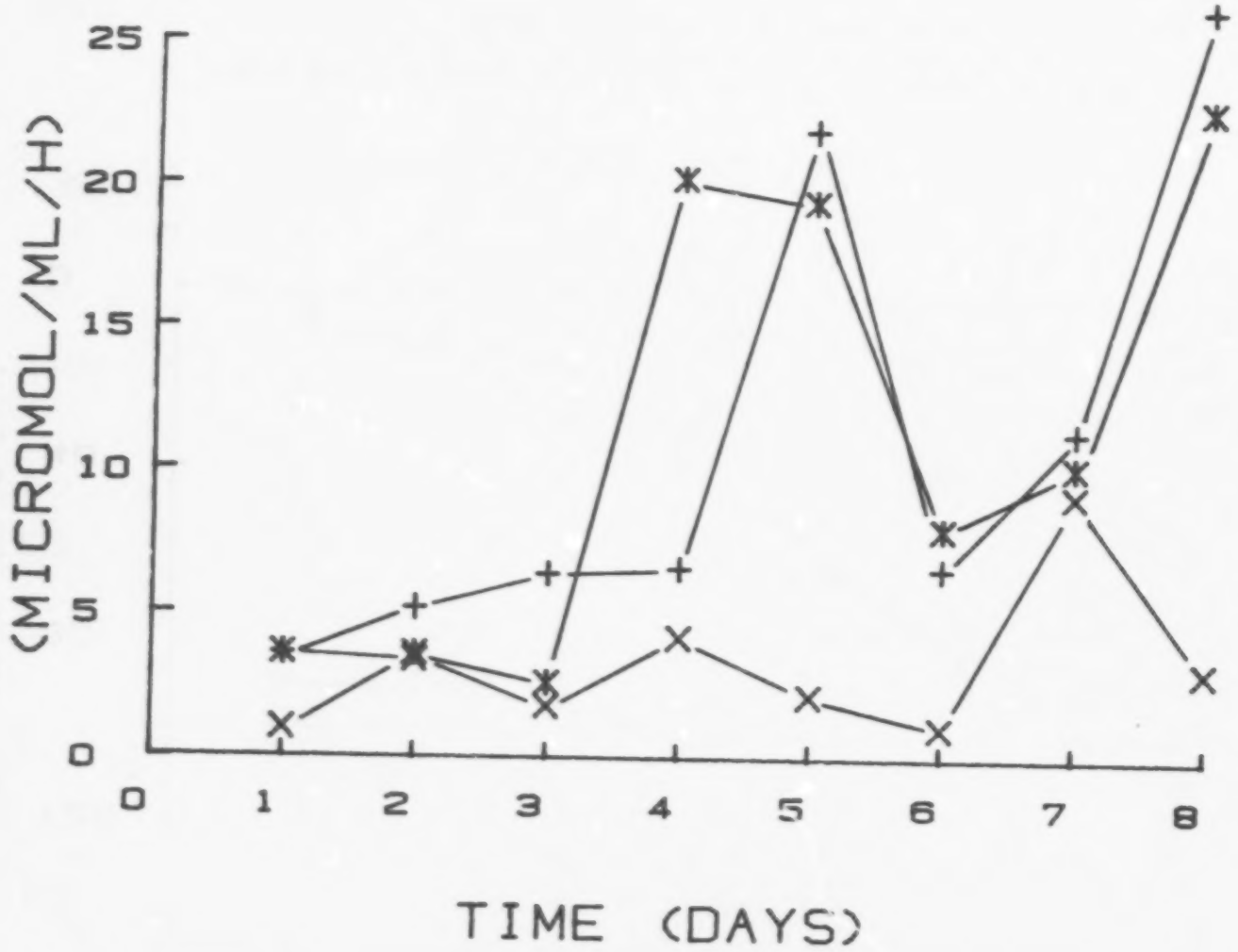

FIGURE 20: Filter paper activity of T. harzianum E58 grown on 2% Solka-Floc. Symbols: (X) culture solids; (+) culture filtrate; (*) whole culture

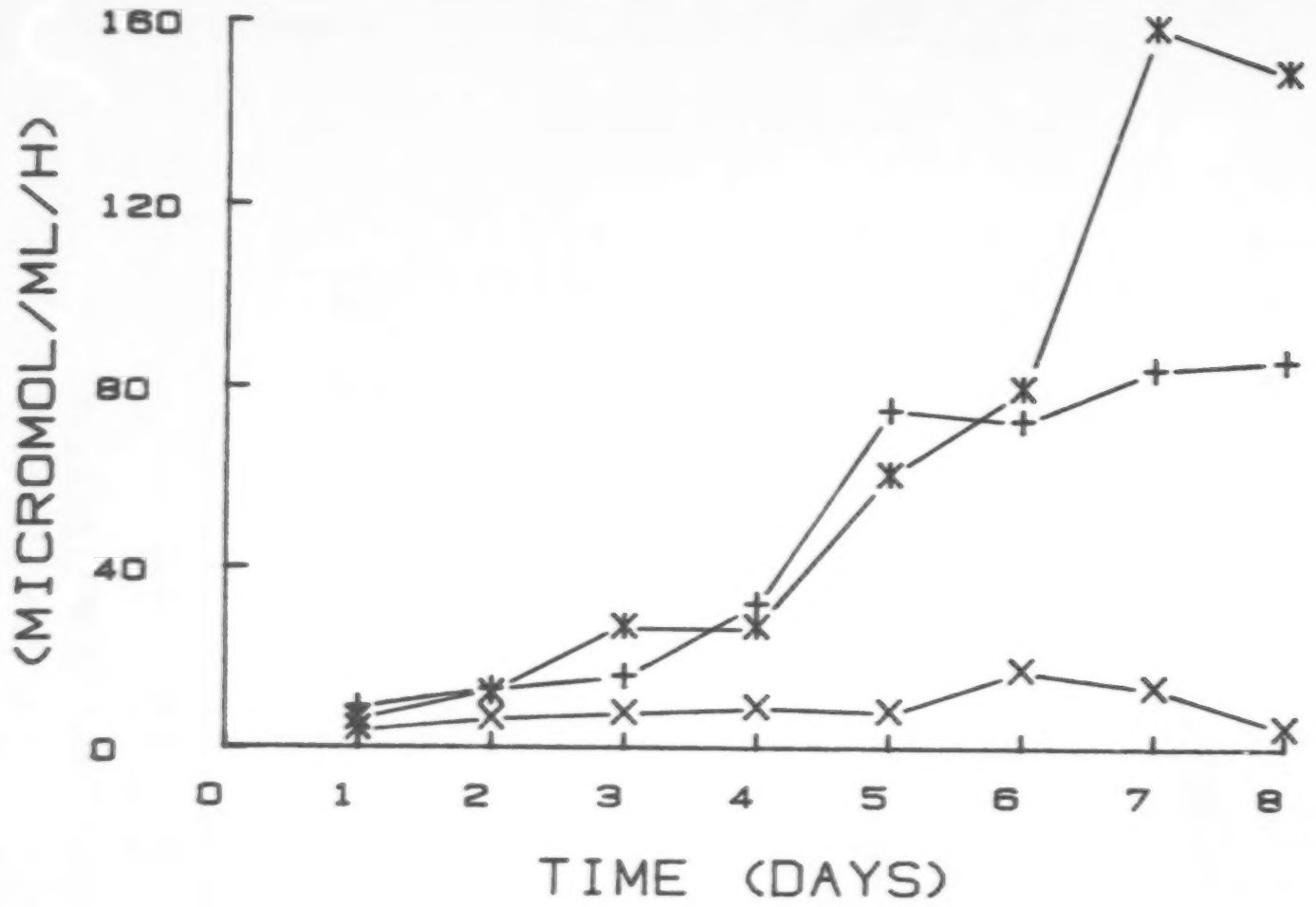

FIGURE 21: Carboxymethylcellulase activity of T. reesei 9414 grown on 2% Solka-Floc. Symbols: (×) culture solids; (+) culture filtrate; (✳) whole culture

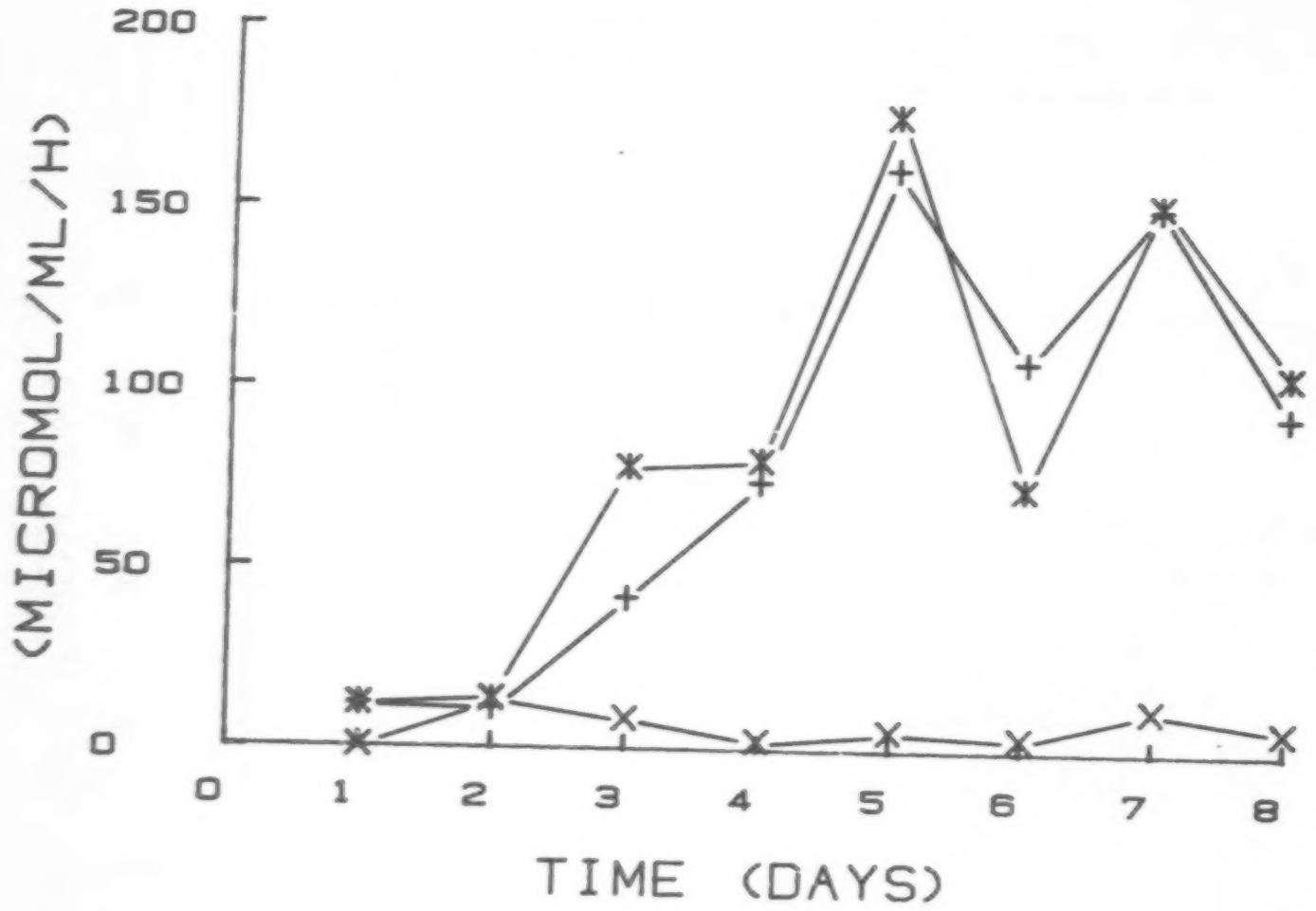

FIGURE 22: Carboxymethylcellulase activity of T. harzianum E58 grown on 2% Solka-Floc. Symbols: (X) culture solids; (+) culture filtrate; (*) whole culture

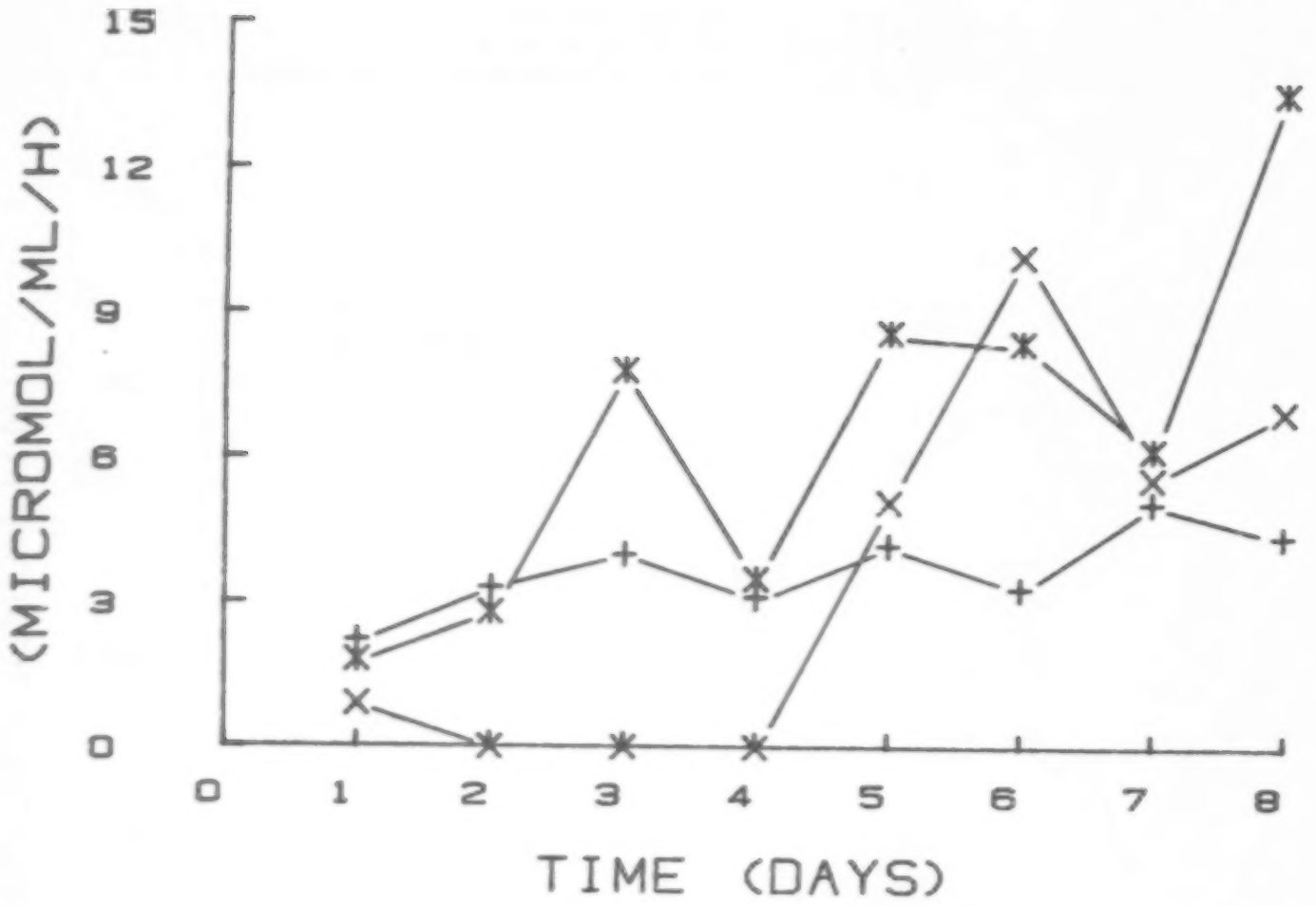

FIGURE 23: β-glucosidase activity of T. reesei 9414 grown on 2% Solka-Floc. Symbols: (X) culture solids; (+) culture filtrate; (✳) whole culture

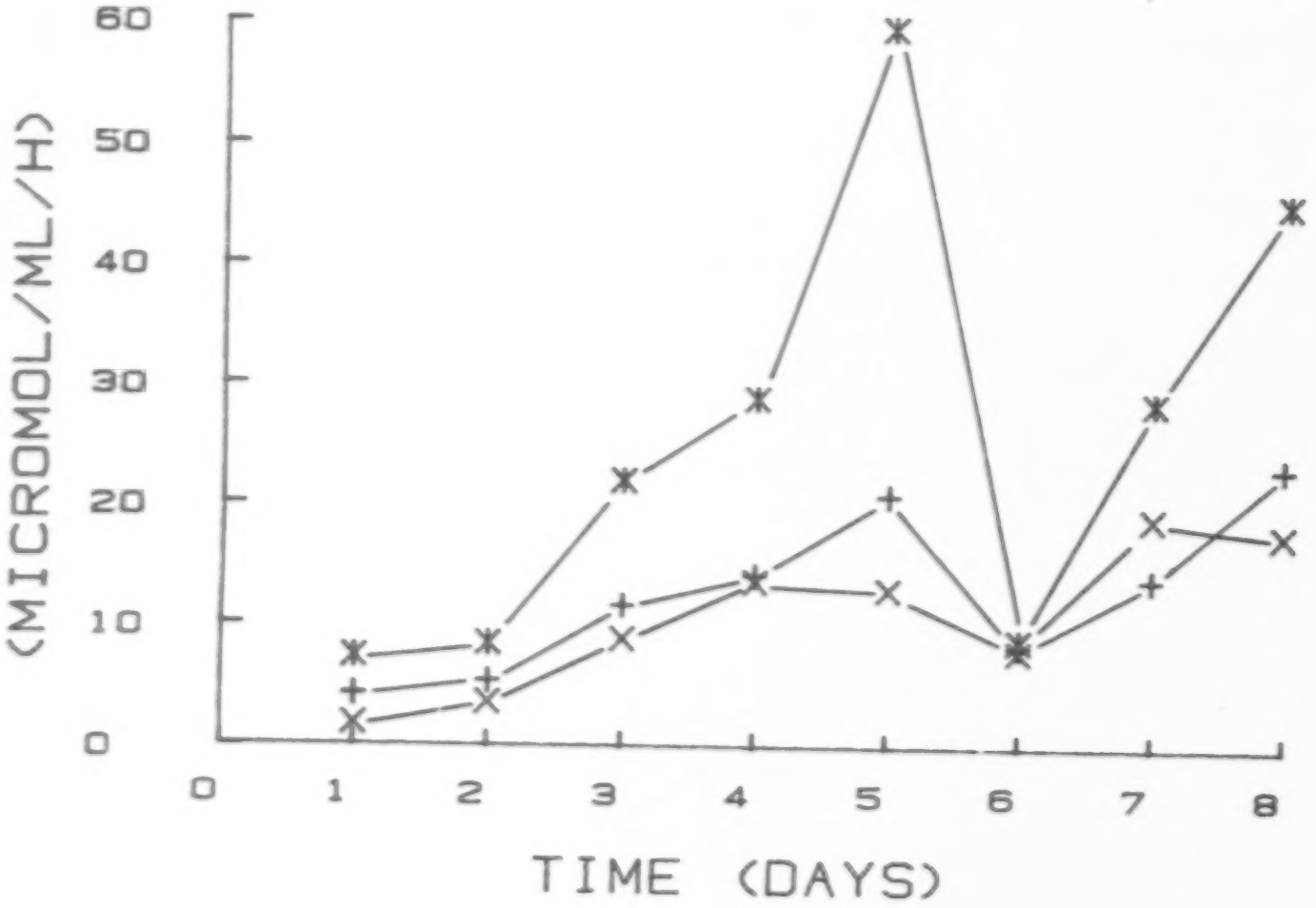

FIGURE 24: ß-glucosidase activity of T. harzianum E58 grown on 2% Solka-Floc. Symbols: (×) culture solids; (+) culture filtrate; (*) whole culture

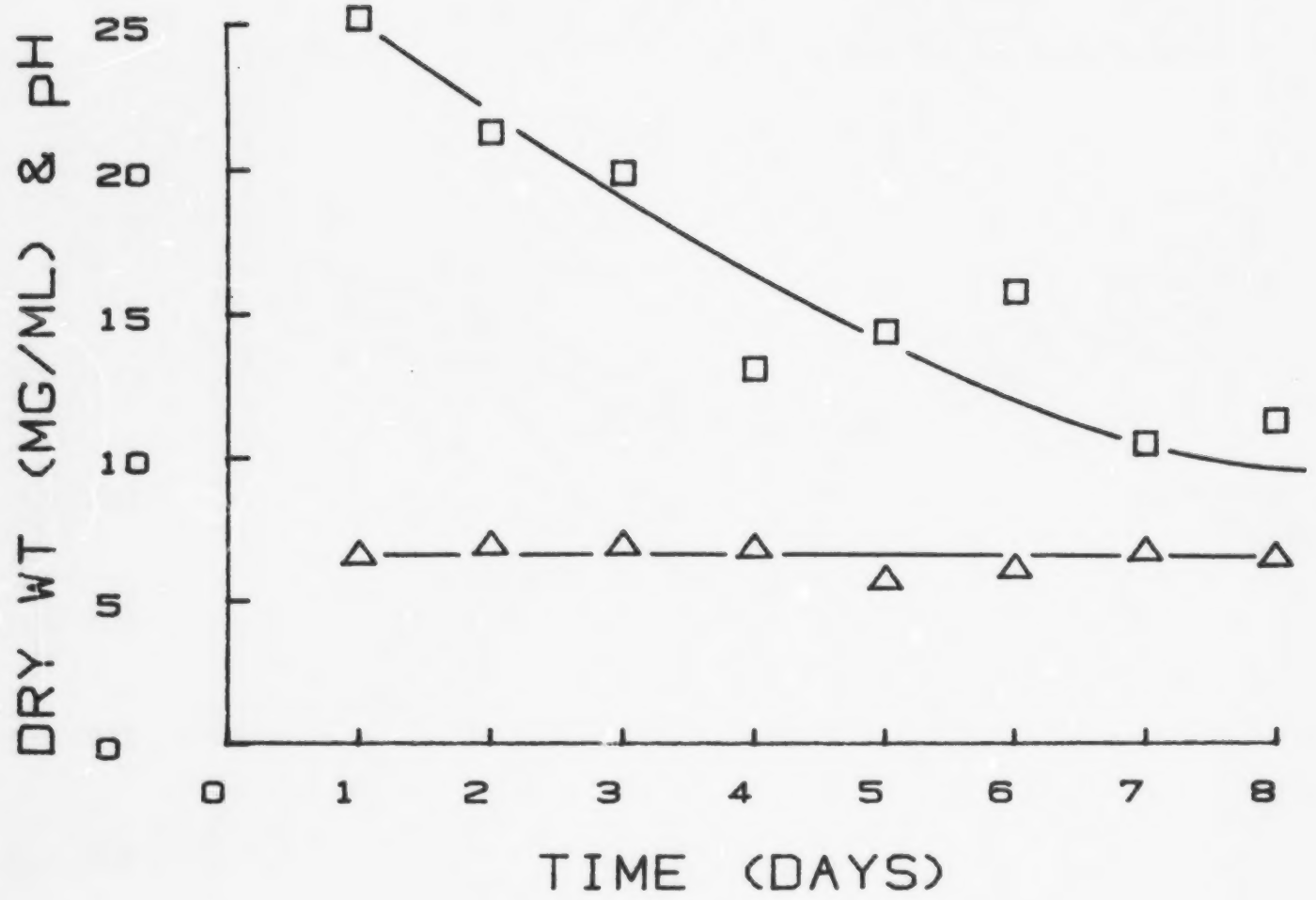

FIGURE 25: Variation in dry weight (□) and pH (△) of T. reesei 9414 culture grown on 2% Solka-Floc

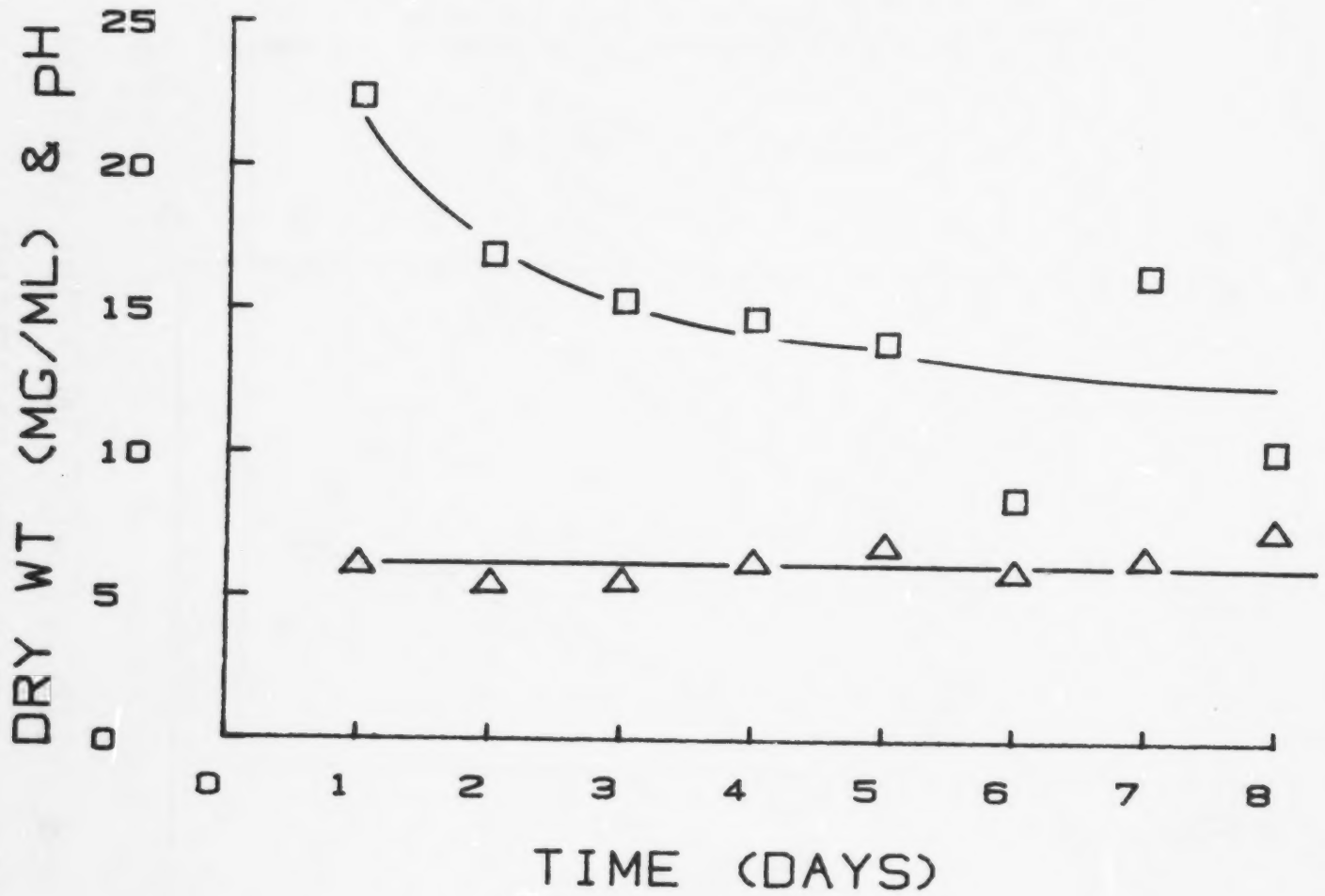

FIGURE 26: Variation in dry weight (□) and pH (△) of T. harzianum E58 culture grown on 2% Solka-Floc

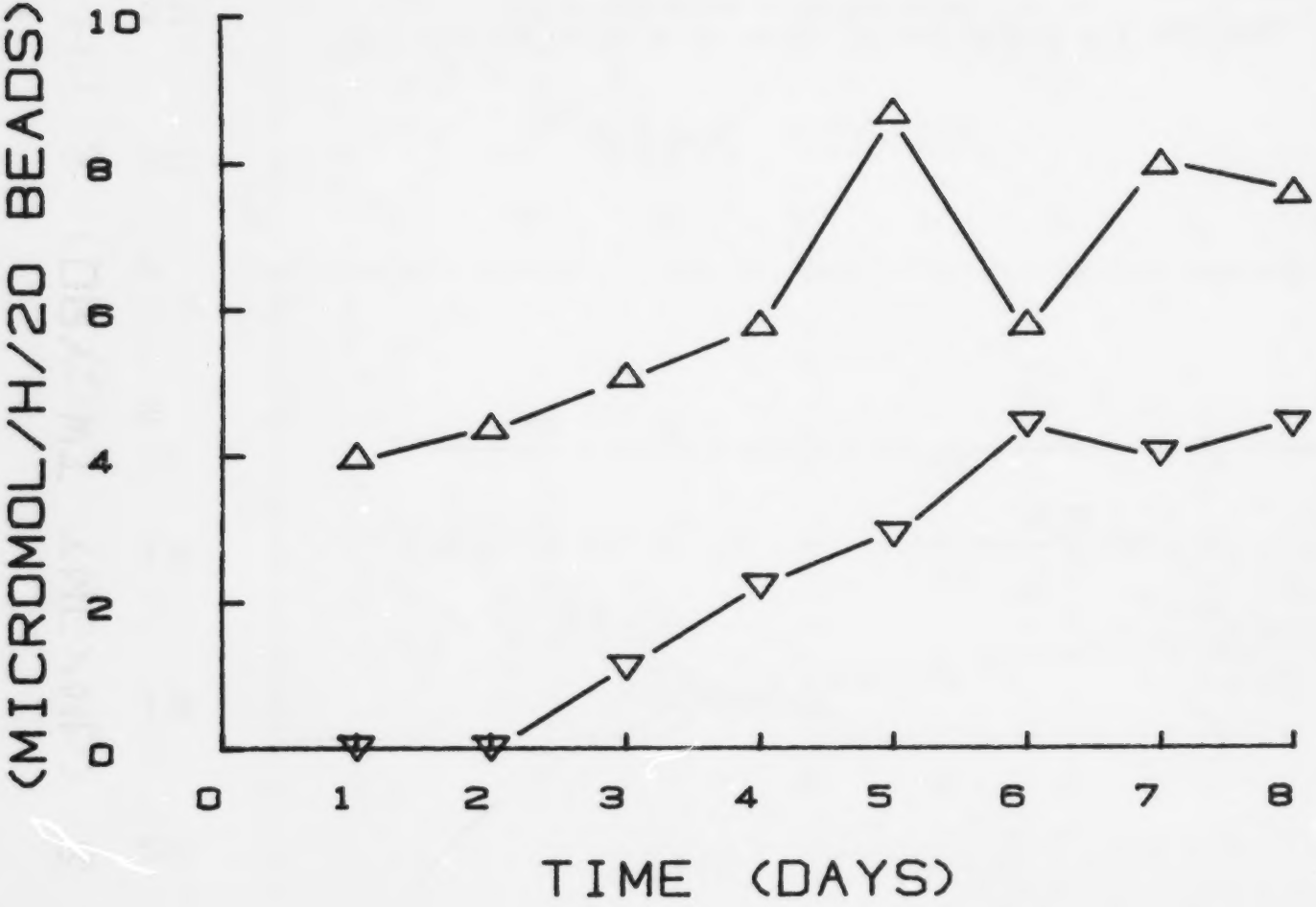

FIGURE 27: Encapsulated cell-associated activity towards salicin of culture solids during growth of T. reesei 9414 (▽) and T. harzianum E58 (△) on 2% Solka-Floc

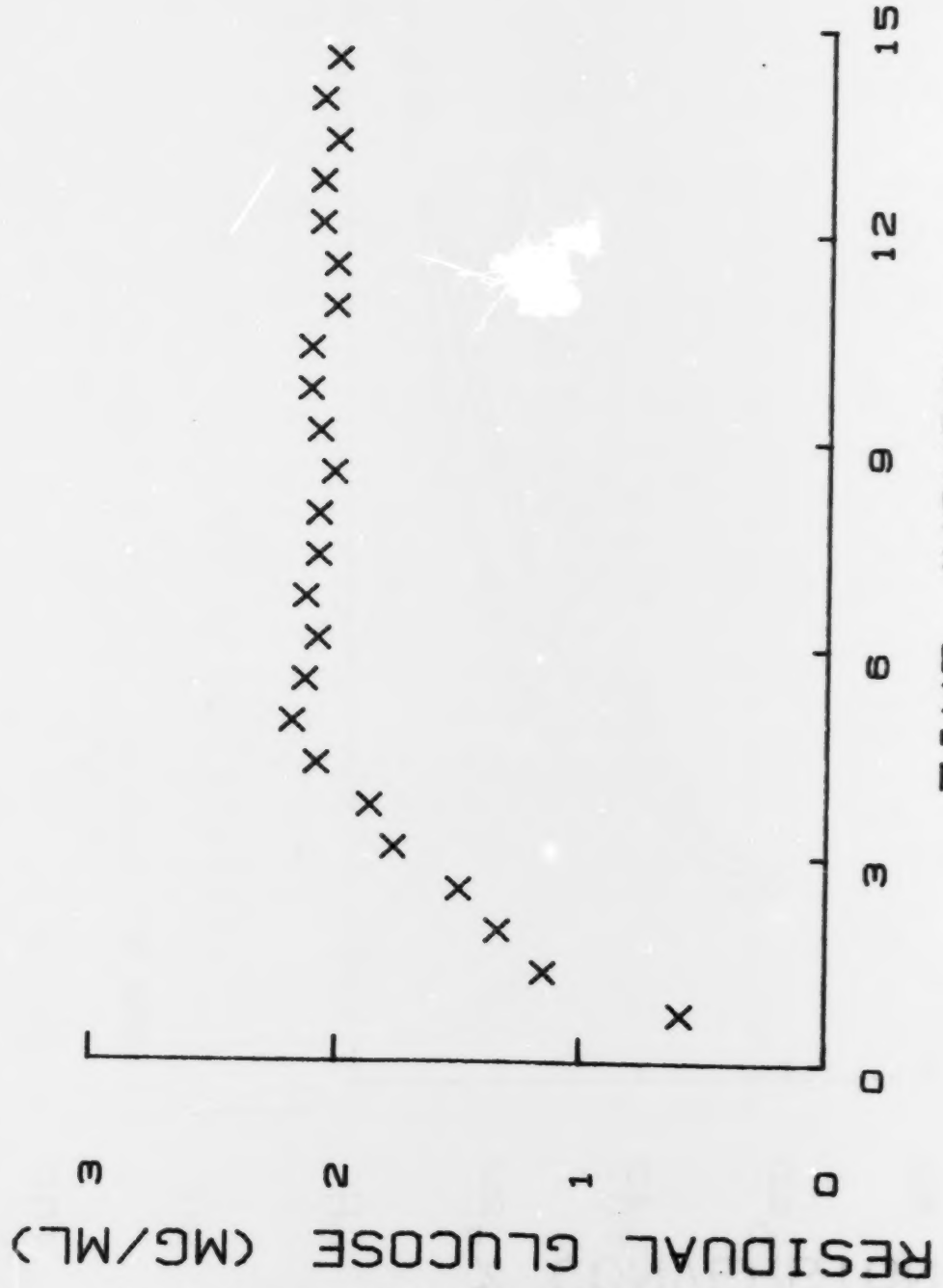

FIGURE 28: Dynamic response of TUB 1 to 10 mM cellobiose at a dilution rate of 0.18 h^{-1}

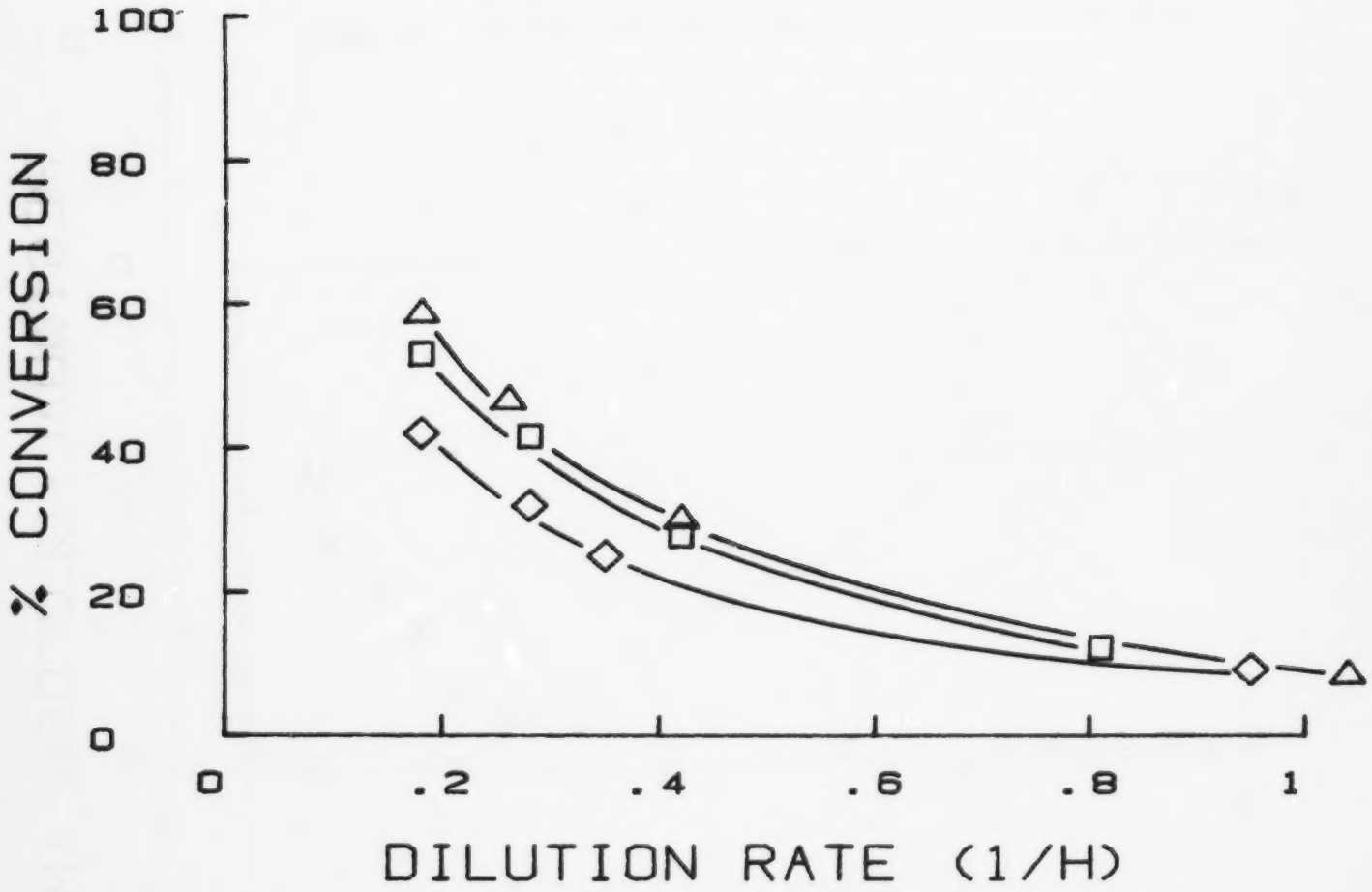

FIGURE 29: Steady-state conversions of 10 mM cellobiose as a function of dilution rate (Run 1). Symbols: (△) TUB 1; (□) TAP 1; (◇) RAD 1

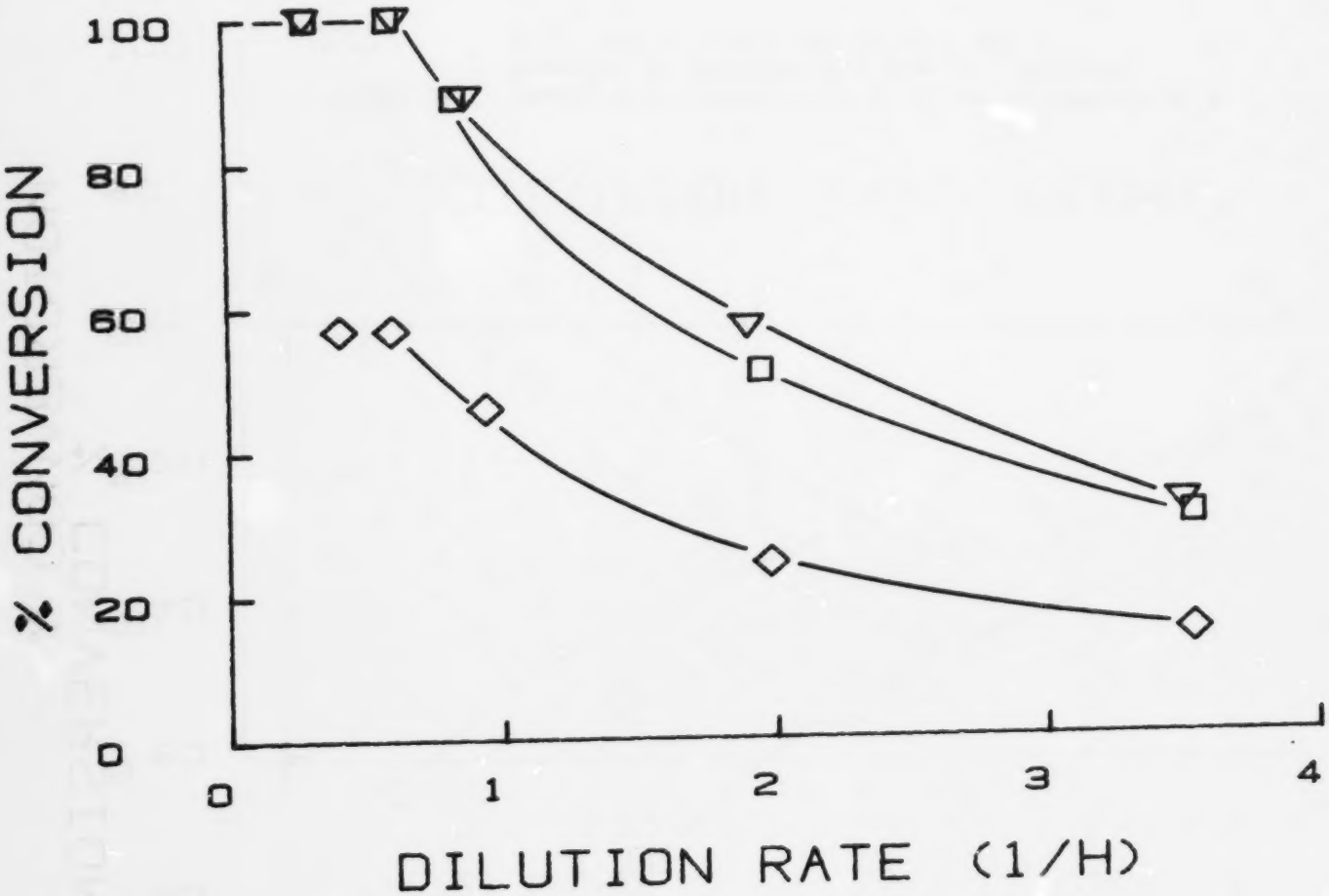

FIGURE 30: Steady-state conversions of 5 mM cellobiose as a function of dilution rate (Run 2). Symbols: (▽) TUB 2; (□) TAP 2; (◇) RAD 1

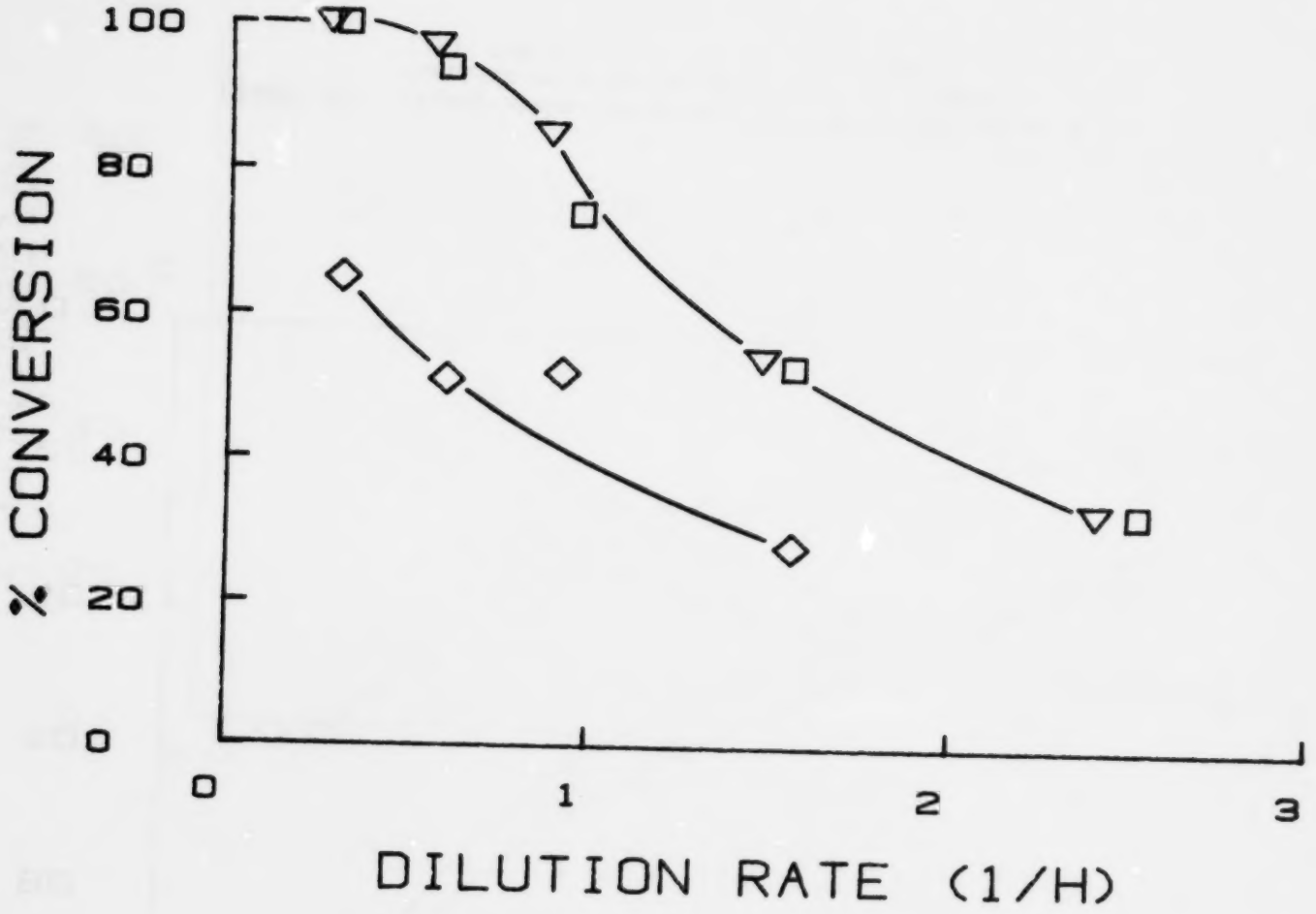

FIGURE 31: Steady-state conversions of 7.5 mM cellobiose as a function of dilution rate (Run 2). Symbols: (▽) TUB 2; (□) TAP 2; (◇) RAD 1

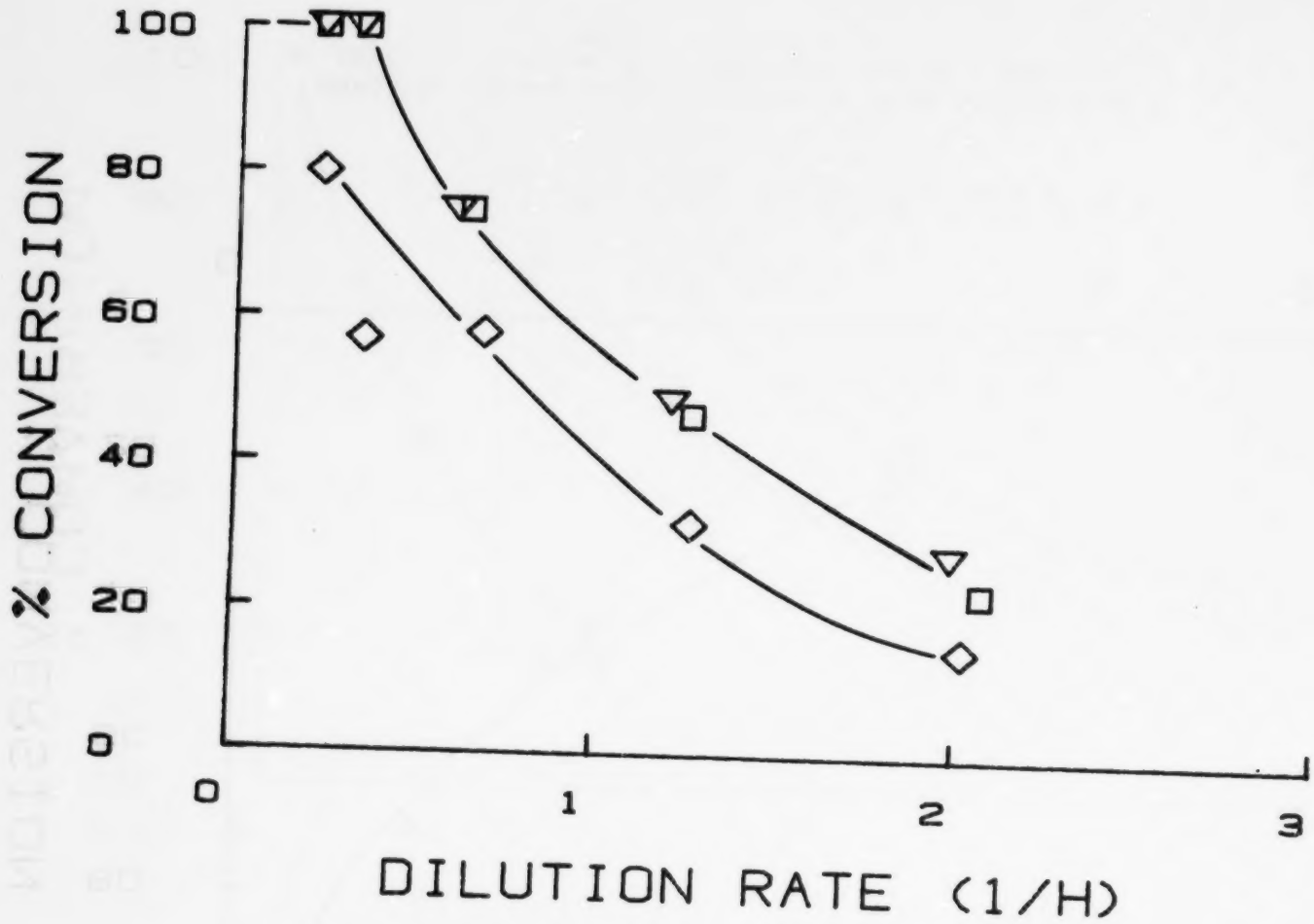

FIGURE 32: Steady-state conversion of 10 mM cellobiose as a function of dilution rate (Run 2). Symbols: (▽) TUB 2; (□) TAP 2; (◇) RAD 1

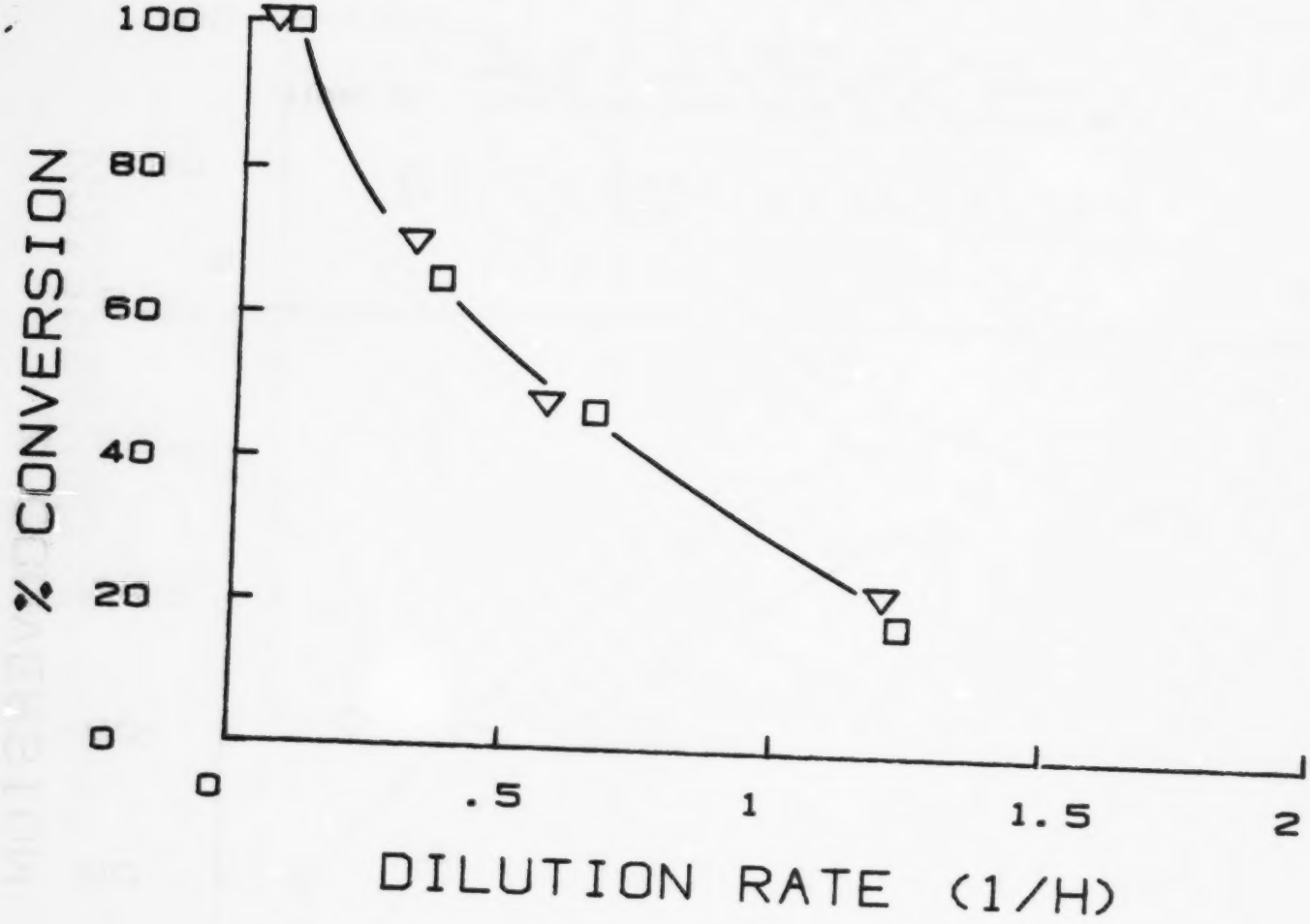

FIGURE 33: Steady-state conversion of 20 mM cellobiose as a function of dilution rate (Run 2). Symbols: (▽) TUB 2; (□) TAP 1

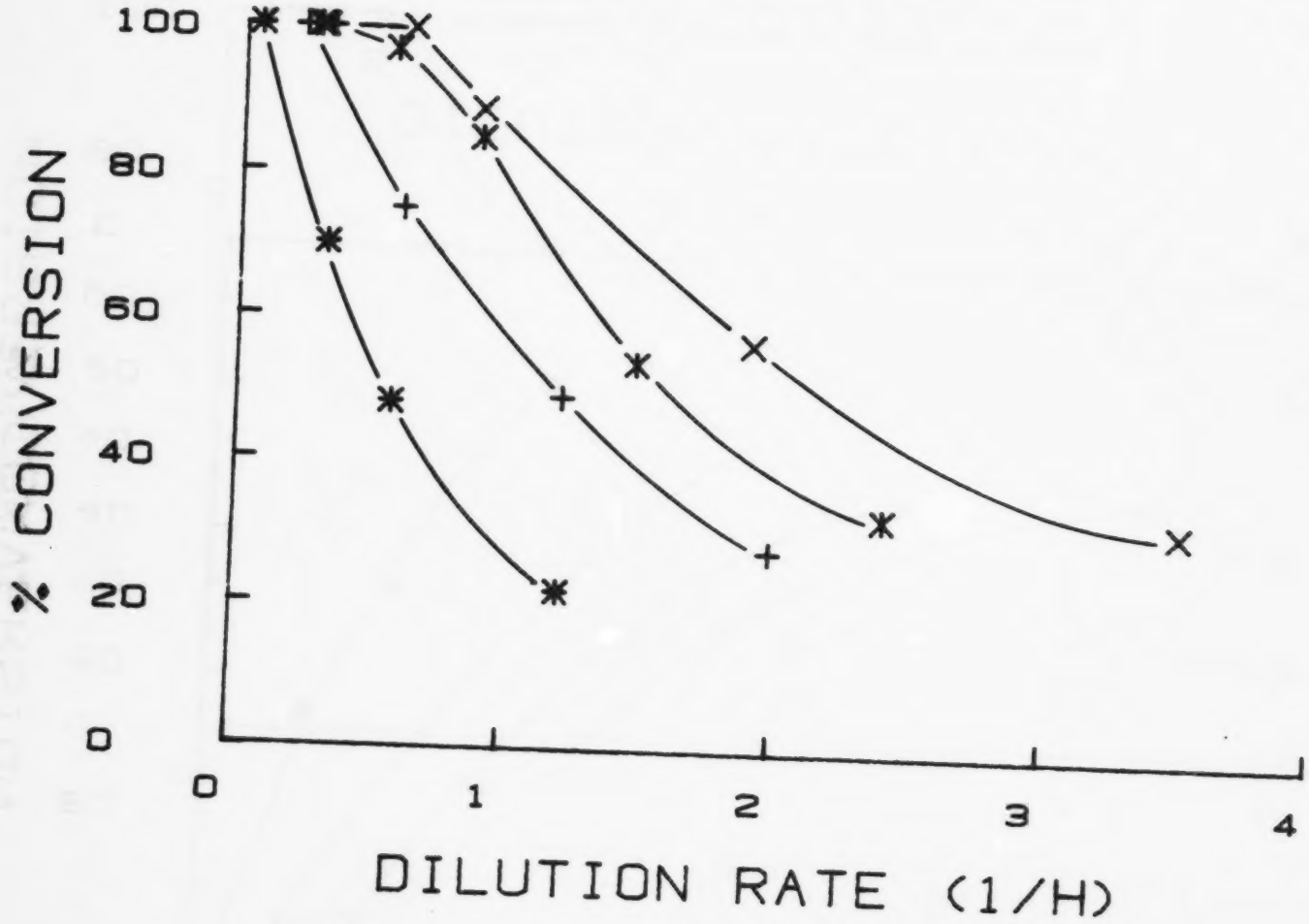

FIGURE 34: Steady-state conversions of various cellobiose concentrations as a function of dilution rate for reactor TUB 2 (Run 2). Symbols: (X) 5 mM; (✳) 7.5 mM; (+) 10 mM; (✳) 20 mM

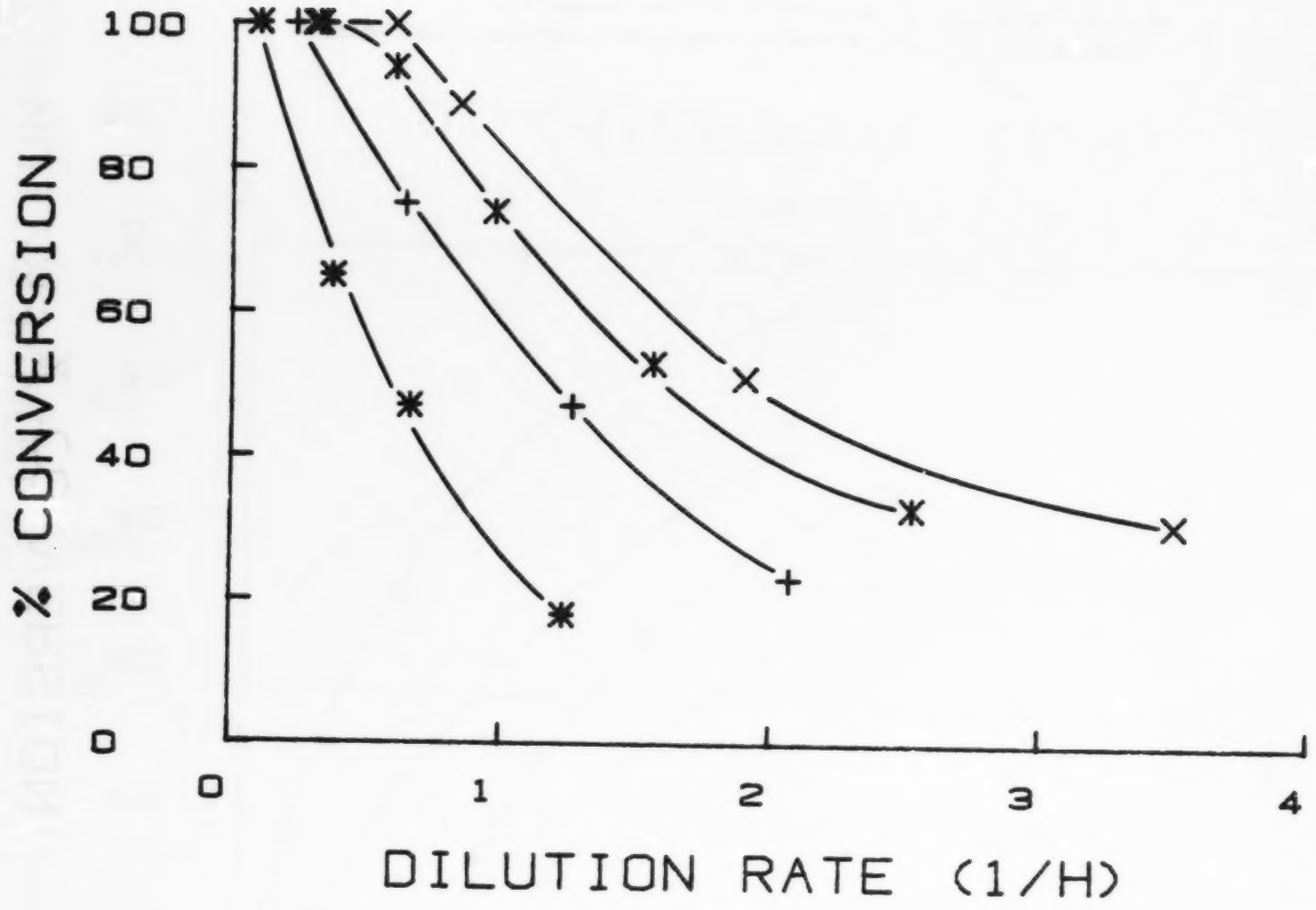

FIGURE 35: Steady-state conversions of various cellobiose concentrations as a function of dilution rate for reactor TAP 2 (Run 2). Symbols: (×) 5 mM; (✳) 7.5 mM; (+) 10 mM; (✳) 20 mM

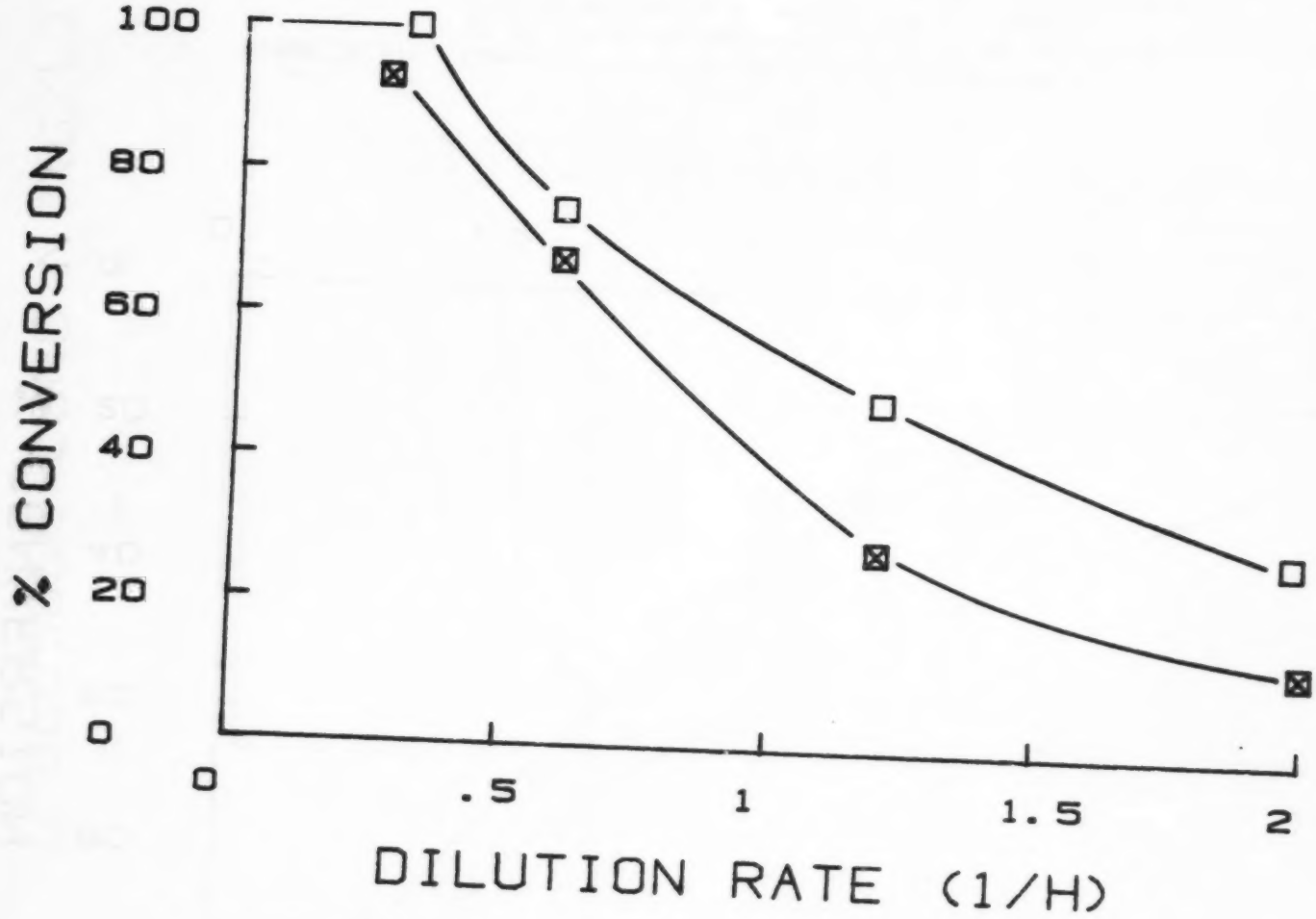

FIGURE 36(a): Comparision of the steady-state conversion of 10mM cellobiose and a mixture of 10 mM cellobiose plus 10 mM glucose in reactor TUB 2. Symbols: (□) 10 mM cellobiose; (⊠) 10 mM cellobiose plus 10 mM glucose

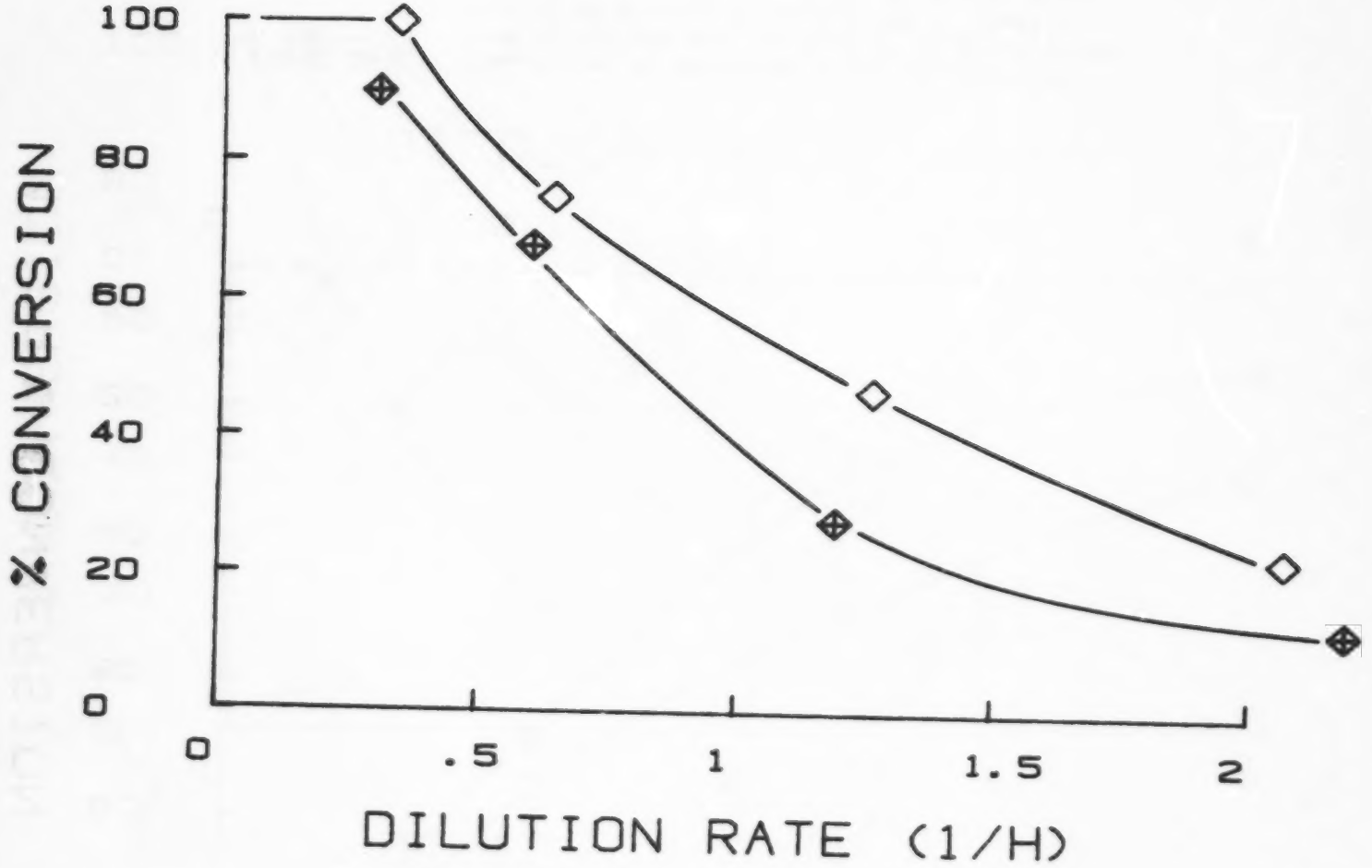

FIGURE 36(b): Comparision of the steady-state conversion of 10 mM cellobiose and a mixture of 10 mM cellobiose plus 10 mM glucose in reactor TAP 2. Symbols: (◊) 10 mM cellobiose; (◆) 10 mM cellobiose plus 10 mM glucose

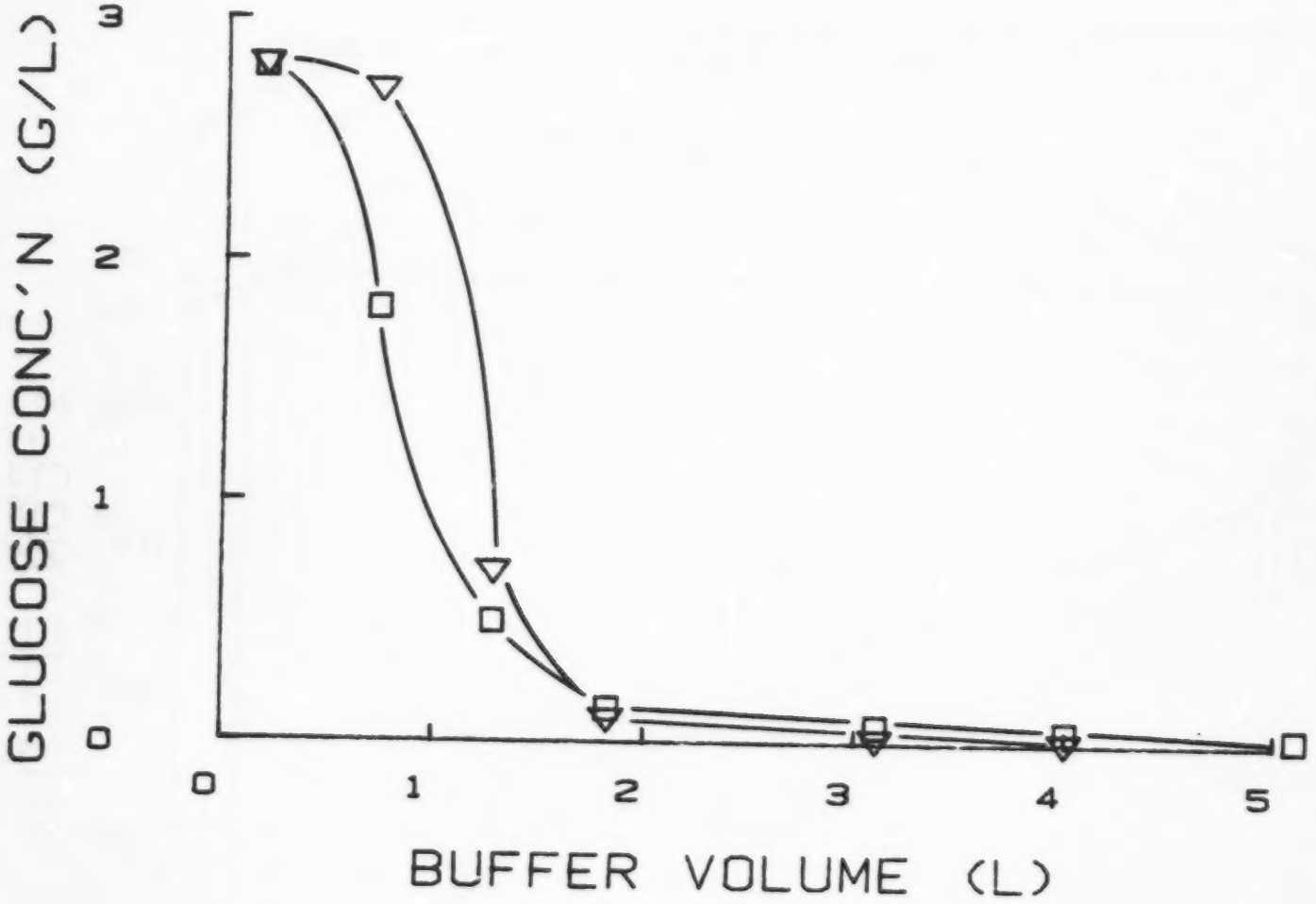

FIGURE 37: Glucose elution profiles obtained after steady-state conversion of 7.5 mM cellobiose had been achieved in reactors TUB 2 and TAP 2. Symbols: (▽) TUB 2; (□) TAP 2

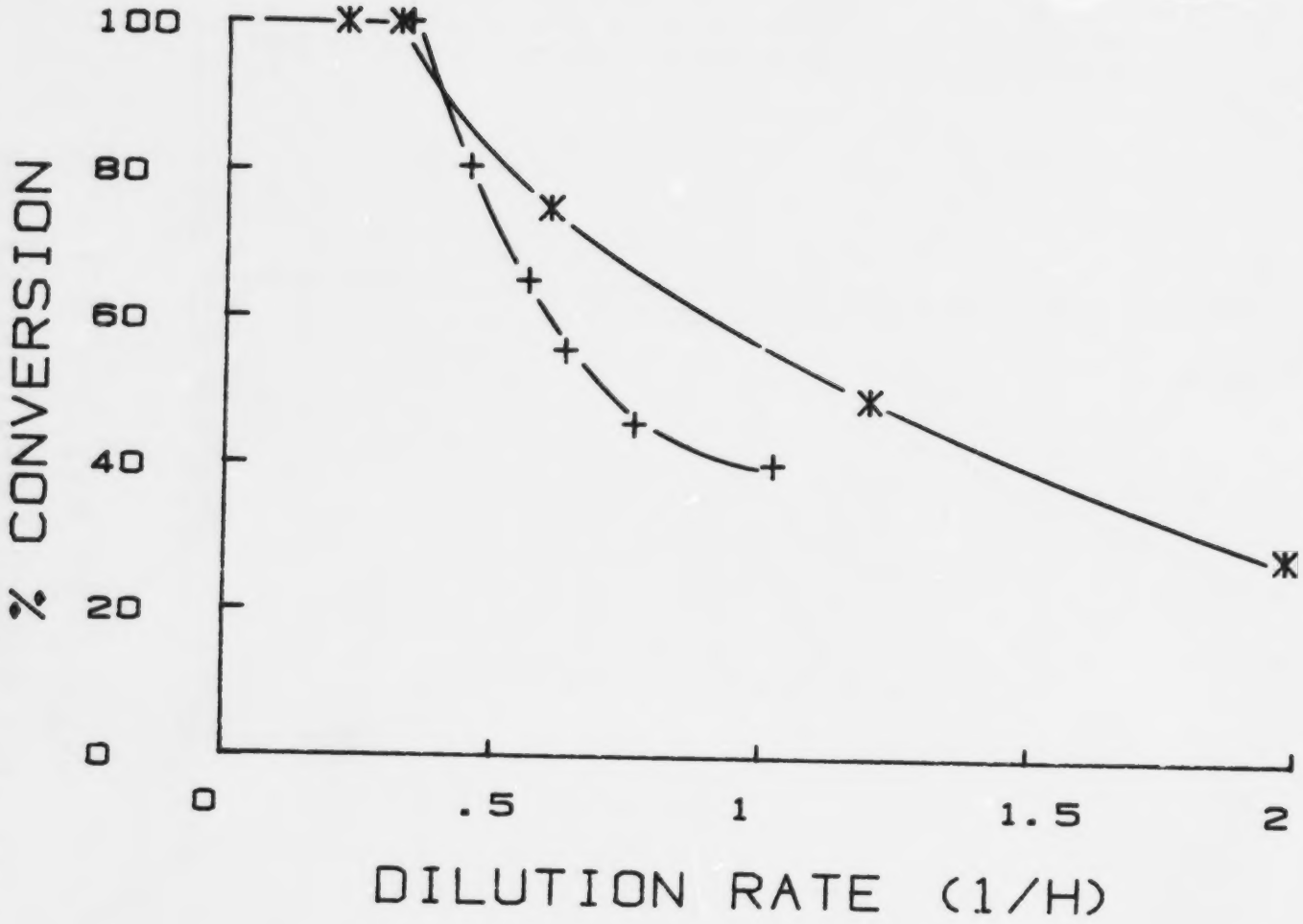

FIGURE 38: Comparision of 10 mM cellobiose hydrolysis using TUB 2 with: (*) 100% active beads; (+) with 50% active beads

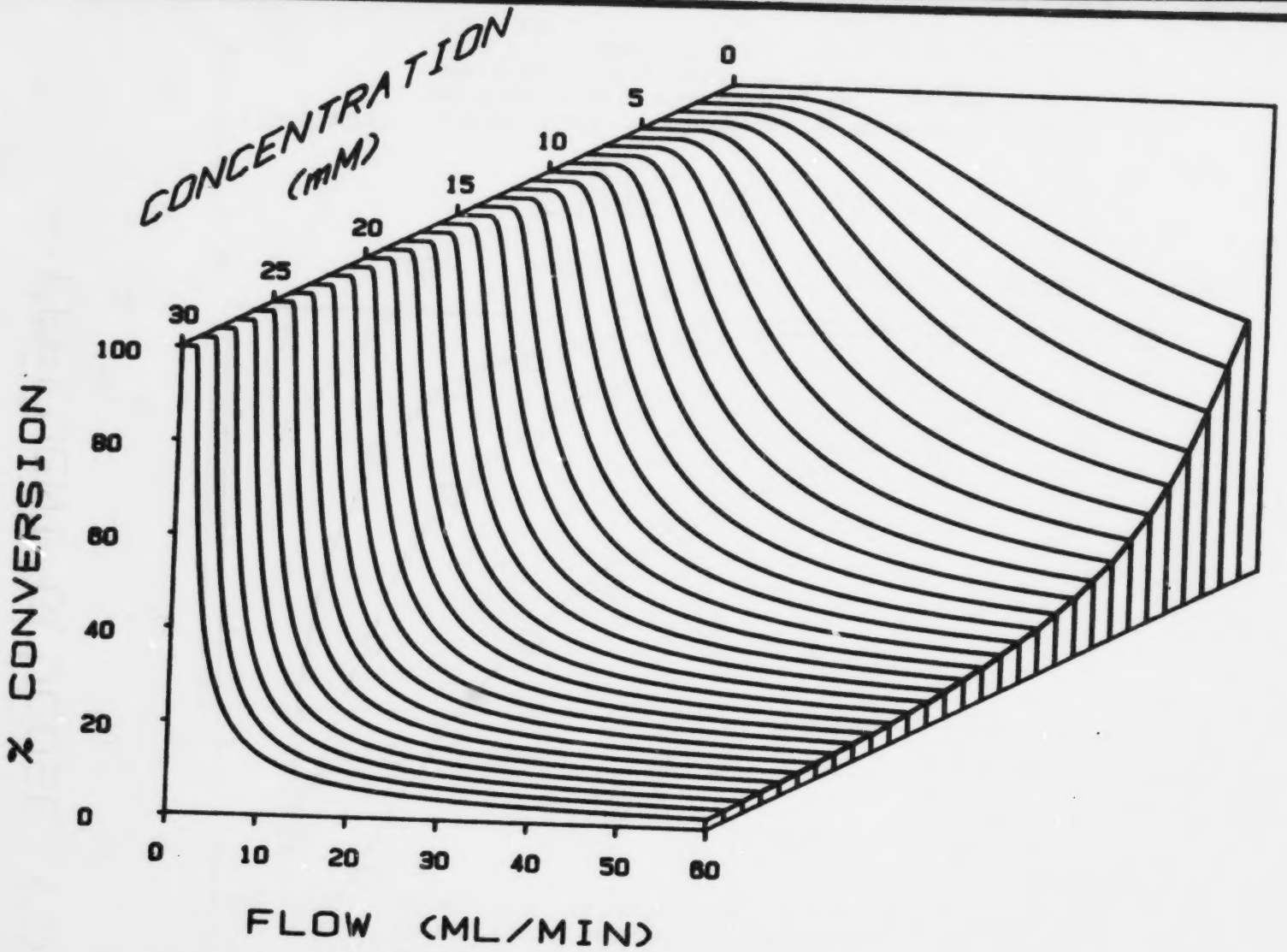

Figure 39: Response surface obtained by modelling of data obtained from cellobiose hydrolysis using TUB 2

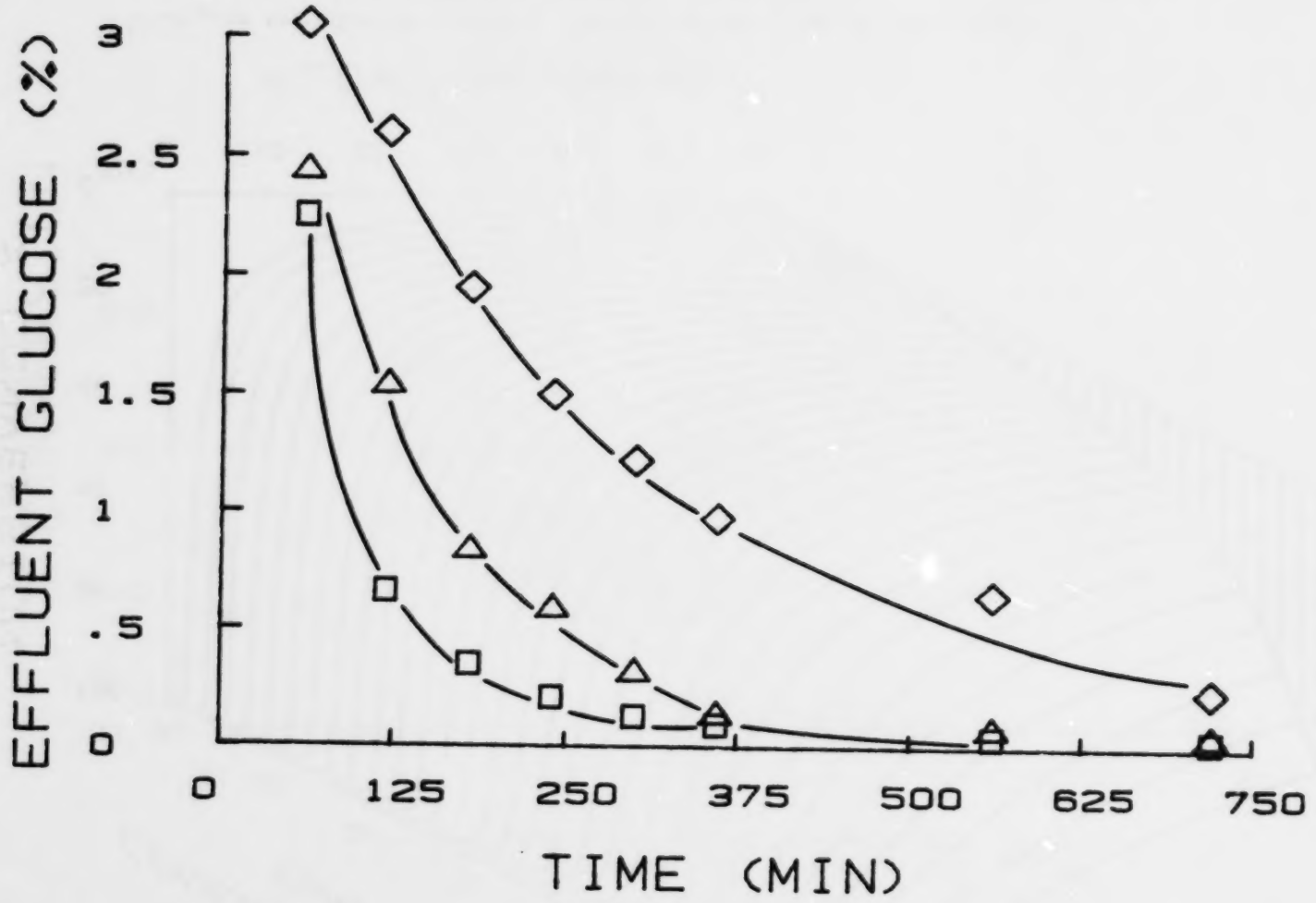

FIGURE 40(a): Dynamic start-up response as reflected by glucose utilization of reactors TUB 1, TAP 2 and RAD 1 operating on 5% glucose feed at a dilution rate of 0.9 h^{-1}. Symbols: (□) TUB 1; (△) TAP 2; (◇) RAD 1

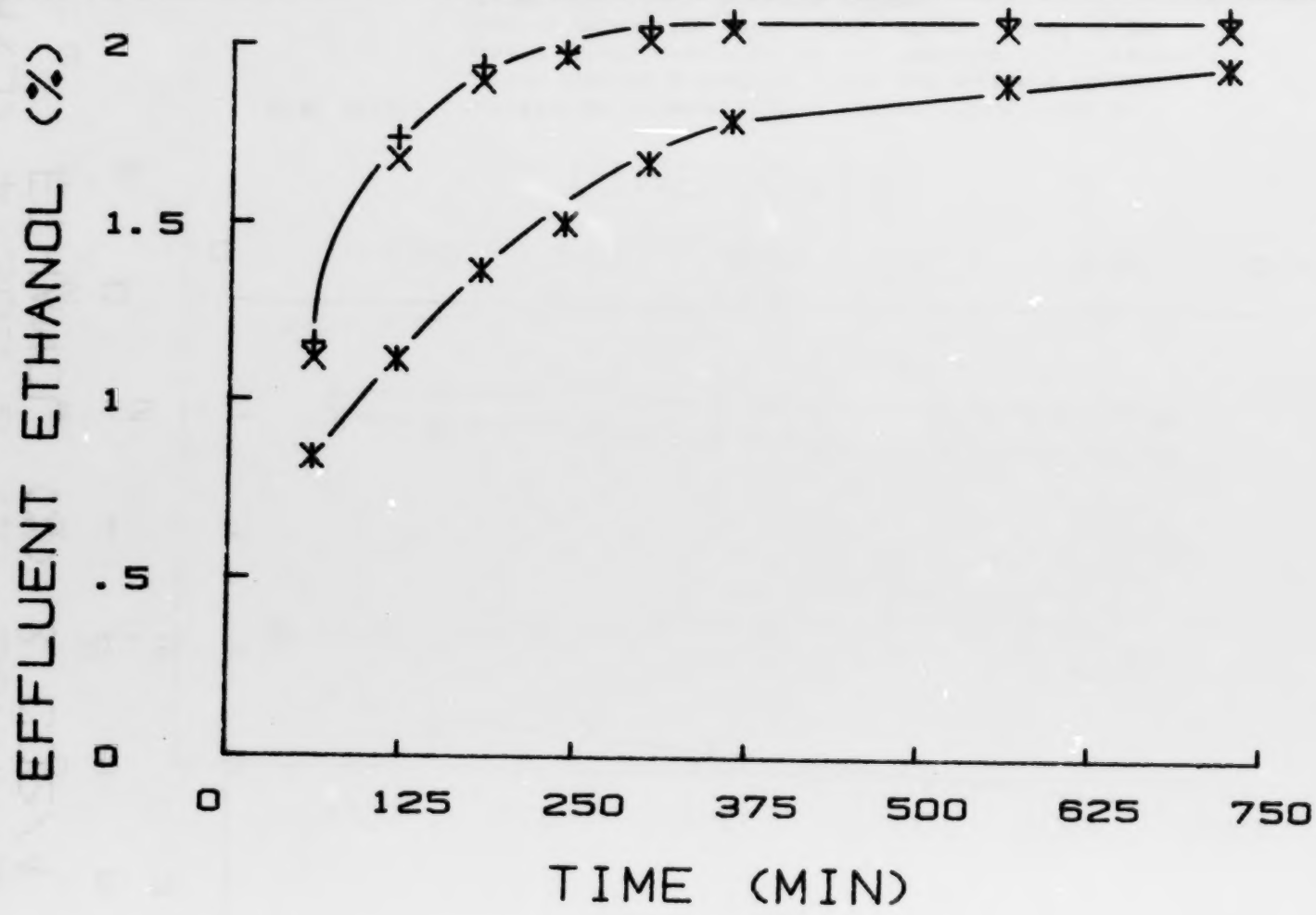

FIGURE 40(b): Dynamic start-up response as reflected by effluent ethanol concentrations from reactors TUB 1, TAP 2 and RAD 1 operating on 5% glucose feed at a dilution rate of 0.9 h^{-1}. Symbols: (+) TUB 1; (X) TAP 2; (*) RAD 1

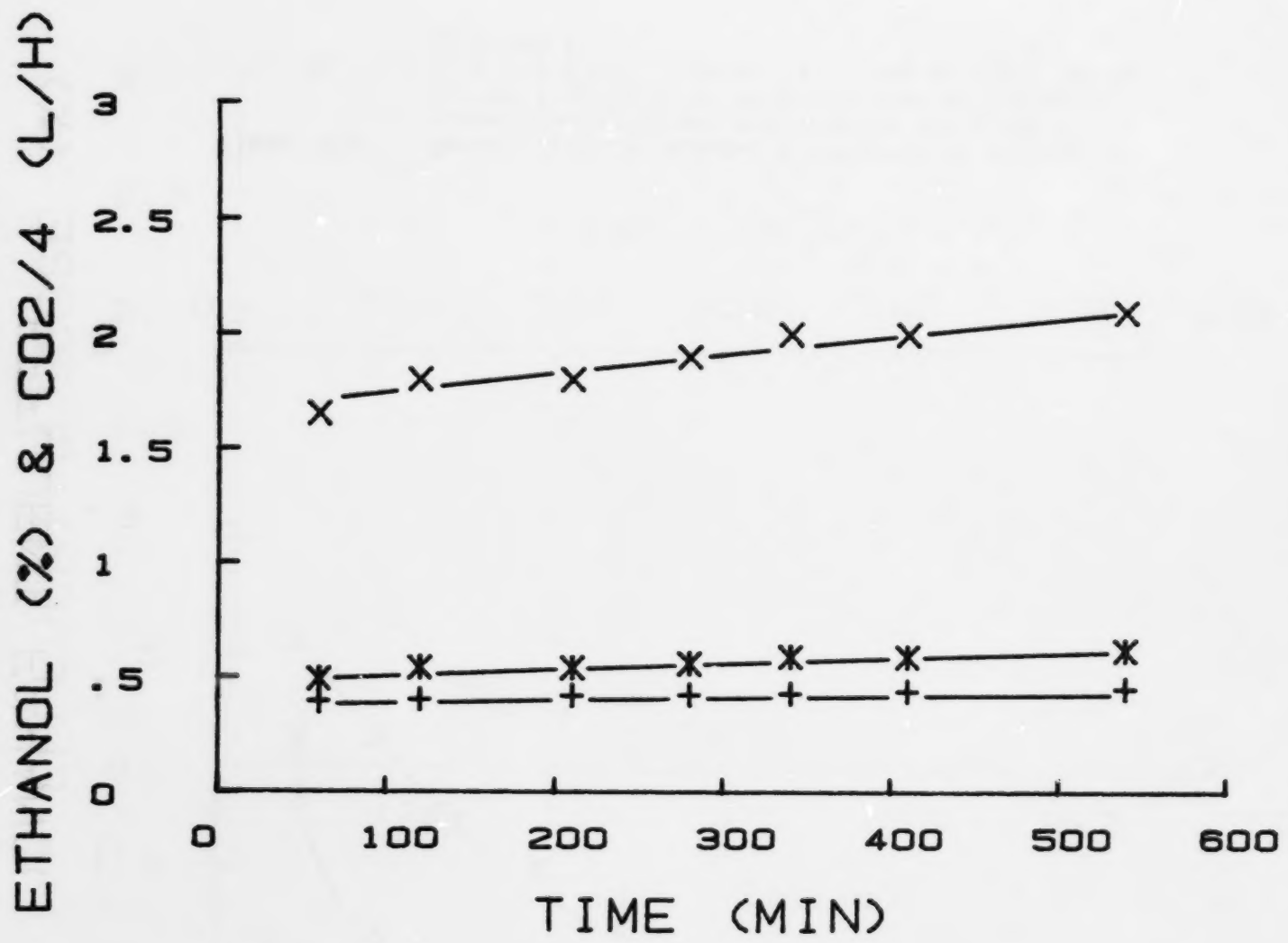

FIGURE 41(a): Correlation between alcohol concentration based on carbon dioxide production rates and measured ethanol levels in effluent from TUB 1. Symbols: (×) carbon dioxide production rate; (✳) ethanol based on gas production; (+) measured ethanol

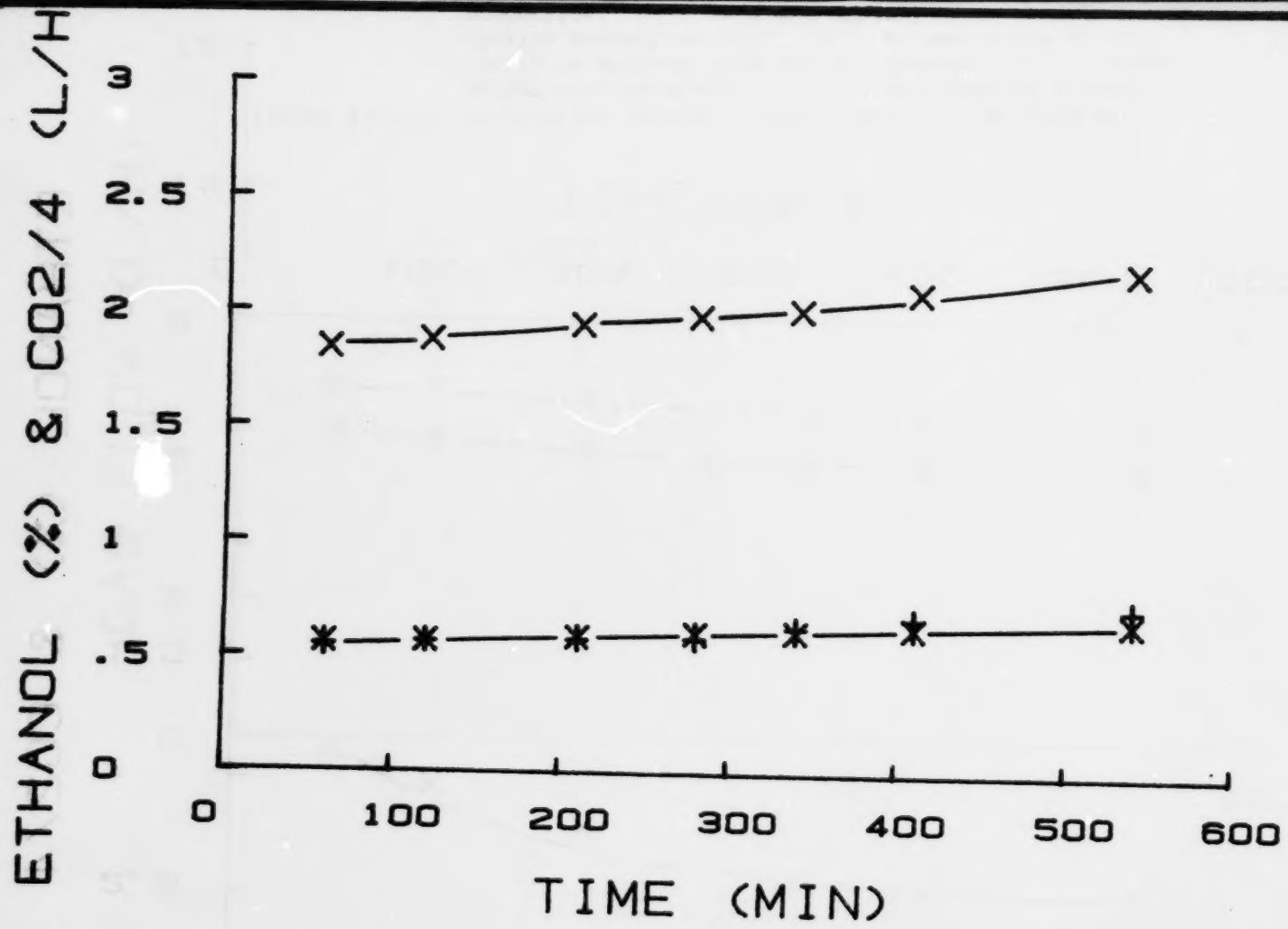

FIGURE 41(b): Correlation between alcohol concentration based on carbon dioxide production rates and measured ethanol levels in effluent from TAP 2. Symbols: (×) carbon dioxide production rate; (*) ethanol based on gas production; (+) measured ethanol

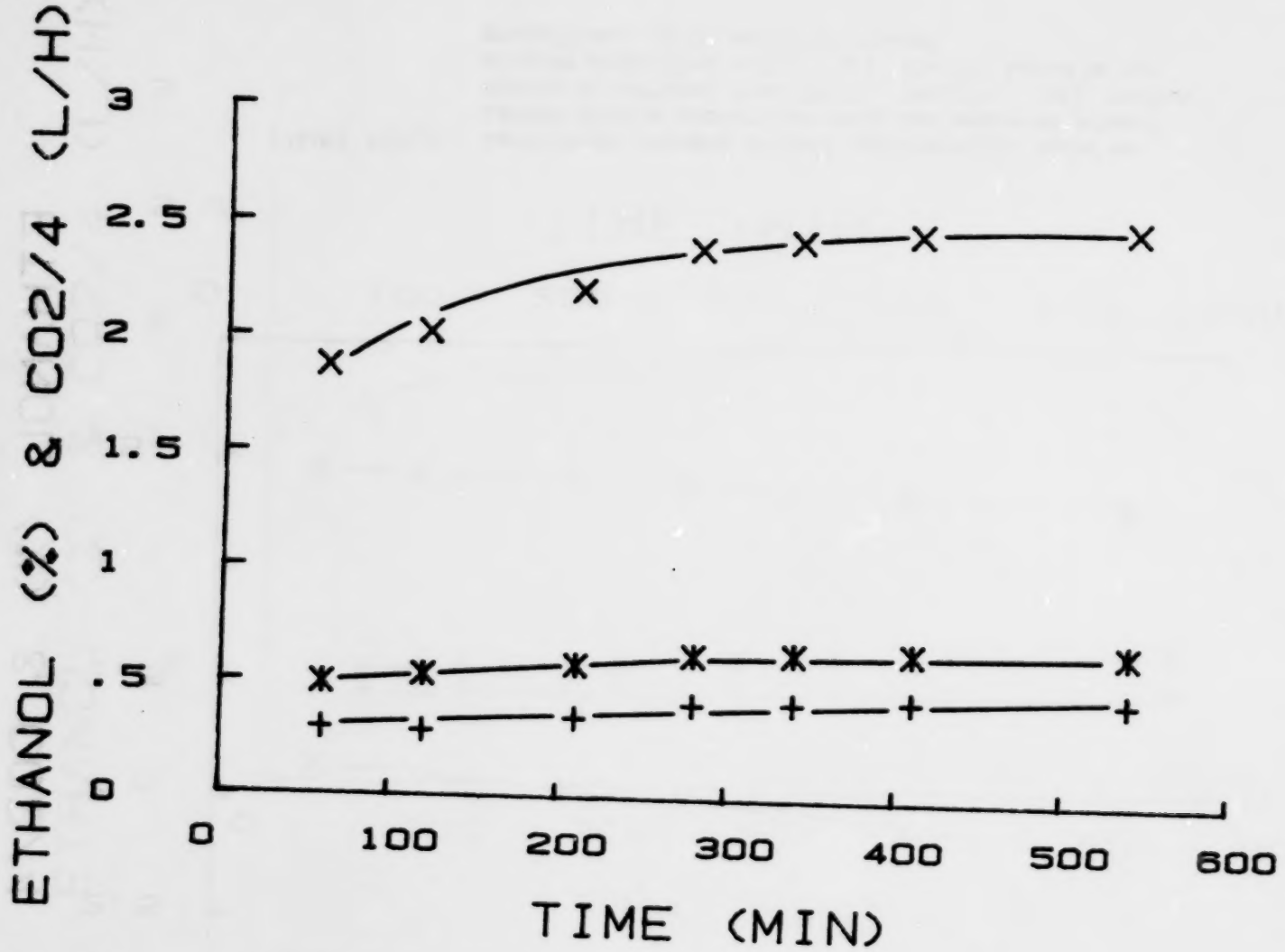

FIGURE 41(c): Correlation between alcohol concentration based on carbon dioxide production rates and measured ethanol levels in effluent from RAD 1. Symbols: (×) carbon dioxide production rate; (✳) ethanol based on gas production; (+) measured ethanol

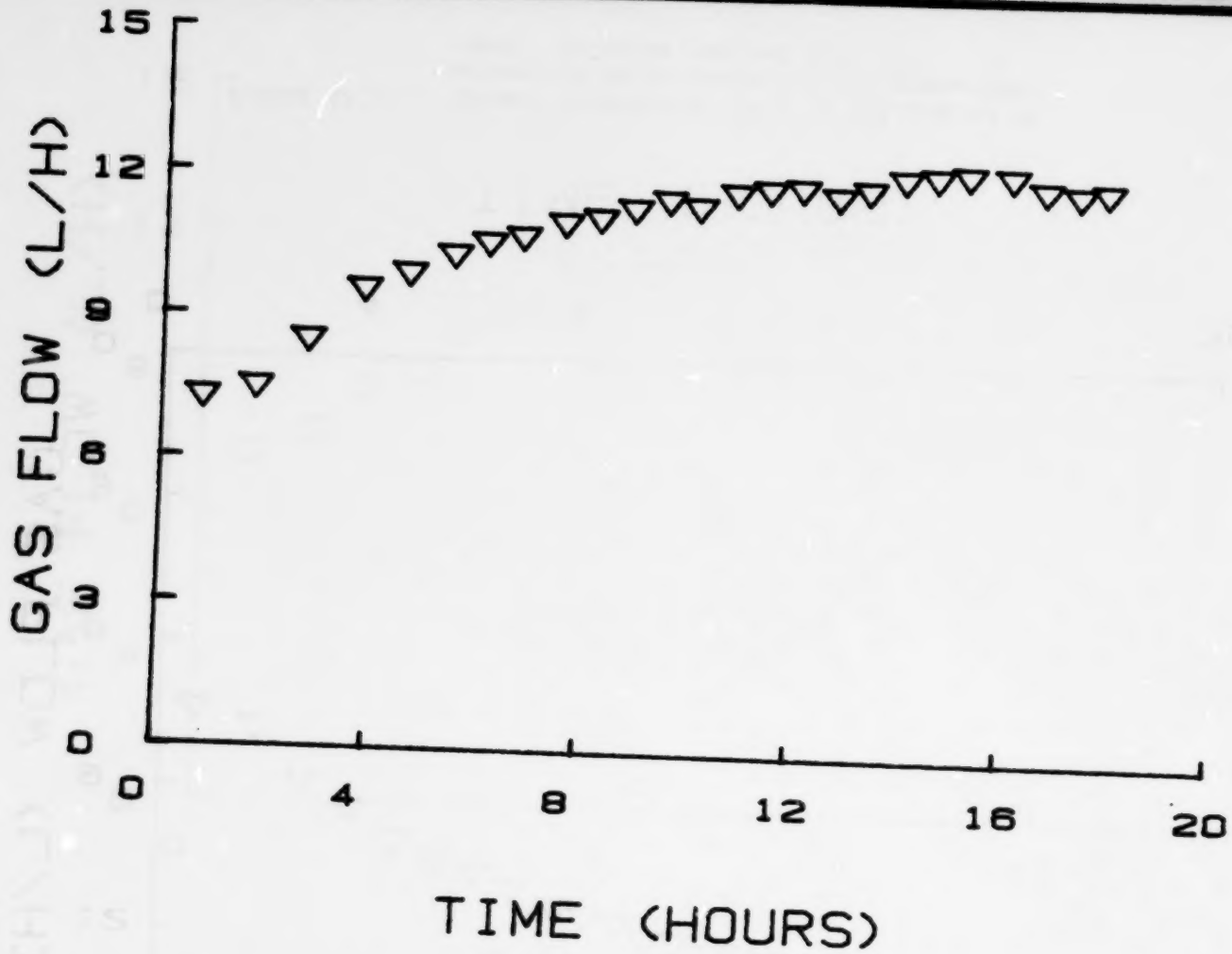

FIGURE 42(a): Dynamic response of TAP 1 to 12% glucose as determined using carbon dioxide production rates. Dilution rate was 0.5 h^{-1}

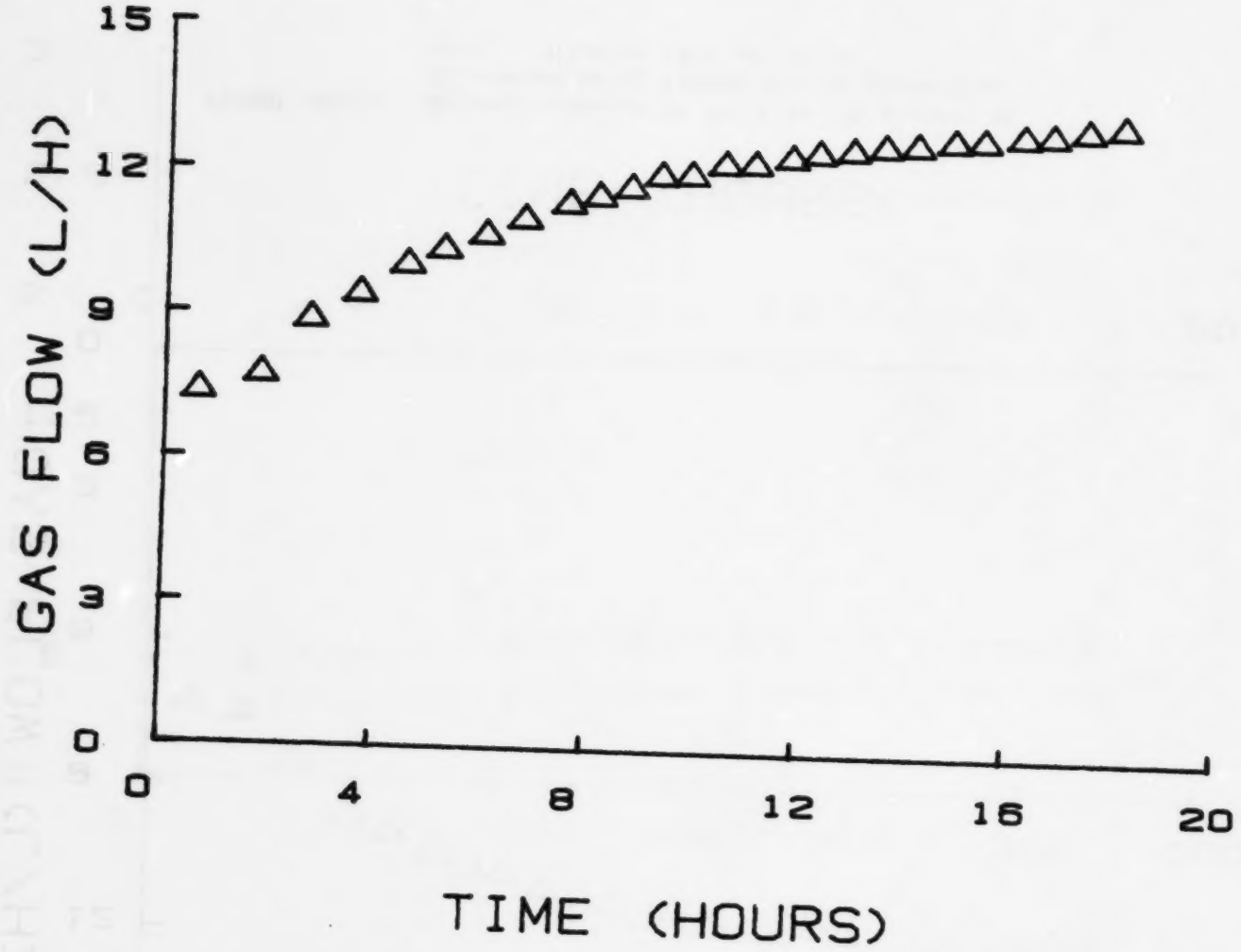

FIGURE 42(b): Dynamic response of TAP 2 to 12% glucose as determined using carbon dioxide production rates. Dilution rate was 0.57 h^{-1}

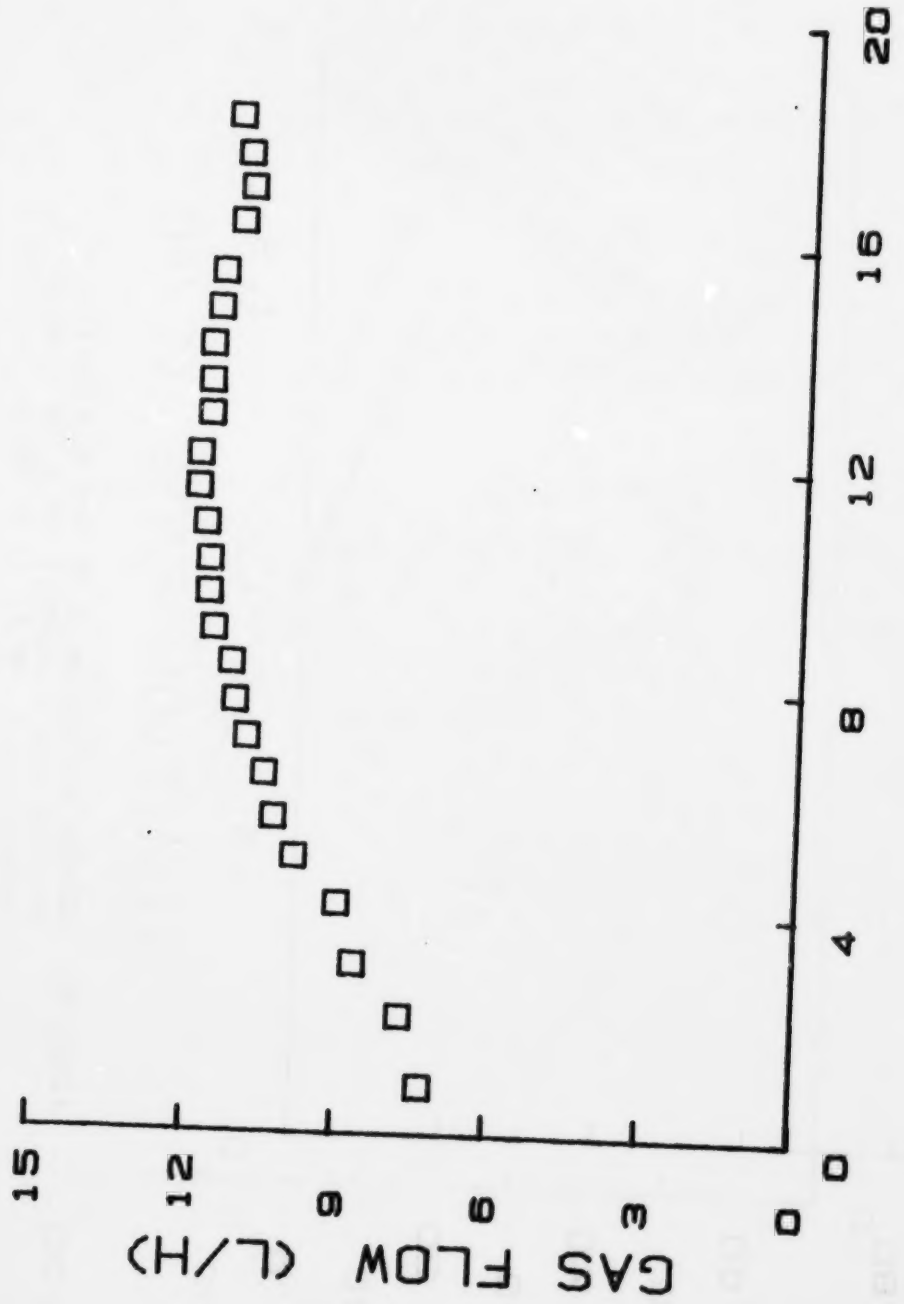

FIGURE 42(c): Dynamic response of RAD 2 to 12% glucose as determined using carbon dioxide production rates. Dilution rate was 0.45 h^{-1}

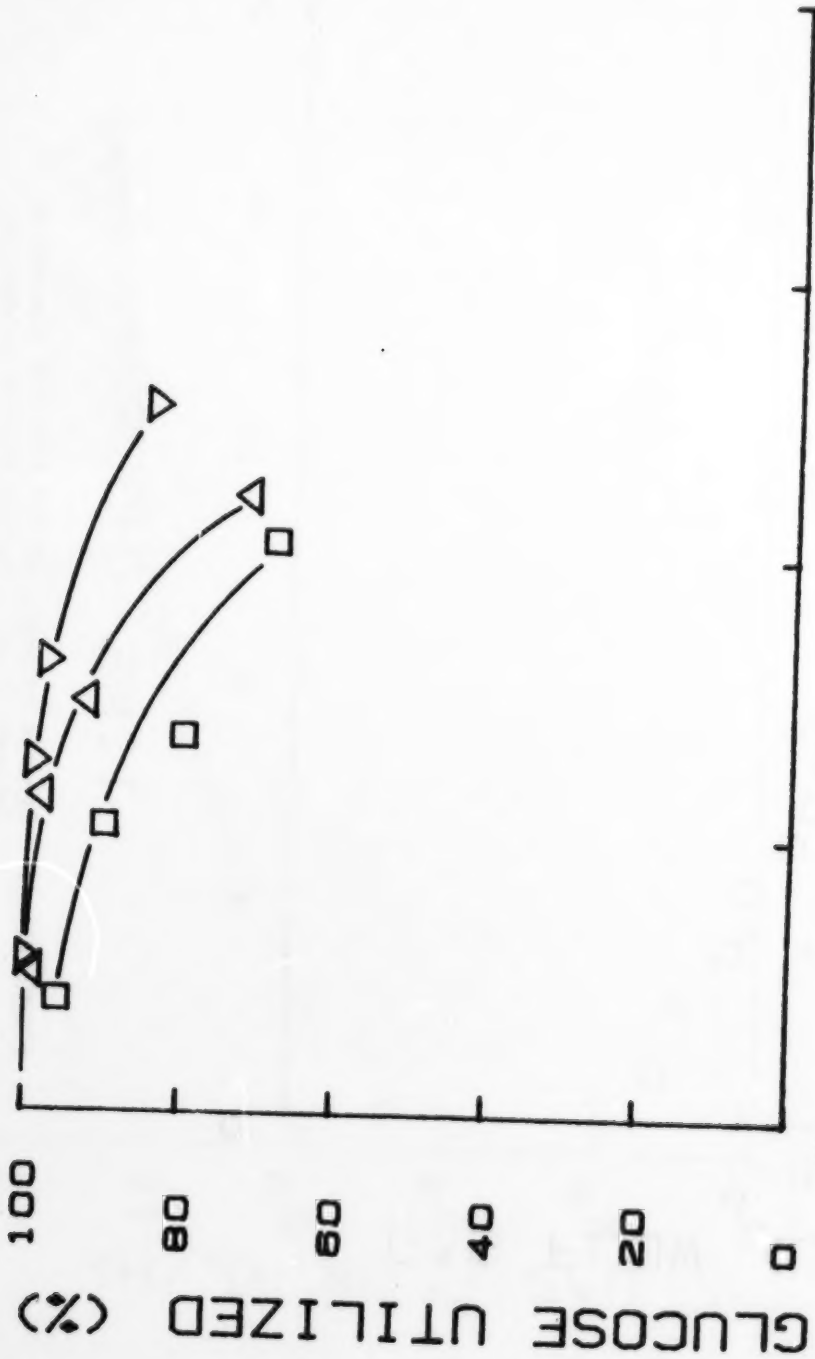

FIGURE 43: Glucose utilization at 8% feed as a function of dilution rate in reactors TAP 1, TAP 2 and RAD 2. Symbols: (△) TAP 1; (▽) TAP 2; (□) RAD 2

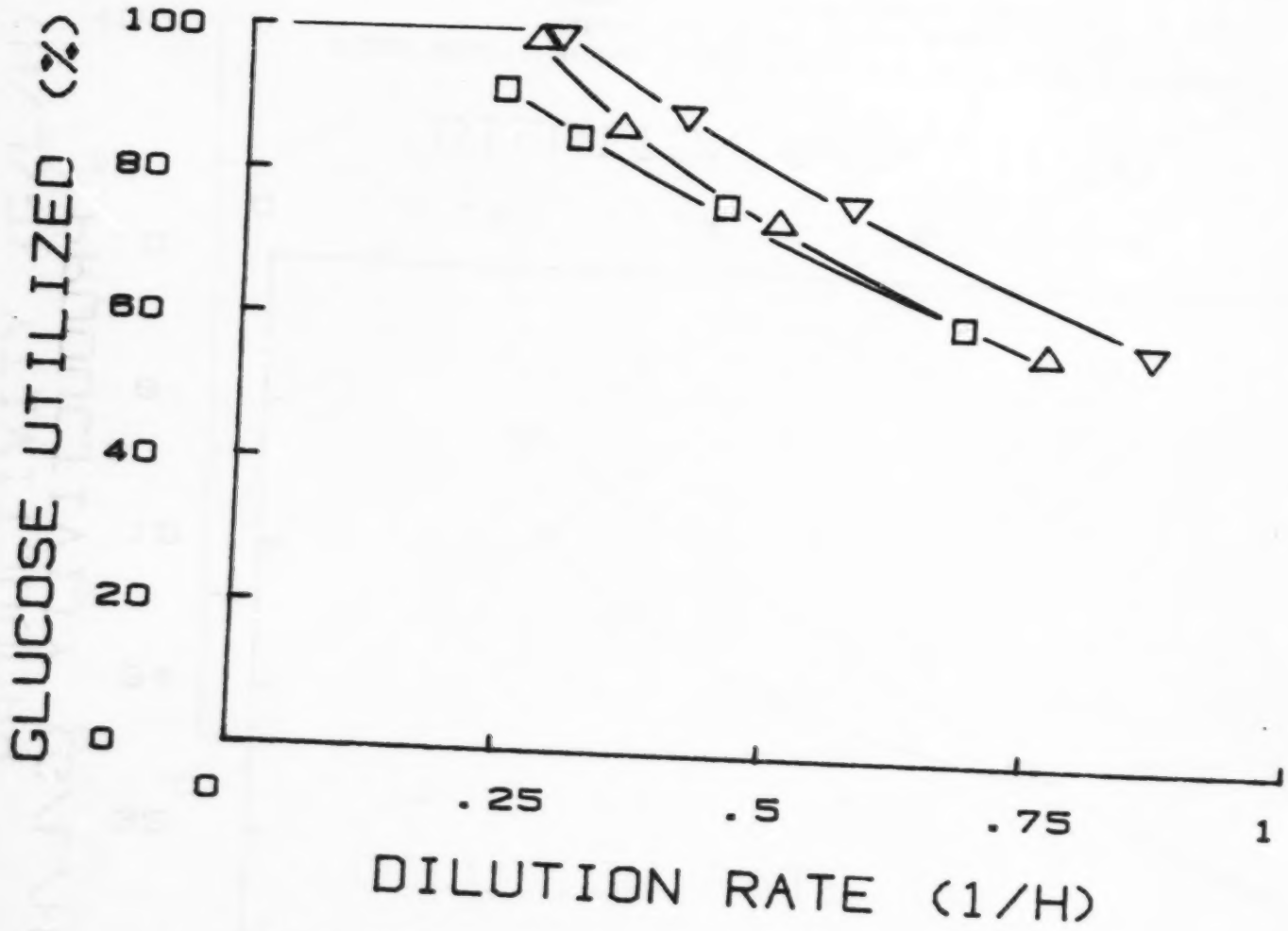

FIGURE 44: Glucose utilization at 12% feed as a function of dilution rate in reactors TAP 1, TAP 2 and RAD 2. Symbols: (△) TAP 1; (▽) TAP 2; (□) RAD 2

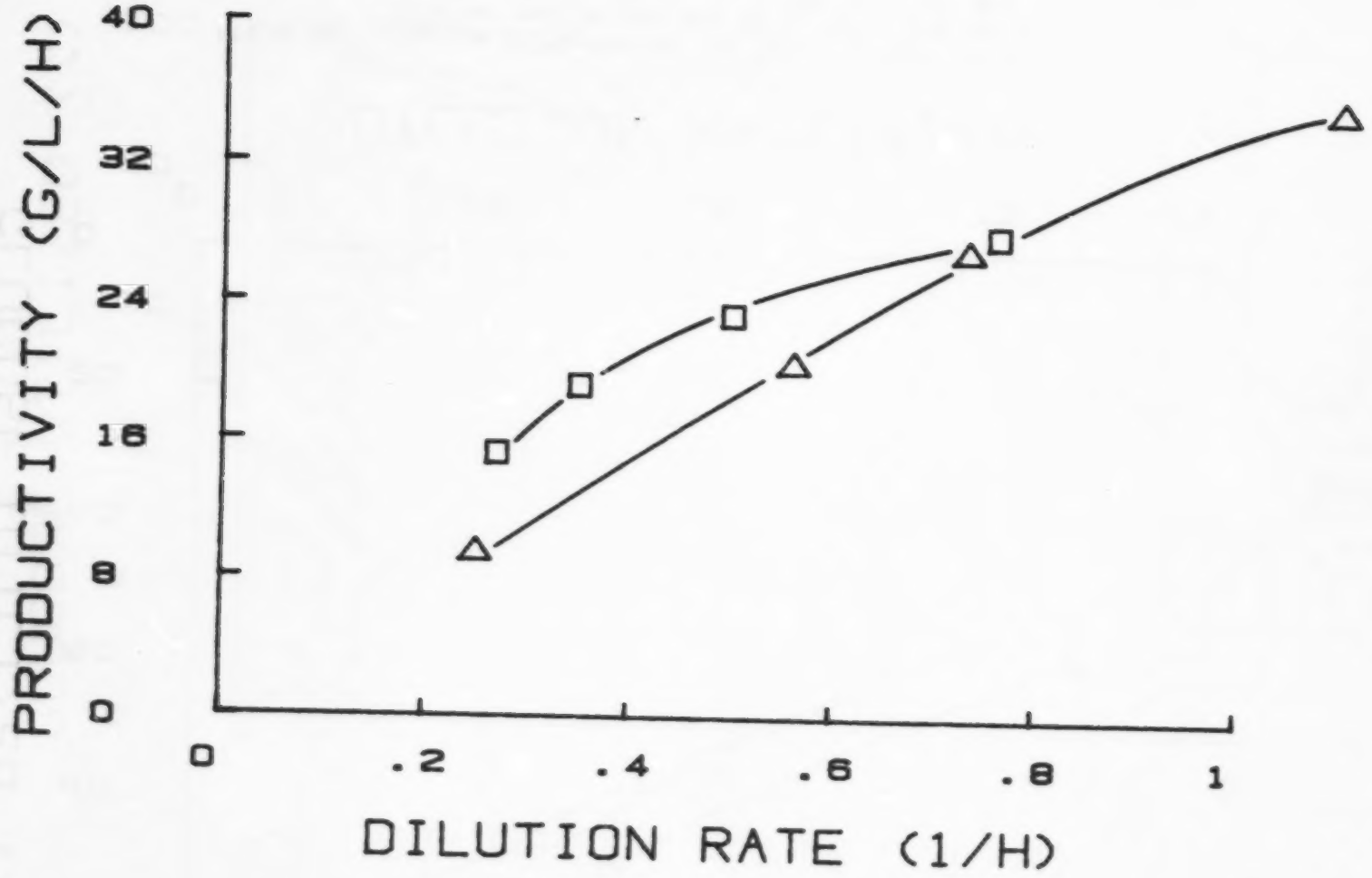

FIGURE 45(a): Alcohol productivities for TAP 1 based on effluent ethanol and carbon dioxide production rates. Symbols: (△) at 8% glucose feed; (□) at 12% glucose feed

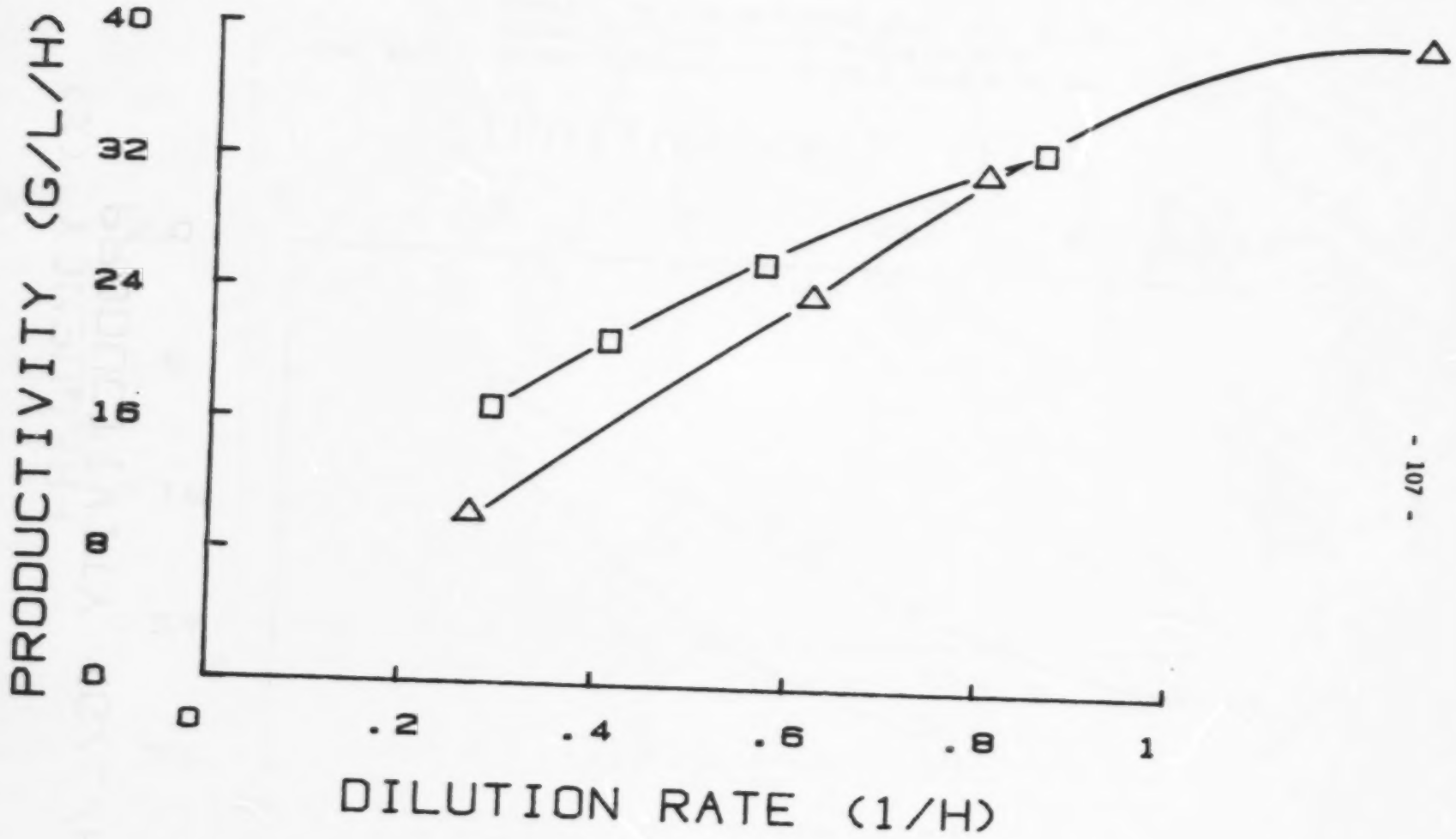

FIGURE 45(b): Alcohol productivities for TAP 2 based on effluent ethanol and carbon dioxide production rates. Symbols: (△) at 8% glucose feed; (□) at 12% glucose feed

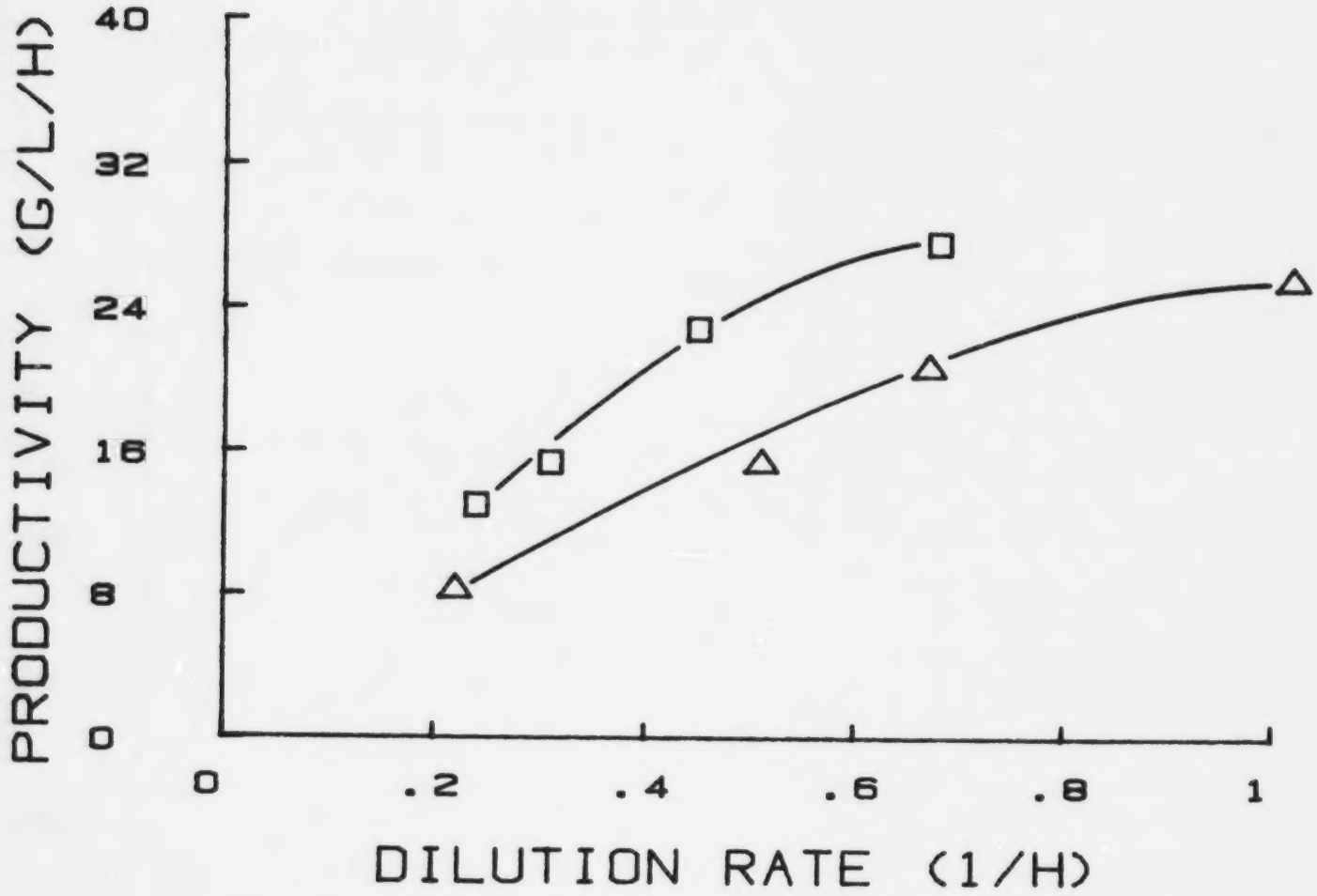

FIGURE 45(c): Alcohol productivities for RAD 2 based on effluent ethanol and carbon dioxide production rates. Symbols: (△) at 8% glucose feed; (□) at 12% glucose feed

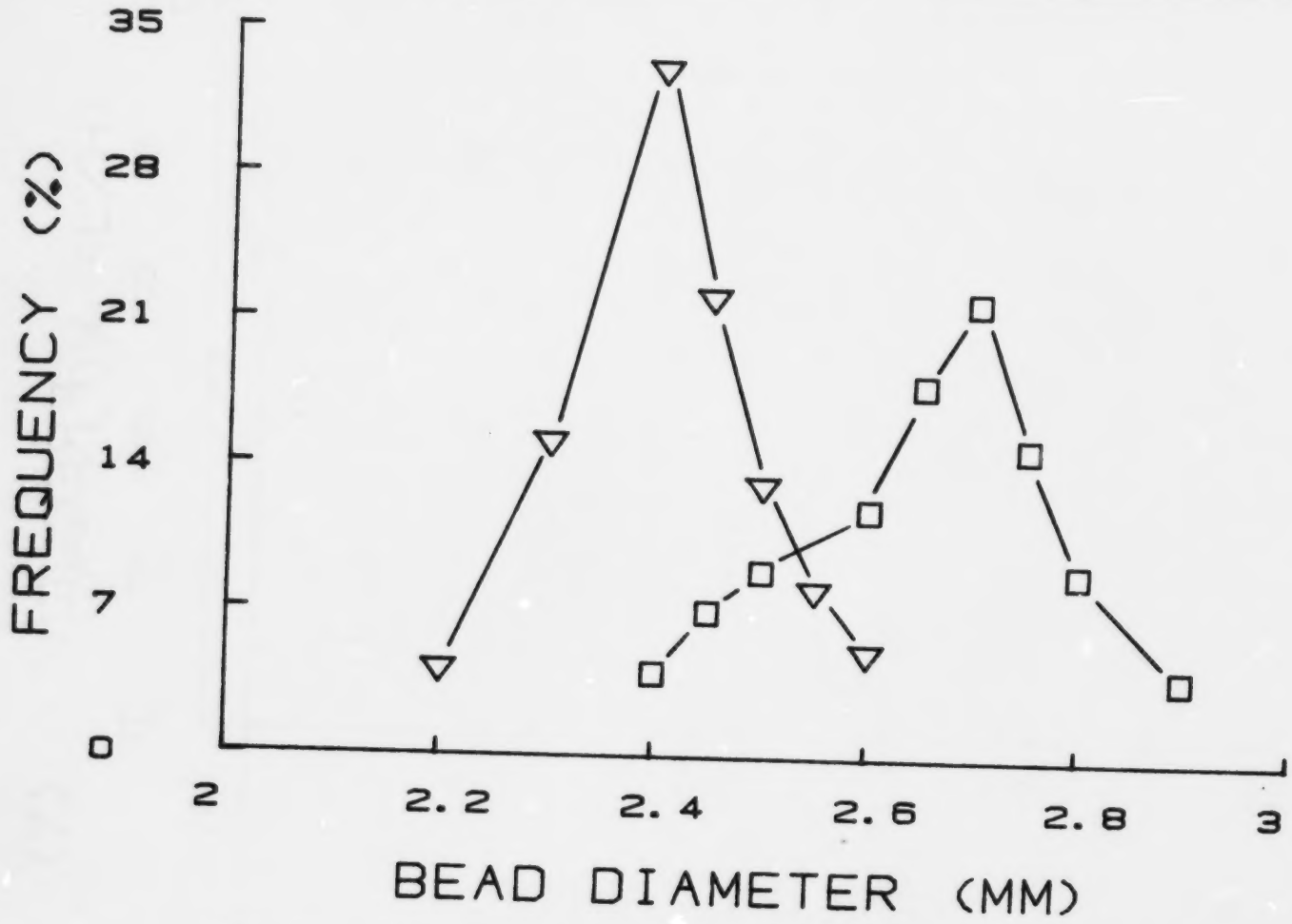

FIGURE 46: Size distribution of yeast-containing calcium alginate beads at various times after initial preparation and use. Symbols: (▽) non-incubated beads; (□) beads incubated in 5% glucose medium at 30°C for four days; (overleaf) (△) beads from TAP 2 after six days operation on either 8% or 12% glucose medium

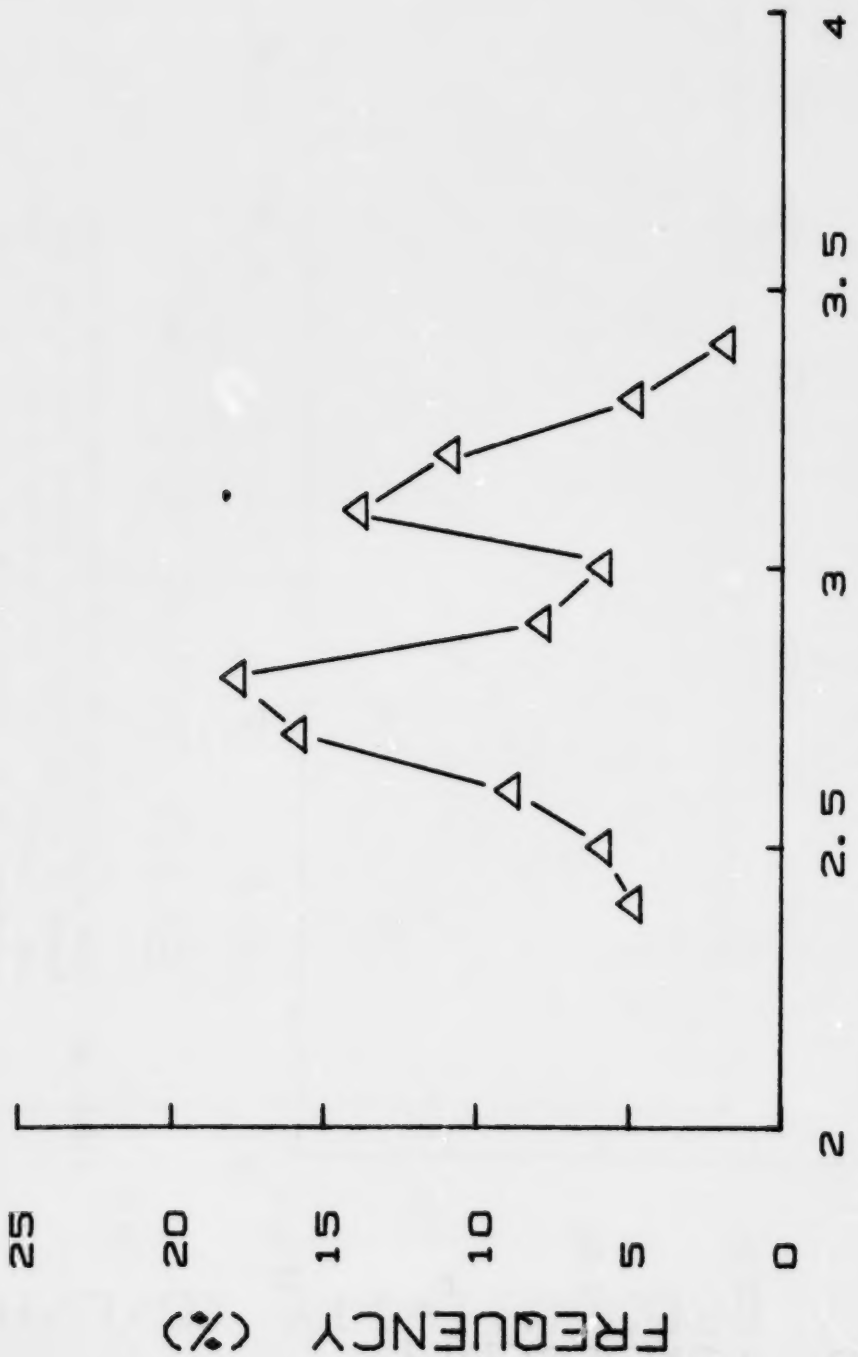

FIGURE 46 (continued)

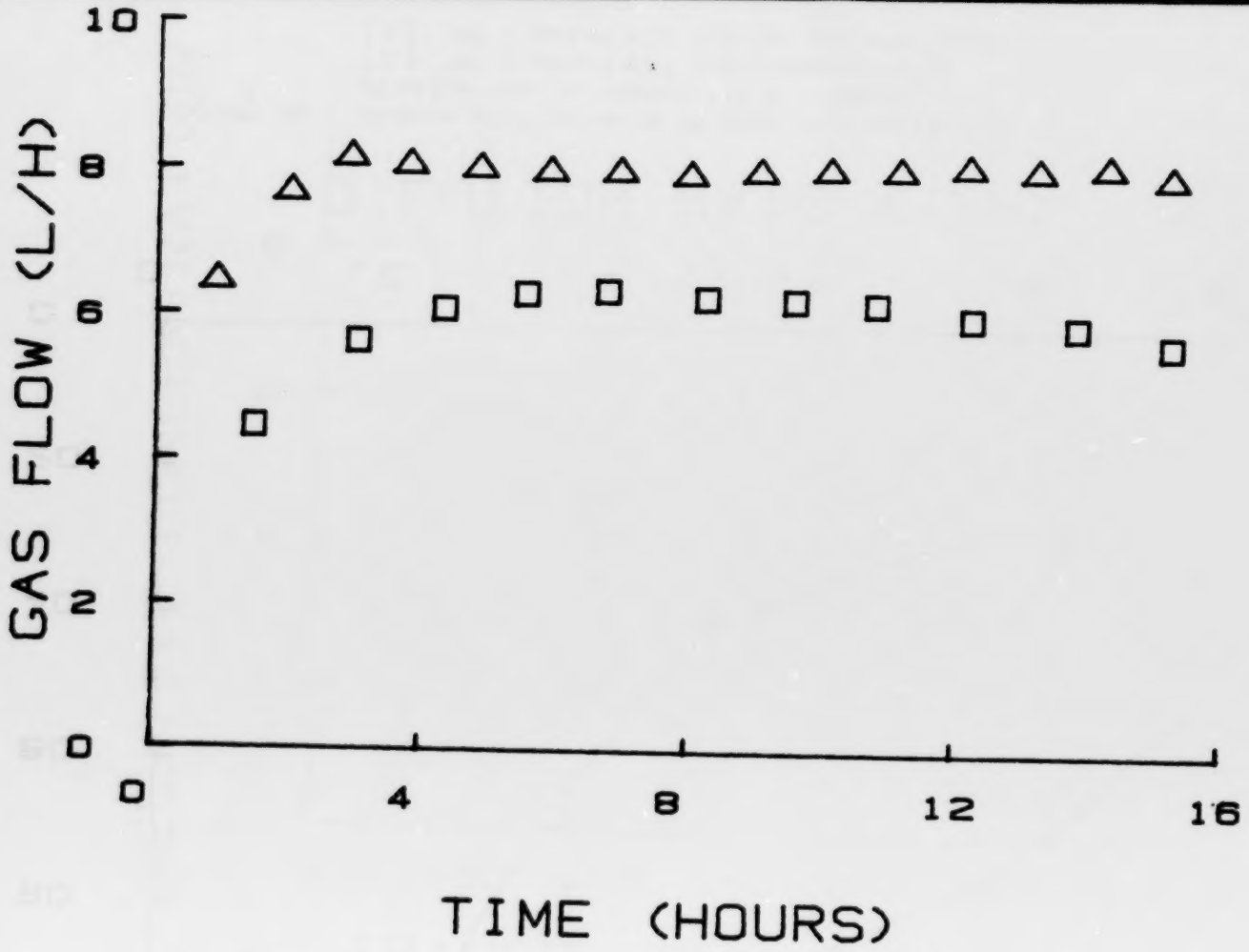

FIGURE 47: Dynamic response of TAP 1 as reflected by carbon dioxide production rate. Reactors were run on 8% glucose medium. Symbols: (□) TAP 1 packed with ion-exchange resin and operated at a dilution rate of 0.52 h^{-1} (△) TAP 1 packed with calcium alginate beads and operated at a dilution rate of 0.36 h^{-1}

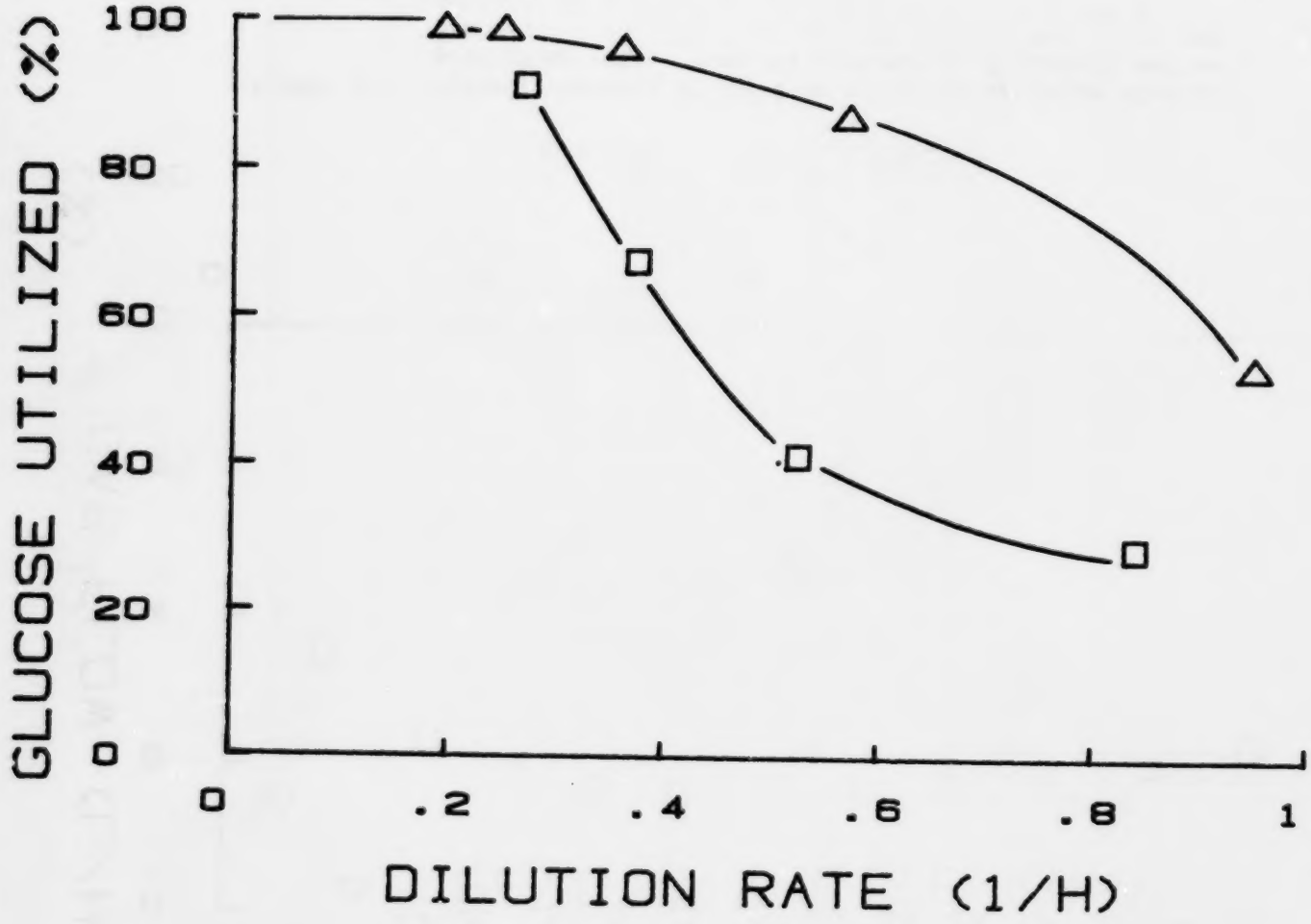

FIGURE 48: Glucose utilization at 8% feed as a function of dilution rate in reactor TAP 1. Symbols:
(□) TAP 1 packed with ion-exchange resin;
(△) TAP 1 packed with calcium alginate beads

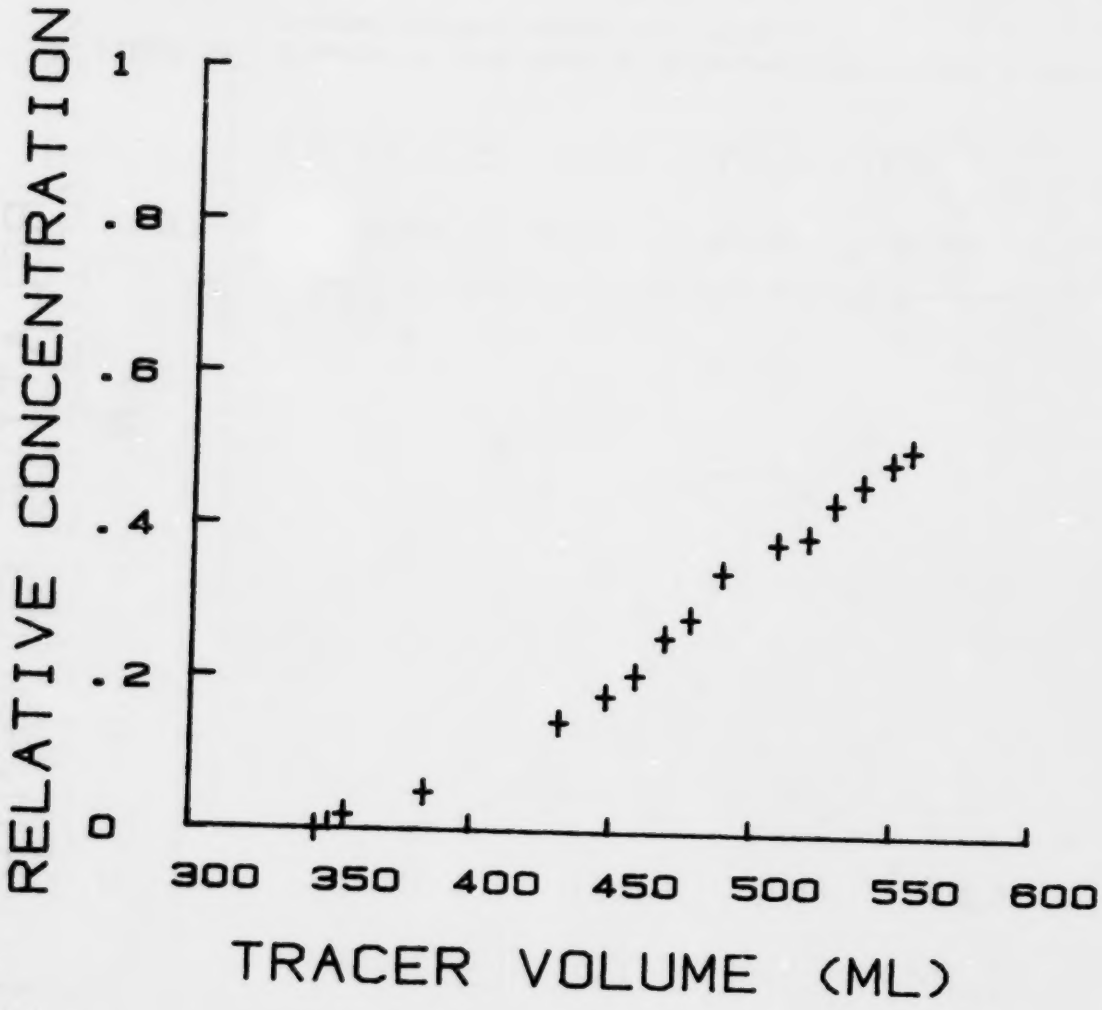

FIGURE 49: Response of step input of 5% isopropanol into TAP 1 containing ion-exchange immobilized yeast cells

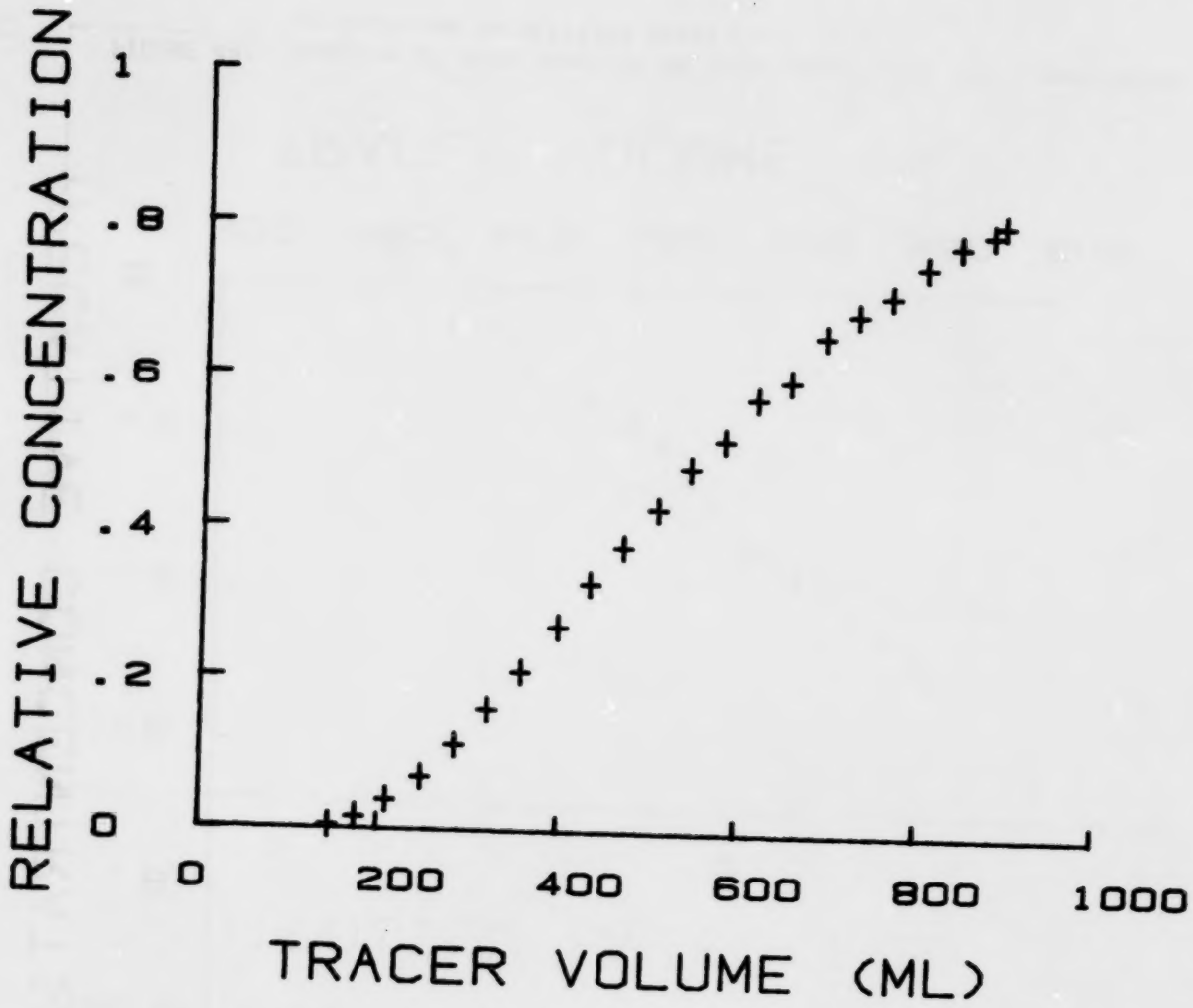

FIGURE 50: Response of step input of 5% isopropanol into TAP 1 containing calcium alginate immobilized yeast cells

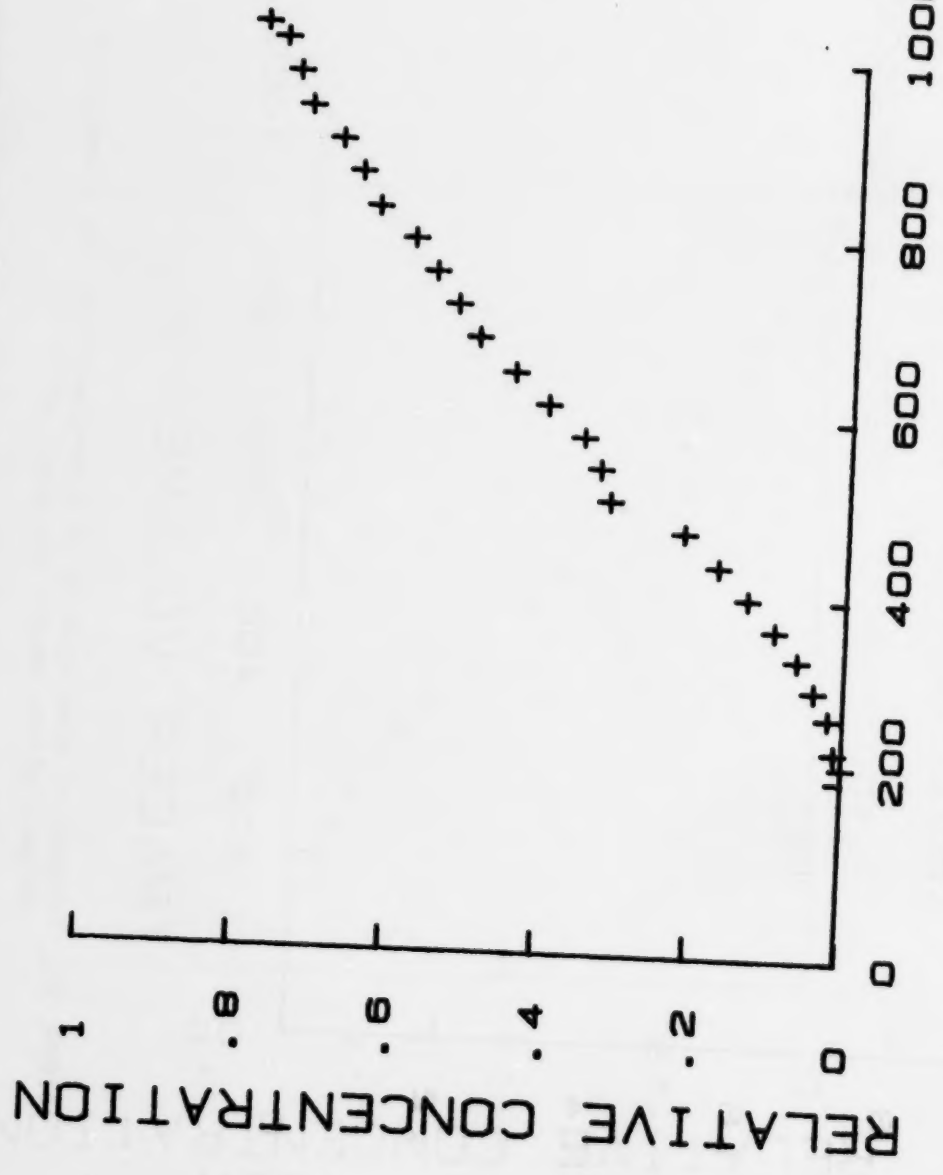

FIGURE 51: Response of step input of 5% isopropanol into TAP 2 containing calcium alginate immobilized yeast cells

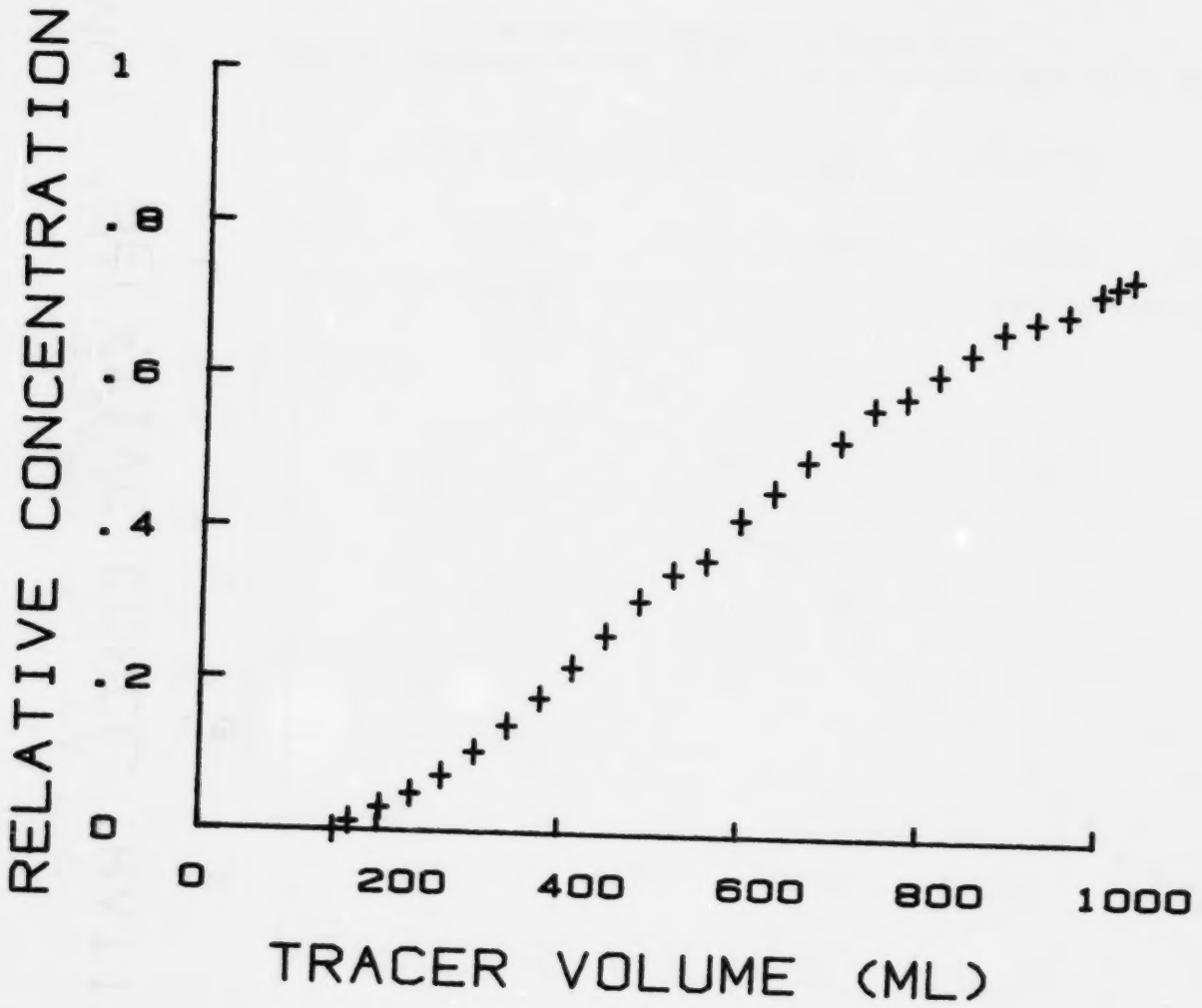

FIGURE 52: Response of step input of 5% isopropanol into TUB 1 containing calcium alginate immobilized yeast cells

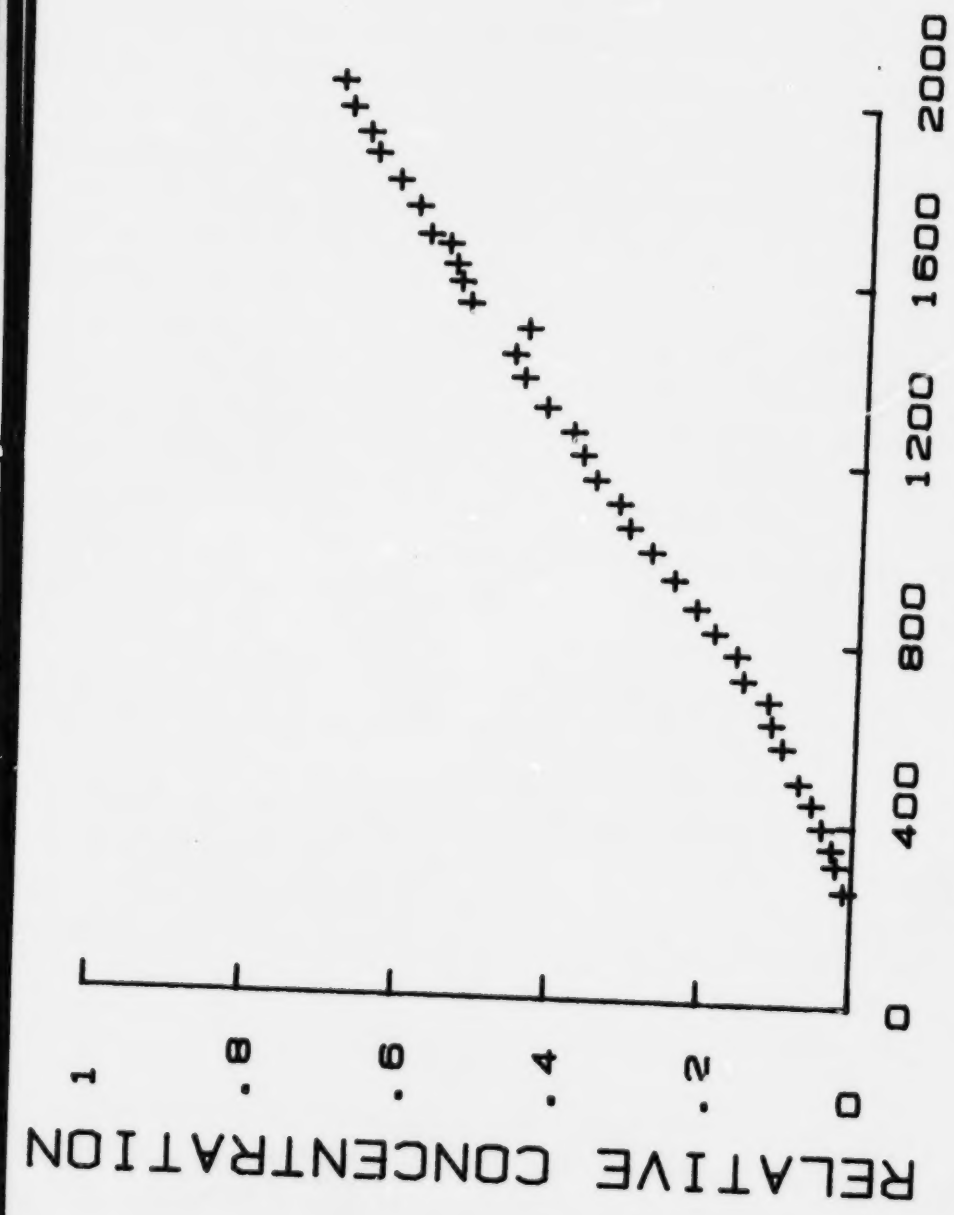

FIGURE 53: Response of step input of 5% isopropanol into RAD 1 containing calcium alginate immobilized yeast cells

APPENDIX 1
Longer-Term Operation of Reactors

Introduction

During a one-month extension of this contract, the longer-term performance of the short tapered-bed reactor as well as the shorter radial-flow reactor were evaluated. The former reactor was evaluated using both calcium alginate immobilized yeast cells and yeast cells which had been absorbed/immobilized using the ion-exchange resin. The latter reactor was evaluated using only the ion-exchange resin immobilization technique. These reactors were chosen as the results obtained previously indicated these units to be the most effective units of the ones tested for the fermentation.

The use of the two immobilization techniques permitted the evaluation of the operation of the short tapered-bed reactor using two different particle sizes in the reactors -- alginate beads of 2.7 mm average diameter; ion-exchange resin of 0.5 - 1.3 mm diameter. This comparison also permitted the continuous evaluation of the two immobilization techniques for a longer period of time -- 21 days. The use of the radial-flow reactor was felt to be worthwhile as this would also permit the concurrent comparison of the two different geometries with little additional effort required. Previous studies using the alginate encapsulated yeast in this reactor had resulted in low productivities wich were attributed to channelling in the reactor. Packing the non-deformable resin more tightly into the reactor might permit a more valid comparison of the geometry of the reactor with the others used in the overall study.

Cell Immobilization and Reactor Packing

Calcium alginate beads containing Saccharomyces cerevisiae NRC 202076 were prepared as described in the main report (page 18). The tapered-bed reactor was wet-packed with 400 ml (displaced volume) of freshly incubated beads. The reactor was then maintained at 30°C and operated on 8% glucose medium at an average dilution rate of 0.63 h^{-1} (based on reactor volume) for a period of 21 days.

Prior to loading the other two reactors with ion-exchange resin, the resin was treated with 0.5% sodium hypochlorite according to the manufacturer's suggested method of preparation. After wet-packing the resin into the reactors, the resin beds were thoroughly washed with distilled water. The volume of resin in the tapered reactor was 510 ml (displaced volume) and that in the radial

reactor was 620 ml (displaced volume). The initial immobilization technique was carried out by recirculating an actively growing culture through the reactors for a period of 48 hours (16 litres of 8% glucose medium). The reactors, maintained at 30°C, were then fed an 8% glucose medium. The initial dilution rates were similar to that used in the alginate system. As will be discussed, these were decreased as a result of a drop in reactor performance.

Results

The operating conditions and results obtained during this longer term run are presented in Tables A1 (TAP 1 -- alginate), A2 (TAP 1 -- resin) and A3 (RAD 1--resin). Averaged values of the gas production rates obtained from the computer-interfaced gas meters are presented in Figures A1, A2, and A3.

The initial dilution rates (based on reactor volumes) were established at 0.62 h^{-1} (TAP 1 -- alginate), 0.54 h^{-1} (TAP 1 -- resin), and 0.64 h^{-1} (RAD 1 -- resin). Two motors were used to run the pump heads, one for the alginate reactor and another for the two resin reactors. The difference in the dilution rates are, therefore, due either to a difference in motor speed, or a difference in pump capacity. These dilution rates resulted in maximum steady-state gas production rates of 12.7 $L.h^{-1}$ (TAP 1 -- alginate), 8.9 $L.h^{-1}$ (TAP 1 -- resin), and 7.7 $L.h^{-1}$ (RAD 1 -- resin) obtained after 5 days, 3 days and 3 days respectively. This indicates that, although the resin immobilization procedure achieves maximum cell loading much more rapidly than does the alginate procedure, the level of active ethanol-producing cells is only 60% - 75% as great. As had been observed previously, the level of free cells eluted from the resin reactors were approximately twice that obtained from the alginate reactor.

After approximately one week of operation, it was noticed that the activity of the resin reactors was deteriorating and an attempt was made to conserve the degree of conversion by decreasing the dilution rates. Although initially this was effective, after an initial restabilization, the levels of conversion again decreased. The dilution rates on the resin reactors were, therefore, reduced to a value of approximately one-half that of the initial values. No such dramatic effect was observed with the calcium alginate immobilized yeast cells. As a result of wear in the feed pump tubing, there was some variation in the average

dilution rates in the alginate reactor and a decrease (12%) in the flow rate during the course of the run. Maximum activity (12.7 $L.h^{-1}$) for this system occurred after one week of operation with a final (21 days) activity of approximately 75% of this value.

Of particular interest from an operational point is the fact that the alginate reactor never had a pressure drop in excess of 14 kPa and that the average value during the run was less than 10 kPa. On the other hand, the pressure drop in the tapered bed reactor containing the resin-immobilized yeast cells increased steadily, even though the dilution rates were decreased. The final differential pressure obtained in this reactor was 114 kPa. The pressure drops in the radial-flow reactor using this latter immobilization procedure, while giving the same conversions, were consistently one-half of those in the tapered-bed reactor.

It should be noted that the mass balances on these systems were not very good at the lowest conversions achieved. It is felt that the error lies with the glucose assay. The extremely large dilution required for the glucose determination seems to consistently result in a wide variation in the data.

At the end of the experiment, the reactors were disassembled and the packings were evaluated. In the alginate reactor, the beads were solidly packed, but not so tightly that they had been compressed or deformed. The beads were firm and as before larger beads were found in the lower sections of the reactor. Dry weight analysis of the beads showed that they contained approximately 67 g of yeast cells. The weight of free cells in this reactor was found to be 11 g.

When the tapered-bed resin reactor was dismantled, the resin bed was seen to be evenly packed, with no obvious signs of channelling. The sides of the reactor were covered with a relatively uniform layer of yeast cells (approximately 2 mm thick) and the bottom of the bed contained a layer of cells approximately 1.5 cm deep. Dry weights of yeast cells were: free cells - 72 g; resin-associated cells - 6 g.

The radial-flow reactor resin bed was similar in appearance to the other. No accumulation of yeast cells was observed on any of the surfaces. Dry weights of yeast cells which were obtained were: free cells - 74 g; resin-associated cells - 7 g. The trend in these results are very similar to those observed with the previous runs.

CONCLUSIONS

As had been predicted, under similar operating conditions, the use of a radial-flow reactor results in lower pressure drops through the packed bed than does the use of a tapered bed reactor. Additionally, as indicatewd from the results for the alginate bed entrapped yeast cells, the pressure drop is substantially reduced when a larger packing is used.

The results indicate that the use of the ion-exchange resin for cell immobilization seems to be more of a "filtration" process rather than a long-term absorption process. In either case, additional studies to clarify the mechanism of immobilization would be of interest. The use of alginate immobilized yeast resulted in good long term activity with little operational difficulties in the tapered-bed reactor. As no modifications were made to the basic medium used for these continuous rermentations, it is suggeested that the 25% loss in activity was likely a result of a nutrient deficiency and not a result of the design of the reactor. Additional studies with this or other yeast in which various growth parameters are evaluated both with free and immobilized cells would be of interest.

There appears to be no inherent difficulty in using the yeast-containing calcium alginate beads in this tapered bed reactor for extended periods of time. This would suggest that the forces present on the alginate beads found in tubular packed-bed reactors are much greater than those experienced in the variable-area reactors. As such, this type of reactor would be more universally applicable for both immobilized enzyme and cell reactions. It is therefore recommended that these reactor systems be more thoroughly investigated.

TABLE A1: Operational parameters[1] and results obtained during long term continuous fermentation of 8% glucose with calcium alginate immobilized yeast in TAP 1.

Time (days)	Dilution (h^{-1})	Ethanol (%)	Residual Glucose (%)	Gas Rate (L/h)	Pressure Drop (kPa)	Effluent Cell Weight (g/100ml)	Productivity[2] (g EtOH/L/h)
1	0.62	1.51	5.3	5.62	5.3	0.036	9.4
2	0.67	2.22	3.5	9.44	3.5	0.051	14.9
3	0.66	2.81	1.6	11.76	5.3	0.055	18.5
4	0.67	3.14	1.4	12.23	6.0	0.053	21.0
5	0.67	3.05	1.3	12.74	5.3	0.047	20.4
6	0.67	3.03	1.5	12.30	5.3	0.054	20.3
7	0.67	3.10	1.3	12.13	5.3	0.050	20.8
8	0.67	2.76	1.7	12.07	5.3	0.045	18.5
9	0.67	2.76	1.9	11.69	5.3	0.043	18.5
10	0.67	2.75	2.0	11.43	5.3	0.047	18.4
11	0.65	2.87	1.8	10.73	5.3	0.050	18.7
12	0.65	2.61	2.2	10.28	13.3	0.051	17.0
13	0.64	2.57	2.2	10.35	10.7	0.053	16.4
14	0.62	2.46	2.6	10.33	12.0	0.055	15.3
15	0.62	2.50	2.4	10.10	6.7	0.056	15.5
16	0.61	2.45	2.8	10.19	6.7	0.065	14.9
17	0.60	2.50	2.8	10.07	6.7	0.065	15.0
18	0.60	2.46	2.7	9.53	6.7	0.063	14.8
19	0.60	2.45	2.7	9.21	8.0	0.051	14.7
20	0.59	2.45	2.8	9.06	6.7	0.055	14.5
21	0.59	2.25	3.0	9.02	8.0	0.056	13.3

[1] Values shown are averages of three samples taken over an 8 hour period at the end of each day

[2] Productivities based on reactor volume (1 litre)

TABLE A2: Operational parameters[1] and results obtained during long term continuous fermentation of 8% glucose with ion-exchange immobilized yeast in TAP 1.

Time (days)	Dilution (h^{-1})	Ethanol (%)	Residual Glucose (%)	Gas Rate (L/h)	Pressure Drop (kPa)	Effluent Cell Weight (g/100ml)	Productivity[2] (g EtOH/L/h)
1	0.54	1.10	6.8	5.45	6.7	0.032	5.9
2	0.56	1.64	5.1	7.17	11.3	0.076	9.2
3	0.57	2.16	3.7	8.89	14.0	0.084	12.3
4	0.56	2.48	2.9	8.81	16.0	0.087	13.9
5	0.57	2.14	3.5	8.53	18.7	0.080	12.2
6	0.55	2.45	2.9	7.41	26.7	0.079	13.5
7	0.45	2.10	3.7	7.39	32.0	0.063	9.5
8	0.45	2.14	3.3	7.31	41.3	0.058	9.6
9	0.45	2.42	2.6	7.68	40.9	0.034	10.9
10	0.45	2.78	1.7	8.33	48.7	0.068	12.5
11	0.45	2.88	1.2	8.15	62.0	0.081	13.0
12	0.43	2.67	1.8	6.84	69.8	0.060	11.5
13	0.42	2.63	1.9	6.63	79.3	0.049	11.0
14	0.41	2.32	2.3	6.04	68.9	0.066	9.5
15	0.42	2.15	3.2	5.43	70.6	0.104	9.0
16	0.35	2.00	3.6	4.15	91.3	0.062	7.0
17	0.28	2.28	2.9	3.83	81.0	0.050	6.4
18	0.28	2.06	3.5	3.58	67.2	0.066	5.8
19	0.28	1.97	3.7	3.86	79.3	0.048	5.5
20	0.28	1.99	4.0	3.57	93.0	0.039	5.6
21	0.28	1.89	4.5	3.40	113.7	0.051	5.3

[1] Values shown are averages of three samples taken over an 8 hour period at the end of each day

[2] Productivities based on reactor volume (1 litre)

TABLE A3: Operational parameters[1] and results obtained during long term continuous fermentation of 8% glucose with ion-exchange immobilized yeast in RAD 1.

Time (days)	Dilution (h^{-1})	Ethanol (%)	Residual Glucose (%)	Gas Rate (L/h)	Pressure Drop (kPa)	Effluent Cell Weight (g/100ml)	Productivity[2] (g EtOH/L/h)
1	0.64	1.05	7.4	5.55	6.7	0.063	6.7
2	0.64	1.37	6.7	6.81	6.7	0.060	8.8
3	0.65	1.71	5.2	7.65	8.0	0.092	11.1
4	0.62	1.80	4.4	7.42	8.0	0.101	11.2
5	0.65	1.57	4.9	7.48	8.0	0.084	10.2
6	0.63	1.70	4.8	7.82	9.3	0.085	10.7
7	0.60	2.07	4.2	8.88	12.0	0.104	12.4
8	0.55	2.29	3.1	7.88	13.3	0.086	12.6
9	0.43	2.68	1.7	6.55	15.3	0.081	11.5
10	0.45	2.43	2.8	7.74	22.7	0.083	10.9
11	0.45	2.42	2.6	7.25	16.7	0.103	10.9
12	0.46	2.40	2.8	7.30	24.0	0.085	11.0
13	0.51	2.15	3.3	7.05	26.7	0.091	11.0
14	0.45	2.22	3.3	6.75	25.3	0.082	10.0
15	0.48	2.19	3.5	5.81	30.7	0.084	10.5
16	0.38	2.24	3.0	5.23	36.0	0.078	8.5
17	0.31	2.56	1.9	5.00	36.3	0.091	7.9
18	0.31	2.63	2.3	4.55	36.7	0.102	8.2
19	0.31	2.13	3.1	3.92	48.7	0.122	6.6
20	0.31	1.95	2.9	4.07	42.7	0.076	6.0
21	0.31	1.92	4.1	4.08	41.3	0.081	5.9

[1] Values shown are averages of three samples taken over an 8 hour period at the end of each day

[2] Productivities based on reactor volume (1 litre)

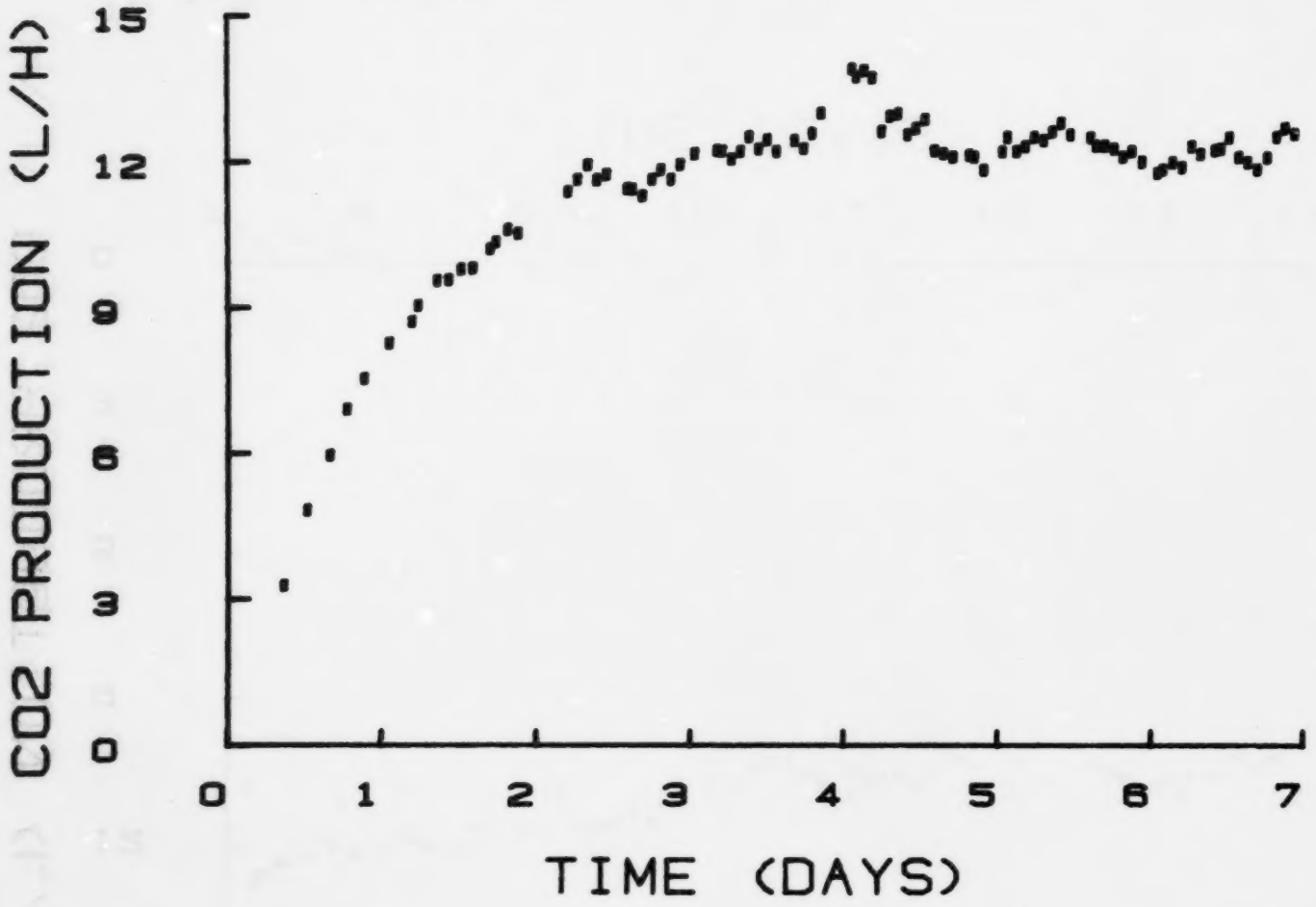

FIGURE A1: Carbon dioxide production rate data for TAP 1 containing calcium alginate immobilized yeast cells

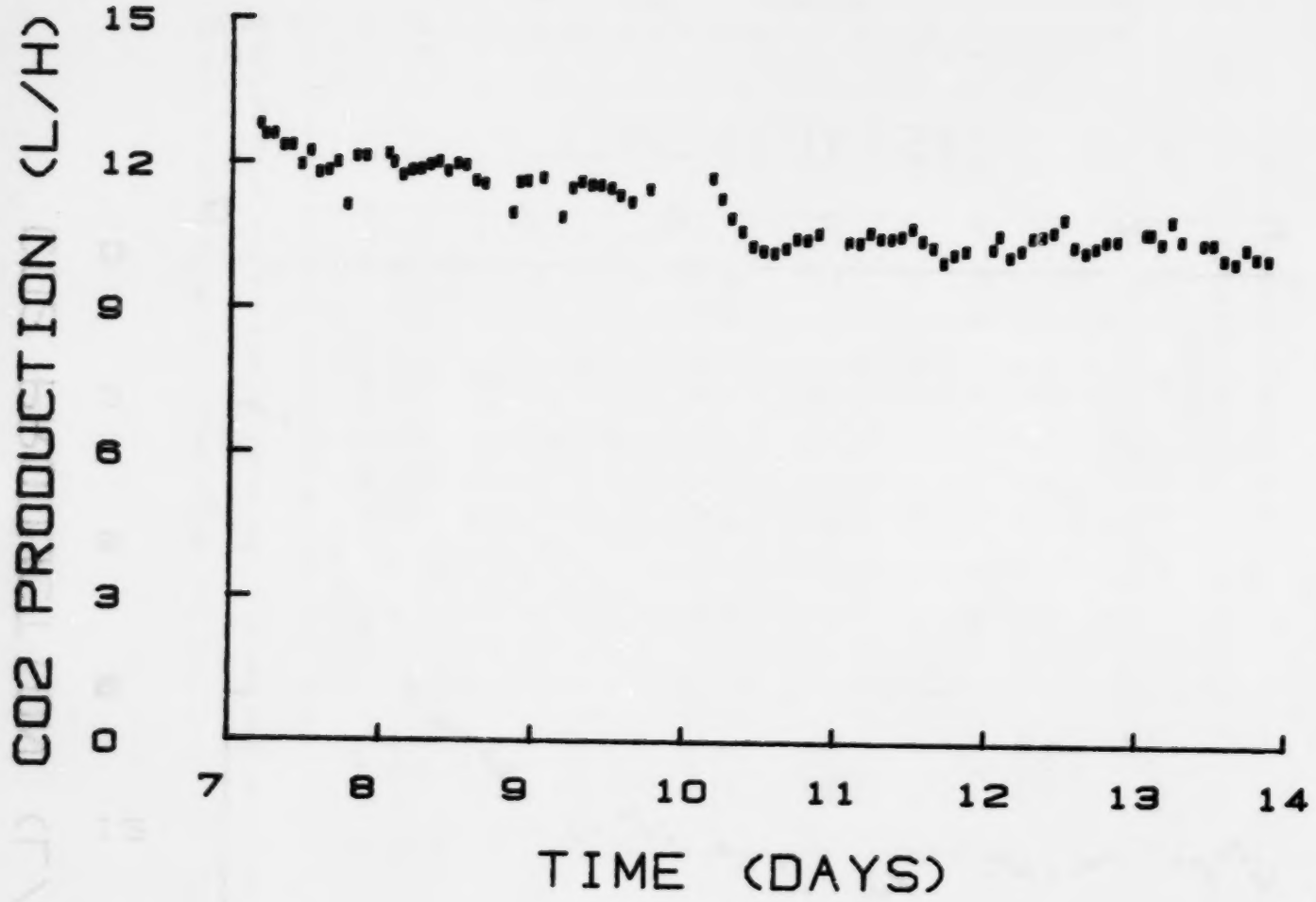

FIGURE A1: (continued)

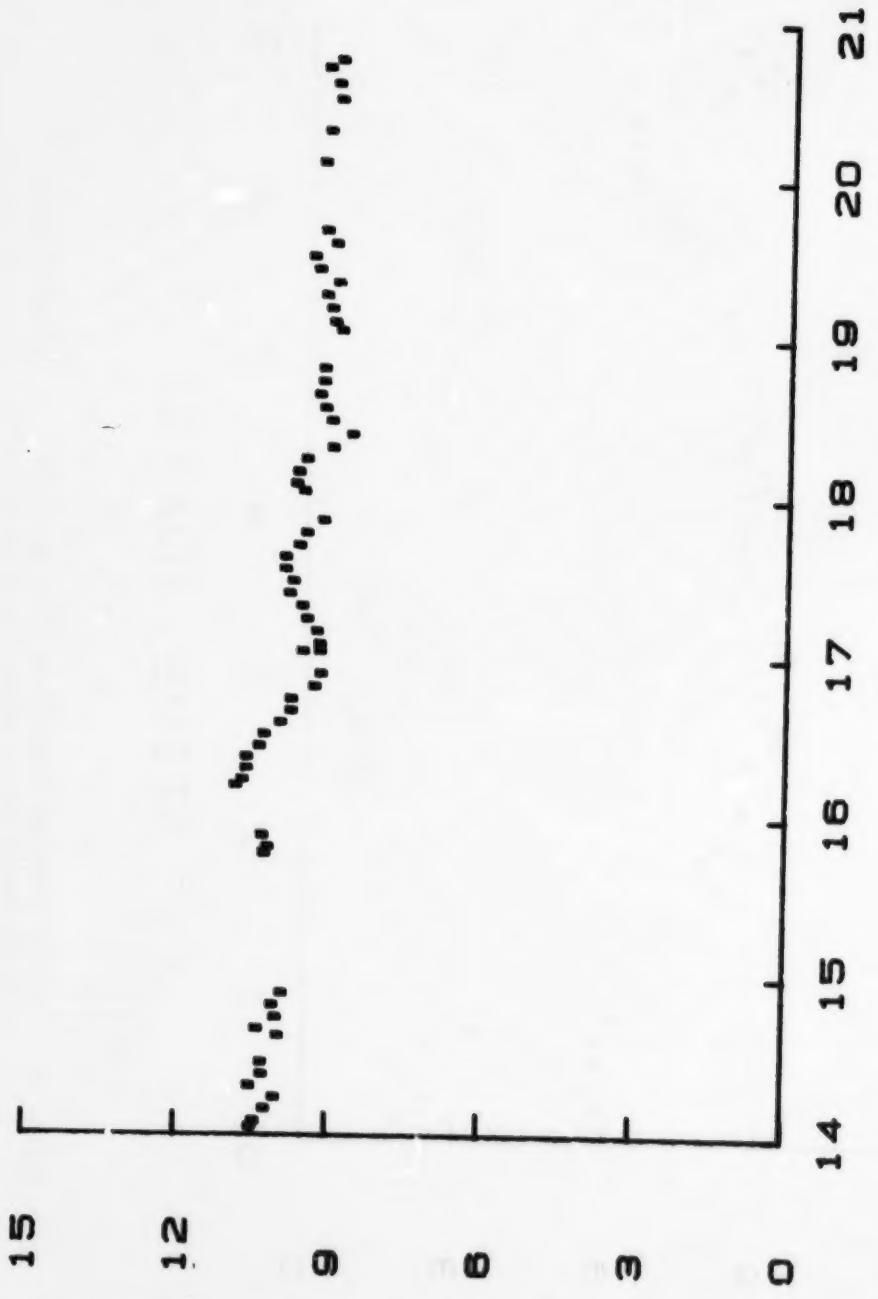

FIGURE A1: (continued)

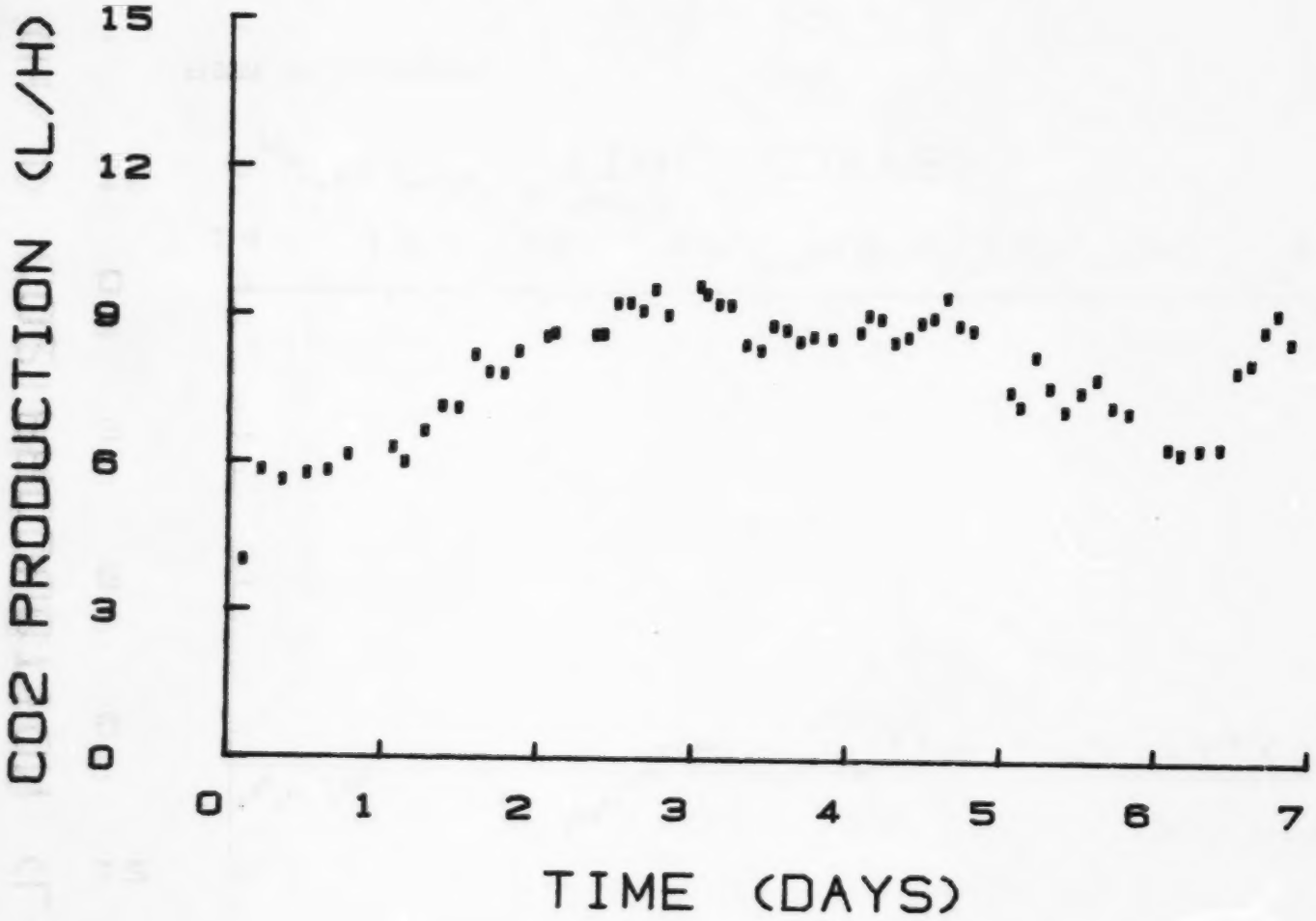

FIGURE A2: Carbon dioxide production rate data for TAP 1 containing ion-exchange resin immobilized yeast cells

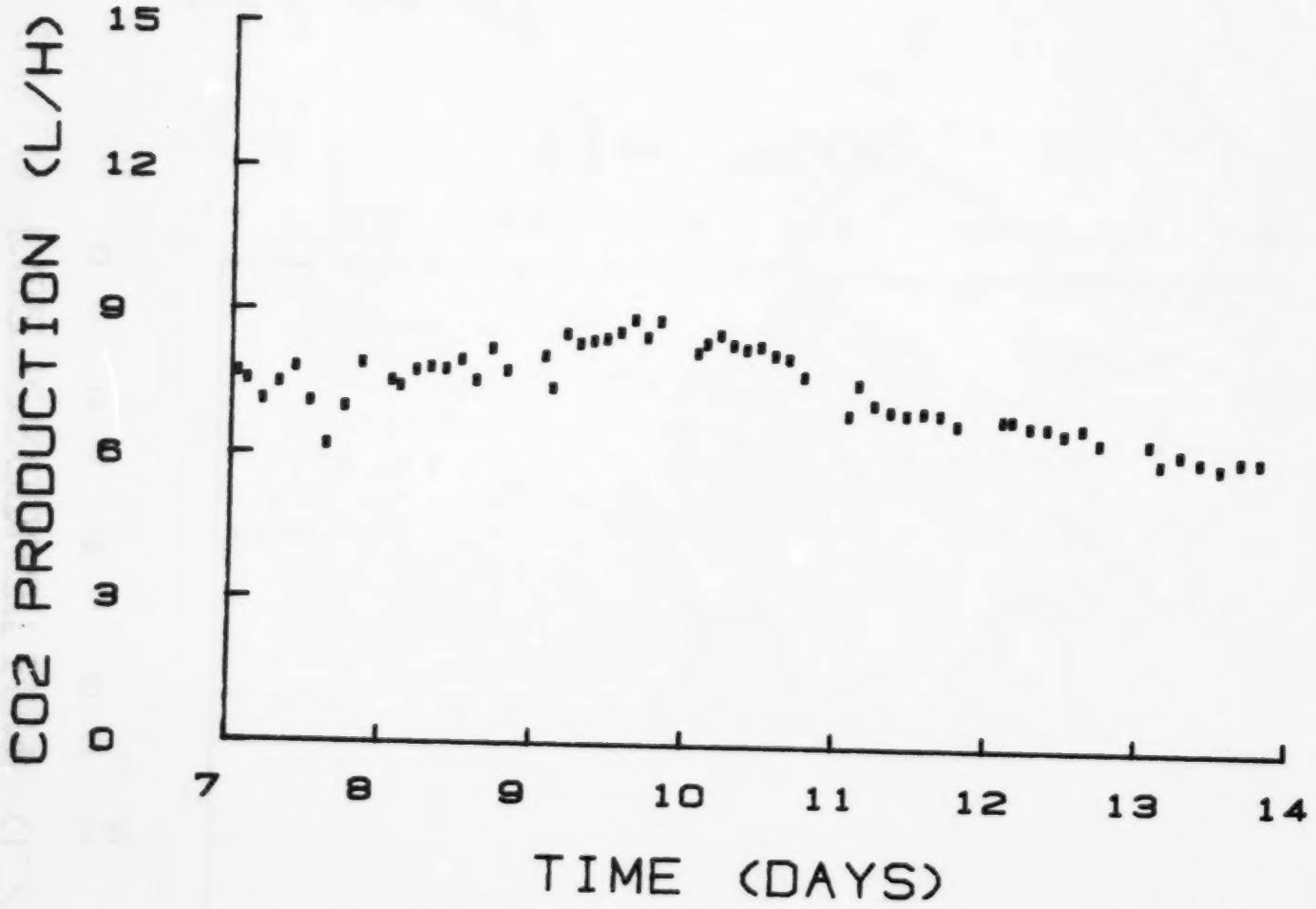

FIGURE A2: (continued)

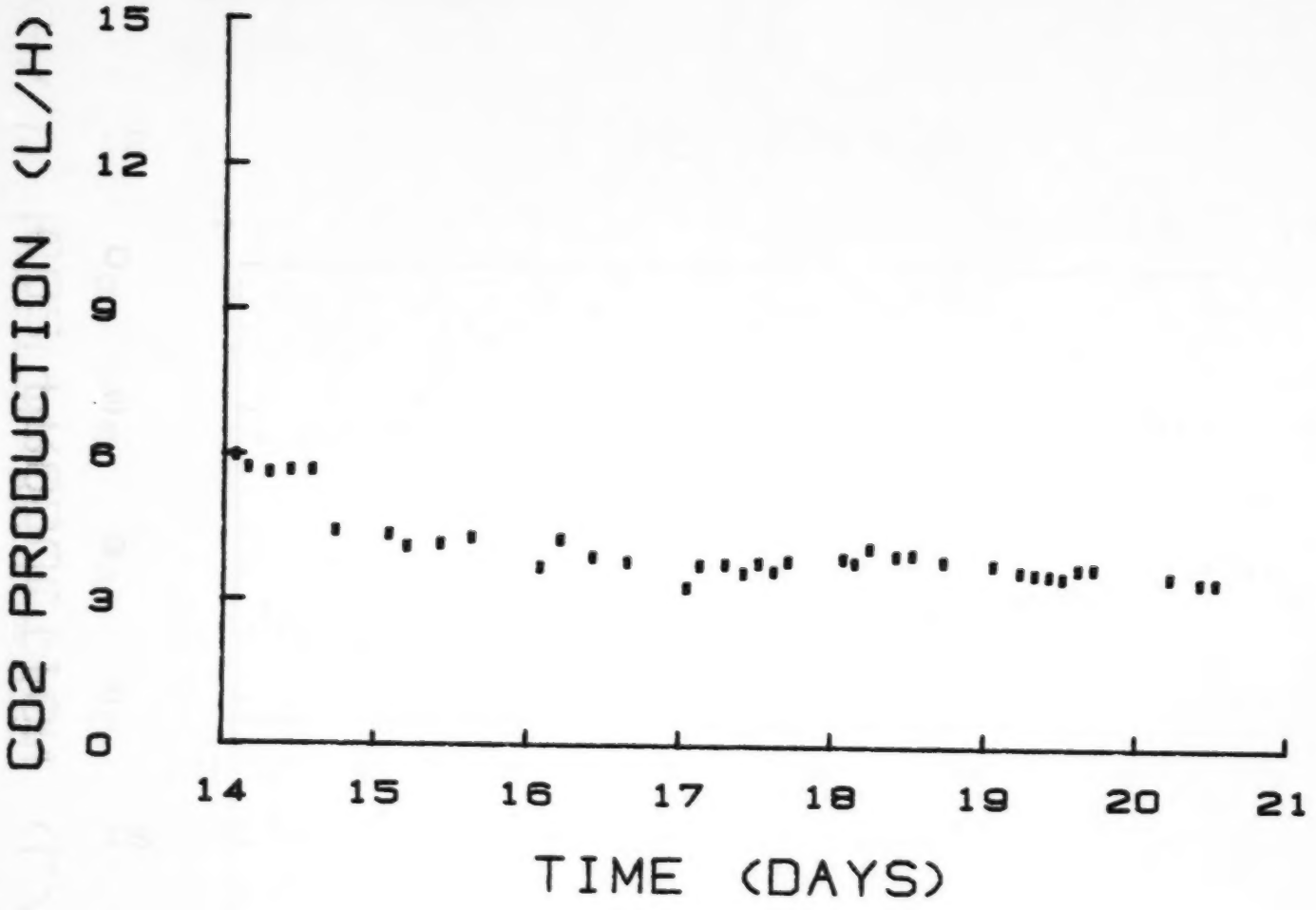

FIGURE A2: (continued)

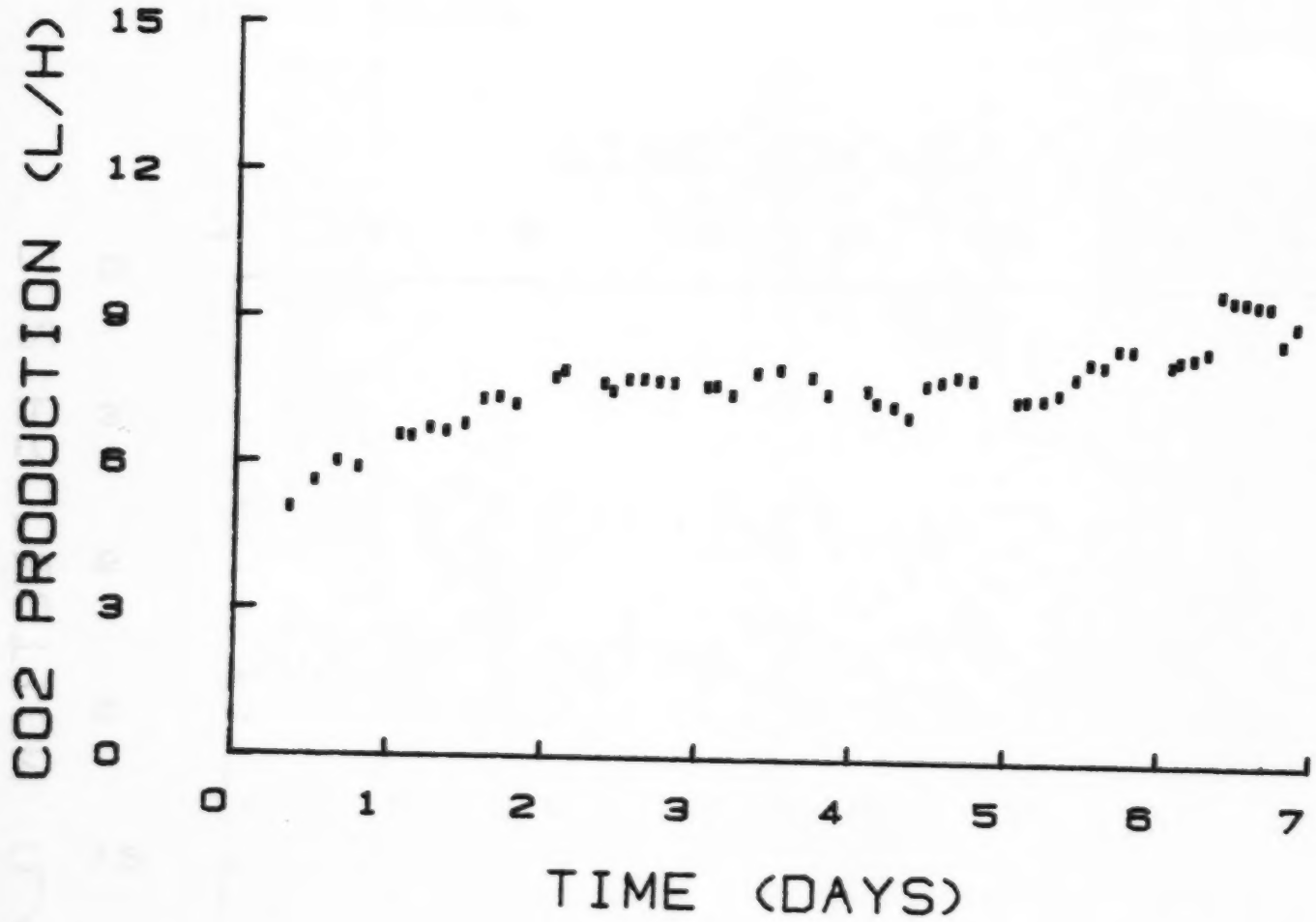

FIGURE A3: Carbon dioxide production rate data for RAD 1 containing ion-exchange resin immobilized yeast cells

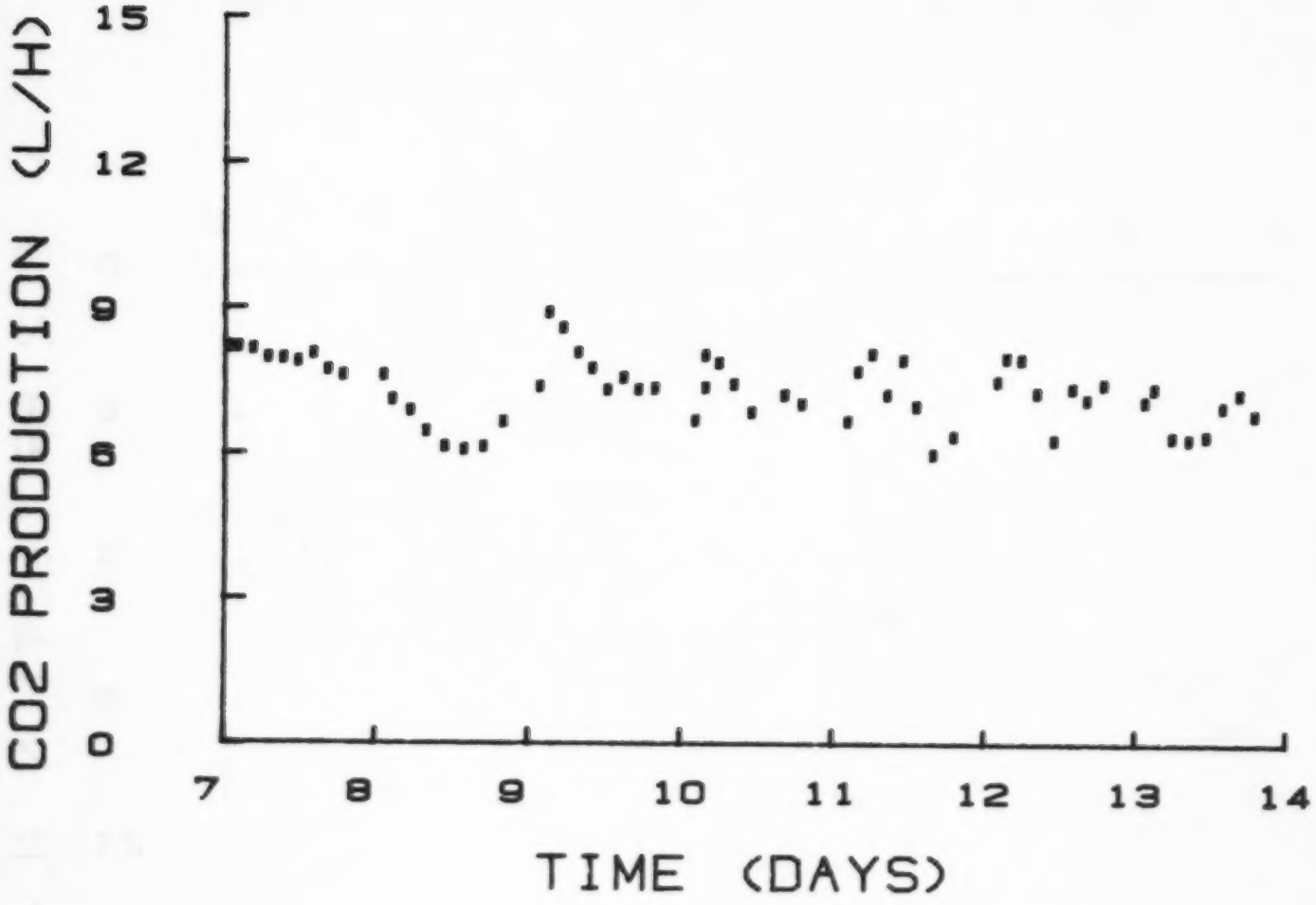

FIGURE A3: (continued)

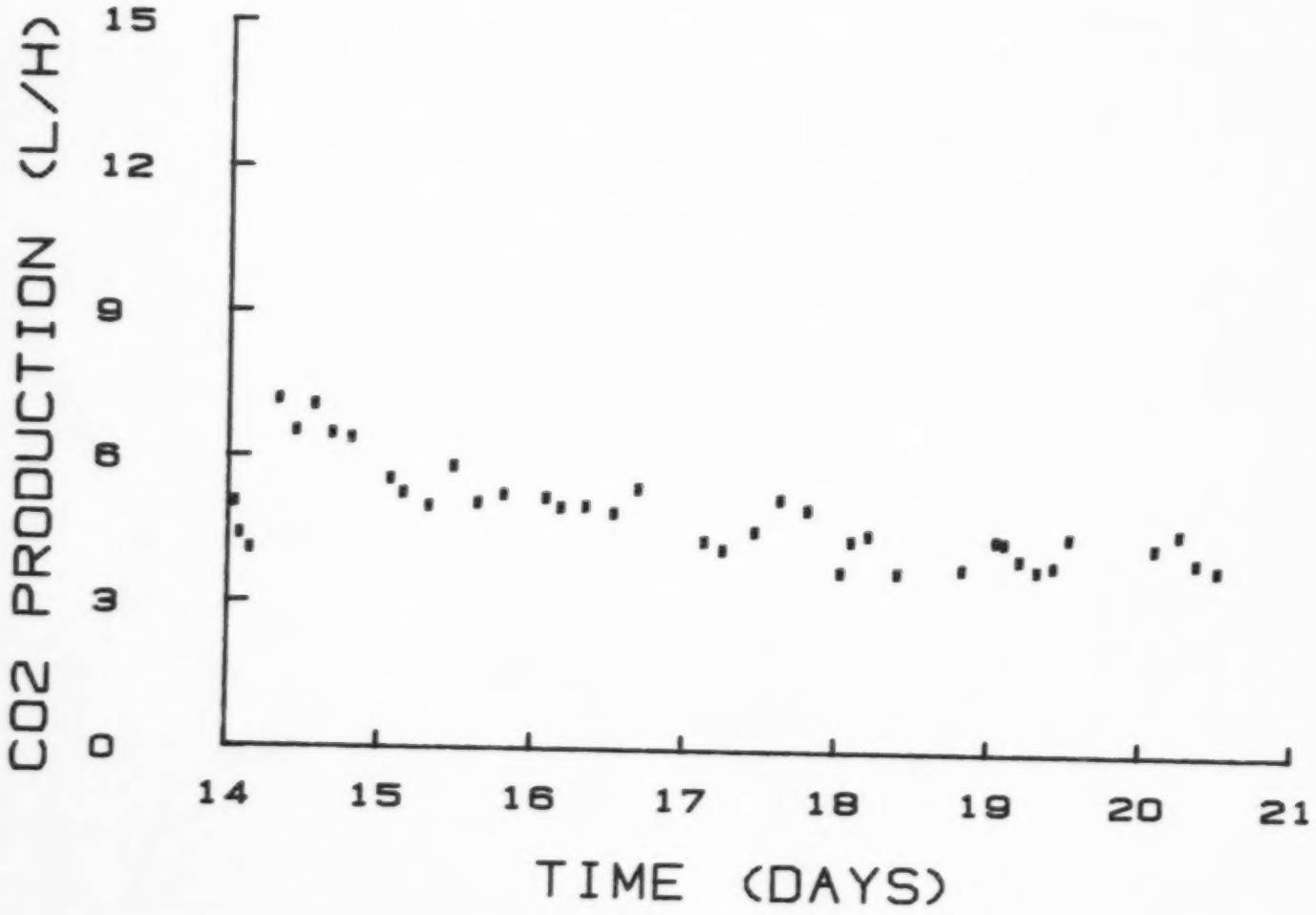

FIGURE A3: (continued)

APPENDIX 2

Paper Presented at 5th Bioenergy R&D Seminar

PERFORMANCE EVALUATION OF VARIABLE-SURFACE AREA BIOREACTORS FOR CELLULOSE UTILIZATION

P.P. Matteau, C.E.T. Choma
BioReact Engineering
Dept. of Chemical Engineering
Royal Military College of Canada
Kingston, Ont. K7L 2W3

The use of high cell densities in continuous reactors can result in severe operational limitations. The objective of this work is to determine the effectiveness of changing the geometry of packed-bed immobilized enzyme/cell reactors. The results of the comparisons of tubular reactors with both tapered-bed and radial-flow reactors will be presented for both the enzymatic hydrolysis of cellobiose and the fermentation of glucose.

ÉVALUATION DU RENDEMENT DE BIORÉACTEURS À SURFACE VARIABLE SERVANT À LA TRANSFORMATION DE LA CELLULOSE

La forte densité cellulaire dans les réacteurs en continu peut considérablement en limiter les possibilités d'exploitation. On veut déterminer s'il est efficace de modifier la géométrie des réacteurs à lit dense de cellules et d'enzymes immobilisées. On compare les réacteurs tubulaires avec les modèles à lit conique ou à écoulement radial pour l'hydrolyse enzymatique de la cellobiose et pour la fermentation du glucose.

INTRODUCTION

The advantages associated with the utilization of immobilized enzymes and whole cells for continuous bioconversions have been well documented and have resulted in the initiation of many new immobilization techniques (1). These novel enzyme and cell immobilization techniques have resulted in a requirement for research to be carried out on the determination of the optimum type of bioreactor to be used in conjunction with the biological catalytic particles. By far the most often employed reactor type for immobilized whole cell and enzyme processes is the packed-bed reactor. When the biocatalyst is in the form of spheres, chips, disks, sheets, beads or pellets, it can be packed readily into a column. In such a reactor, there is a steady movement of substrate across the bed of immobilized cells/enzymes in a chosen spatial direction. If the velocity profile is perfectly flat over the cross section, the reactor is said to operate as a plug-flow reactor (PFR).

Packed-bed reactors have the advantage of simplicity of operation, high mass-transfer rates, and high volumetric reaction rates (for processes which are not inhibited by the substrate concentration). On the other hand, a unique feature of the packed-bed reactor is that there exists a pressure drop or resistance to flow across the reactor. This pressure drop depends on such parameters as bed height, feed rate, feed temperature, and composition as well as the catalyst packing density. This feature can result in gas hold-up, channelling of the fluids and compaction of the bed. This drawback is further compounded during the course of certain biological reactions where a substantial amount of gas is produced. The increased pressure drop across the reactor which thus results from inefficient gas removal poses an even greater problem as a reduction in liquid flow will occur. Augmenting the flow merely acts to further increase the pressure differential across the packed-bed and results in an additional compaction of the bed and a greater reduction in the hydraulic permeability of the resulting bed. New reactor designs which have been proposed to overcome these problems have included fixed-film reactors with large void volumes (2), fluidized-bed reactors (3), inclined tubular reactors with in situ gas/liquid separators (4) and membrane reactors (5).

In order to maintain the positive features of the packed-bed reactor, two novel reactor geometries have been considered: a radial-flow packed-bed (RFPBR) and a tapered packed-bed reactor (TPBR). In both geometries, there is an increase in bed surface area in the direction of flow. This increased area produces a reduction in the fluid velocity through the bed and thus lowers the pressure drop across an equivalent bed in a tubular reactor. This increased surface area should reduce the bed resistance to flow of gases which are produced during fermentation reactions.

The present work has involved the design, construction and testing of four variable-surface area packed-bed reactors (two radial-flow units and two tapered-bed units). The performance of these reactors were then compared to that of tubular packed-bed reactors for an enzymatic and a fermentation reaction using calcium alginate encapsulated whole cells. The enzymatic reaction tested was the hydrolysis of cellobiose to glucose using a mycelium-associated enzymatic activity of Trichoderma harzianum E58. The model fermentation of glucose to ethanol and carbon dioxyde was carried out with the yeast Saccharomyces cerevisiae NRC 202076.

Reactor Design and Flow Characteristics

In order to test the hypothesis of the effect of the change in surface area of a reactor on the pressure drop across the packed bed, the pressure drop predicted by the Kozeny-Carman equation (6) was determined for various volumetric flow rates through one-litre packed-bed reactors. The results obtained from these simulations along with the general characteristics of each of the tubular, radial and tapered-bed reactors are presented in Figure 1. Based on these simulations, under identical reactor operating conditions, the pressure drops encountered in the tubular packed-bed reactors will be approximately twice those encountered in tapered-bed reactors and up to 20 times greater than those encountered in radial-flow packed-bed reactors.

The dimensions of the reactors (all of 1 litre capacity) used in this study along with the pressure drops obtained while passing distilled water through various sizes of bed packing are presented in Table 1. The data suggests that little resistance to flow is encountered in any of the reactors under these conditions. These reactors were subsequently loaded with either yeast cells or fungal mucelium encapsulated in calcium alginate beads, and their performance evaluated for either a model fermentation (glucose to ethanol and carbon dioxide) or a single-step enzymatic reaction (cellobiose to glucose). The test system which was used in each case is shown in Figure 2. During the fermentation, continuous evaluation of the performance of the reactor was carried out by determining the rate of carbon dioxide production from the reactor by interfacing a gas meter with a minicomputer.

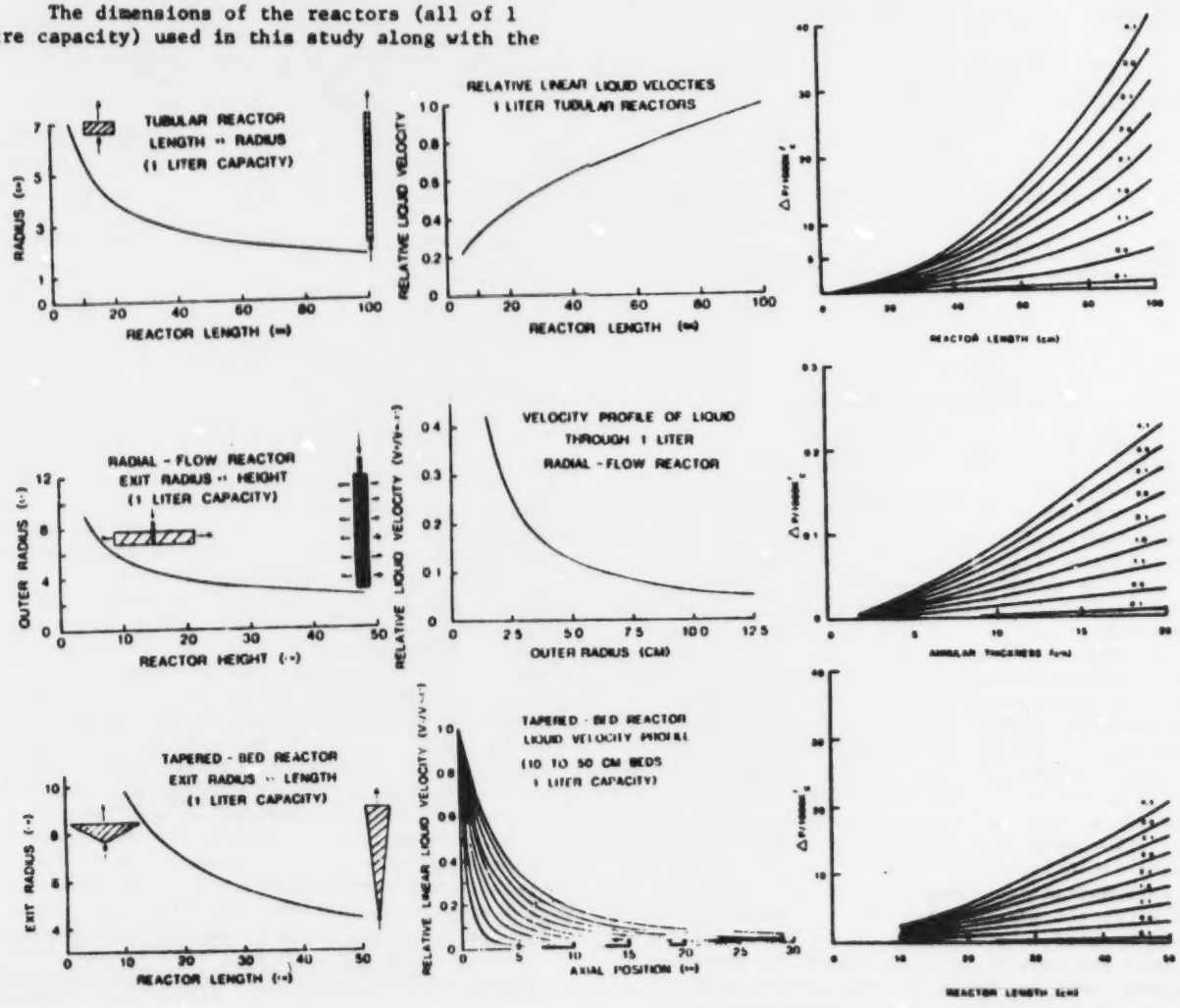

FIGURE 1: Effects of variation in reactor geometries of one-litre capacity reactors for tubular reactor (top row), radial-flow reactor (middle row), and tapered-bed reactor (bottom row). First column -- height to diameter relationships. Second column -- variation in flow rates. Third column -- pressure drop across the bed as a function of volumetric flow rates (0.1,0.6,1.1,1.6,2.1,2.6,3.1,3.6,and 4.1 L/h)

TABLE 1: Description of, and Pressure Drops Observed in Packed-Bed Reactors Using Different Sizes of Packing

Reactor and Type of Packing*	Reactor Height (cm)	Diameter		Maximum Flow Rate (L/h)	Pressure Drop (kPa)
		Inlet (cm)	Exit (cm)		
Short Tubular	49.3	5.1	5.1		
IER				5.0	1.3
Small				6.1	0.1
Medium				6.1	2.3
Large				6.1	0
Tall Tubular	87.7	3.8	3.8		
IER				5.0	4.9
Small				5.9	2.0
Medium				N/A	N/A
Large				5.9	3.0
Short Tapered	16.0	1.9	15.0		
IER				N/A	N/A
Small				6.1	0
Medium				6.1	0
Large				6.1	3.0
Tall Tapered	45.0	1.3	7.6		
IER				5.0	1.2
Small				6.1	0.4
Medium				6.1	0
Large				6.1	6.0
Short Radial	8.2	1.3	17.7		
ALL				6.0	0
Tall Radial	24.7	1.3	7.6		
ALL				6.0	0

* IER -- Ion-Exchange Resin
Small -- Calcium Alginate Beads Formed from 0.813 mm Needle
Medium -- Calcium Alginate Beads Formed from 1.024 mm Needle
Large -- Calcium Alginate Beads Formed from 2.0 mm Orifice

TABLE 2: The Effect of Reactor Geometry on Pressure Drop. Pressure Drops and Productivities Were Measured After 10 Hours Operation on 5% Glucose Medium at the Given Dilution Rate

Dilution Rate (h^{-1})	Reactor					
	Short Tubular		Tall Tapered-Bed		Short Radial-Flow	
	Pressure Drop (kPa)	Productivity (g EtOH/L/h)	Pressure Drop (kPa)	Productivity (g EtOH/L/h)	Pressure Drop (kPa)	Productivity (g EtOH/L/h)
0.9	13	18.5	13	18.5	1.3	17.6
1.5	28	16.5	21	22.5	2.7	19.5
2.1	41	23.1	14	33.6	6.0	27.3
2.7	80	25.7	27	35.1	2.7	21.6

TABLE 3: The Effect of Reactor Geometry on Pressure Drop in the Two Tapered-Bed Reactors. Pressure Drops and Productivities Were Measured After 16 Hours Operation on 5% Glucose Medium at the Given Dilution Rate

Glucose Feed (%)	Dilution Rate (h^{-1})	Reactor			
		Short Tapered-Bed		Tall Tapered-Bed	
		Pressure Drop (kPa)	Productivity (g EtOH/L/h)	Pressure Drop (kPa)	Productivity (g EtOH/L/h)
8	0.25	21	9.7	24	10.3
	0.6	17	20.4	39	23.5
	0.75	17	27.7	43	31.8
	1.2	17	35.0	31	40.7
12	0.28	14	15.2	19	16.6
	0.38	10	19.7	12	22.4
	0.54	12	23.7	26	27.0
	0.81	10	28.7	24	34.7

Enzymatic Hydrolysis

Use of the variable-surface reactors for the hydrolysis of cellobiose to glucose using the encapsulated mycelium of Trichoderma harzianum E58 resulted in no operational advantage over the use of the tubular reactors. Nor was any variation in the kinetics of the reactions seen to occur as a result of a change in reactor geometry. On the other hand, tracer studies showed that the radial-flow reactor was susceptible to channelling as a result of a shrinkage of the packed bed volume. The conversion rates for the radial-flow reactors were, therefore, consistently lower than that obtained with either the tubular or tapered-bed reactors. A typical set of data obtained from the tall tubular reactor is presented as Figure 3. As can be expected, the fractional conversion drops as a function of an increase in the dilution rate (flow rate) and an increase in substrate concentration. A least-squares fit of the data to exponential equations resulted in a good fit and permitted the construction of a model which could be used in evaluating other data. Simulation of this exponential model produced the response surface shown in Figure 4. The results dramatically show that for substrate concentrations above approximately 10 mmol.L^{-1} very low conversions will take place at even low dilution rates.

Fermentation

The fermentation of glucose to ethanol was carried out using calcium alginate encapsulated cells of Saccharomyces cerevisiae NRC 202076. The reactors were wet-packed with yeast-containing calcium alginate beads and the glucose medium was passed through at a low dilution rate for 24 to 48 hours to permit the growth of the yeast. The testing procedure then consisted of operating the reactors at various dilution rates and of analyzing the effluent and the state of the reactor continuously until a steady-state level of conversion had been achieved. A typical transient response of three different reactors operating with a 5% glucose feed is presented in Figure 5. Of particular interest during the course of reactor operation were the pressure drops which were encountered in each reactor. Table 2 presents data obtained for each type of reactor operating with 5% glucose feed. The pressure differentials which were obtained were in keeping with what had been predicted. The tubular reactors, in fact, developed such high pressure drops (Ca. 200 kPa) that it was decided to not use them at higher glucose concentrations.

The data in Table 3 at 8% and 12% feed is a comparison of the performance of two tapered-bed reactors. The shorter of the two units is seen to be almost as productive while giving pressure drops of approximately one-half that of the taller reactor. The degree of conversion of

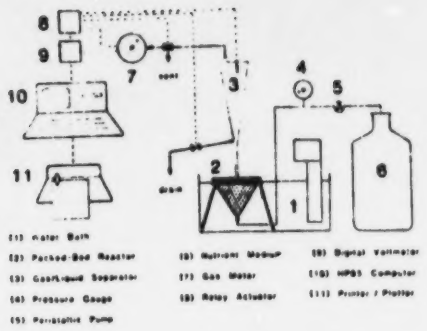

FIGURE 2: Schematic diagram of system used for reactor evaluation

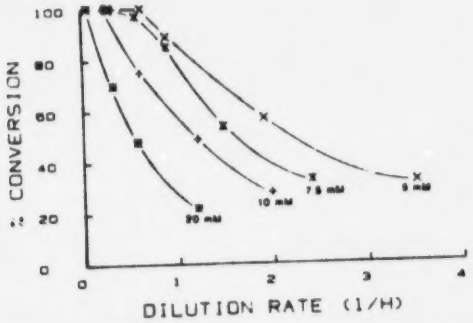

FIGURE 3: Enymatic hydrolysis of cellobiose using a 1-litre capacity tubular reactor (tall) filled with calcium alginate encapsulated mycelium of Trichoderma harzianum E58

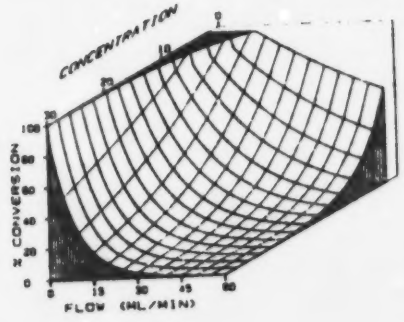

FIGURE 4: Simulation of the response surface generated from an exponential model of the enzymatic hydrolysis data obtained from the tall tubular reactor

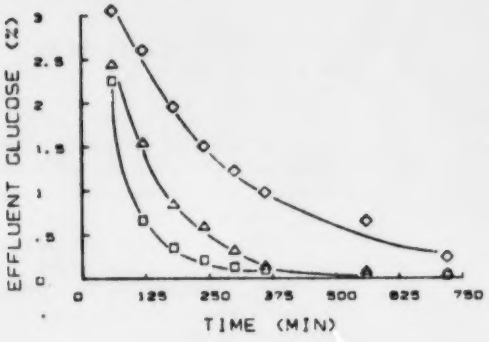

FIGURE 5: Dynamic start-up response of the short tubular reactor (◇), tall tapered-bed reactor (△), and the short radial-flow reactor (□), operating at a dilution rate of 0.9 h^{-1} and a 5% glucose feed concentration

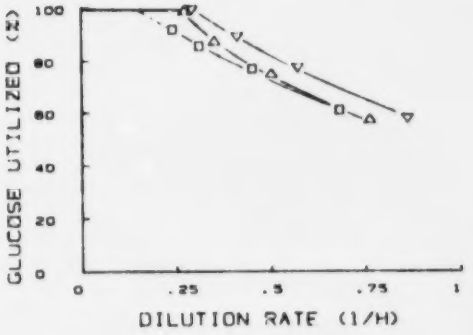

FIGURE 6: Glucose utilization in the short (△) and tall (▽) tapered-bed reactors and the tall radial-flow reactor (□) using a 12% glucose feed concentration

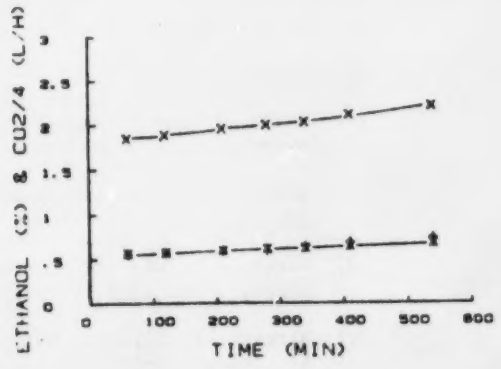

FIGURE 7: Correlation between alcohol concentration in effluent as determined by gas chromatography (⧗) and as calculated from the rate of carbon dioxide production (+). Rate of carbon dioxide production (X)

these reactors as well as that of the tall radial-flow reactor for a 12% glucose feed is presented in Figure 6.

During the course of the work, it was determined that the use of a computer to continually monitor the fermentation reaction would be useful. As shown in Figure 2, an HP 85 computer was interfaced to the gas-meter which was used to determine the gas flow rates. This permitted the continuous acquisition of carbon dioxide production rates and the calculation of the conversion efficiency of the reactor. In order to show that such data were consistent with that which could be obtained by analysis of the reactor effluent, a comparison was made of the analyzed alcohol concentration and the alcohol concentration based on the carbon dioxide production rate. One set of results, presented as Figure 7, shows the correlation to be very good.

Conclusions

This work has shown that:

(1) The use of variable-surface area packed-bed reactors have major operational advantages over tubular packed-bed reactors.

(2) No kinetic advantage was observed during the use of variable-surface area bioreactors during either a single-step enzymatic reaction or a complex multi-step fermentation.

(3) Of the reactors tested, the short tapered-bed reactor proved to be the best overall performer.

(4) The use of a computer data acquisition and control system proved effective for determining the continuous performance of the fermentation reactors.

Acknowledgements

This work was supported by a contract from the Division of Energy, NRC and by a grant from the Department of National Defence.

References

(1) Klein, J. and F. Wagner. Appl. Biochem. Bioeng., 4, 12 (1983).

(2) Sitton, O.D. and J.L. Gaddy. Biotechnol. Bioeng., 24, 1735 (1980).

(3) Scott, C.D. and C.W. Hancher. Biotechnol. Bioeng., 18, 1393 (1976).

(4) Margaritis, A., P.K. Bajpai and J.B. Wallace. Biotechnol. Lett., 3, No. 11, 613 (1981).

(5) Kan, J.K. and M.L. Shuler. Biotechnol. Bioeng., 20, 217 (1978).

(6) Aiba, S., A.E. Humphrey and N.F. Mills. Biochemical Engineering, Academic Press, New York (1973).